GEORGE W. WOODRUFF SCHOOL OF MECHANICAL ENGINEERING
Georgia Institute of Technology
Atlanta, Georgia 30332

Manipulation Strategies for Massive Space Payloads

Semiannual Progress Report
May 16, 1989 - November 15, 1989
Wayne J. Book, Principal Investigator

NASA Grant NAG 1-623
(E25-517)

Technical Officer: Donald Soloway

TABLE OF CONTENTS

SUMMARY 1

RESEARCH TOPIC

Control of a Flexible Bracing Manipulator 4

Modeling of the Contrained Dynamics of a Flexible Robot 6

Control of a Small Working Robot on a Large Flexible Manipulator for Suppressing Vibrations 7

Control Strategy for Cooperating Disparate Manipulators 9

Dynamics of Cooperating Robots 11

Control of a Large Flexible Arm 12

Characterization of the Limits of Control of Flexible Arms 13

APPENDIX 14

High Speed, Precision Motion Strategies for Lightweight Structures

SUMMARY

During the period of this report, from May 16 to November 15, 1989, work continued on (1) control for bracing of light weight arms and (2) modeling of closed chain flexible dynamics. Work on (3) control of a small arm mounted on a large flexible arm to meet demanding application requirements was supported for the first time, although the work has been in progress for some months.

Mr. Dong-Soo Kwon has been looking at control for the bracing strategy. His early work concluded that trajectory planning must be improved to best achieve the bracing motion. He has now achieved very interesting results which enable the inverse dynamics of flexible arms to be calculated for linearized motion in a more efficient manner than previously published. The desired motion of the end point beginning at $t = 0$ and ending at $t = t_f$ is used to calculate the required torque at the joint. The solution is separated into a causal function that is zero for $t < 0$ and an accusal function which is zero for $t > t_f$. He has explored a number of alternative end point trajectories in terms of the peak torque required, the amount of anticipatory action, and other issues. The single link case is the immediate subject of this study, and an experimental verification of that case is being performed. An abstract was submitted to the 1990 American Control Conference and that paper is now in preparation.

Modeling with experimental verification of closed chain dynamics continues and will soon result in the Ph.D. thesis of Mr. Jeh-Won Lee. Mr. J-W Lee is no longer supported under this grant since he is completing his thesis while employed at the NASA Marshall Space Flight Center. His work there is closely related to the thesis work carried out with this NASA Grant. His modeling effort has pointed out inaccuracies that result from the choice of numerical techniques used to incorporate the closed chain constraints when modeling our experimental prototype RALF (Robotic Arm Large and Flexible). Since he

is comparing his results to TREETOPS, a multi body code developed for and used by NASA, direct improvements in the NASA modeling capabilities are expected. The experimental verification work is suggesting new ways to make comparisons with systems having structural linearity and joint and geometric nonlinearity. Mr. J-W Lee should complete his Ph.D. degree in the first quarter of 1990.

Work on the small arm mounted on a large arm currently involves three students. Mr. Soo-Han Lee has been studying the generation of inertial forces with a small arm that will damp the large arm's vibration. Since the centralized control is complex to implement and dependent on close coordination for stability (hence less robust) he has concentrated recently on a "nearly decoupled" control. Decoupling is enhanced by the proper configuration of the small arm. During the large arm motions this is reasonable, since the small arm may not have a specified configuration. When the small arm configuration is specified by the task other approaches may be necessary. Experimental verification using the planar motions of RALF, a 20 ft arm, and SAM (Small Articulated Manipulator), a 3 degree of freedom arm, are proceeding. The control computer interfaces have now been constructed. These experiments should begin in early 1990.

Mr. Jae Lew has orally presented his Ph.D. thesis proposal and is making several adjustments to the draft document. He is studying the control and coordination problems that arise in task execution using a small and large arm combination like RALF and SAM. The disparate size of these arms and the serial mounting challenge us to use the advantages of each arm most effectively to provide reach, precision, payload and speed improvements. Existing approaches for redundant and dual arms are relevant, but not directly applicable. In particular, by attaching the heavy payload to the large arm at the same point the small arm is attached, a topology similar to the construction crane results. The small arm can make precise adjustments to the payload position much as the construction worker places the crane's load by pushing on it.

Mr. Jonathan Cameron joined the project in the Fall quarter. He has now successfully completed his qualifying exams and will be studying the multiple arm dynamics and

coordination problem. His experience in the space program at JPL and his computer experience make him an immediately valuable team member.

Previous researchers under this grant are continuing to publish papers on the research it supported. Dr. Bau-San Yuan, currently with American Semiconductor Equipment Technologies, has co-authored papers on his control results, and the draft of a paper on symbolic modeling has been prepared. Dr. Sabri Cetinkunt, now at the University of Illinois, Chicago, has submitted and published papers to several journals as documented in the following.

RESEARCH TOPIC: Control of a Flexible Bracing Manipulator

RESEARCH ASSISTANT: Dong-Soo Kwon

SHORT TERM OBJECTIVE: Inverse Dynamics Calculation for Following The Desired End Point Trajectory

1) INVERSE DYNAMICS

An inverse dynamic equation is derived from the direct dynamic equation of a flexible one-link manipulator using the assumed mode method. The required torque for a certain desired trajectory is obtained by synthesizing two solutions of the causal part and the anticausal part of the inverse dynamic equations. Applying the calculated torque to the ideal model of the system as open loop, the reference values of all state variables, which match the desired end point trajectory, are provided. These can be used as reference command values of all state variables for full state feedback tracking control. The characteristics and the performance of the open loop control and the combination of the open loop feedforward control and feedback control are studied in simulation and experiment.

2) EXPERIMENTAL EQUIPMENT

To implement the torque profile which was obtained from the inverse dynamics, a flexible 47" long aluminum single link manipulator is setup with a direct DC servo motor and a current amplifier. Two strain gauges are attached at the base and the mid point of the beam to measure the flexible vibration. A joint angle position sensor and a tachometer are attached at the shaft of the motor. At the end of the beam, a mass is attached to model the payload, and a force sensor is installed to measure the contact force for bracing applications.

PUBLICATION

The abstract of the paper "A Causal Approach to The Inverse Dynamics of a Flexible Link Arm" was submitted to the 90' American Control Conference.

RESEARCH TOPIC: Modeling of the Constrained Dynamics of a Flexible Robot

RESEARCH ASSISTANT: Jeh-Won Lee

Jeh-Won Lee is nearing the completion of his thesis. He is currently working for NASA Marshall Space Flight Center while he completes his degree.

The numerical simulations of RALF (Robotic Arm Large and Flexible) were compared to results obtained from TREETOPS, a NASA sponsored code. Discrepancies found appear to be due to the means of enforcing the constraints for the TREETOPS code. Mr. Lee is working with TREETOPS in his job at Marshall, and so has an excellent opportunity to influence the direction of its development.

Experiments with the large motion behavior of RALF are being examined for various geometrical nonlinearities, Coriolis and centrifugal forces influencing the behavior. Experimental results for nonlinear systems lack an accepted way to categorize the results. Mr. Lee is looking at sinmoidal motions and the resulting harmonics that appear in strain and joint measurements.

Initial drafts of all chapters of Mr. Lee's thesis have been received. He should complete his degree early in the Winter '90 quarter.

PUBLICATIONS

Lee, Jeh-Won and Wayne J. Book, "Efficient Dynamic Models for Flexible Robots," submitted to 1990 IEEE Robotics and Automation Conference, May 13-18, Cincinnati, OH.

RESEARCH TOPIC: Control of a Small Working Robot on a Large Flexible Manipulator for Suppressing Vibrations

RESEARCH ASSISTANT: Soo Han Lee

The main research activities during this period were working for the construction of the I/O interface boards of the small robot, and studying for the development of the control algorithms for the small robot (SAM, Small Articulated Manipulator).

1) Although a prototype I/O board designed by Douglas J. Paul, who earned his MS in March of this year, worked well for single joint operation, the board had reliability and noise problems. In order to solve these problems, printed circuit boards were constructed. In addition to the construction of the I/O boards, the kinematics, inverse kinematics, and dynamic equations of motion of the small robot were obtained for testing and calibrating the total robot system that consisted of a controller, I/O interface boards, and mechanical hardware.

2) Inertial forces are generated by the movement of SAM around a nominal configuration. The nominal configuration is related to the direction of the inertial forces. The direction of the inertial forces affect the stability of the vibration control of the large arm on which SAM is mounted, RALF (Robotic Arm, Large and Flexible). The stability analysis has been done using lumped mass-spring analogy and force diagrams. This analysis shows that decoupling is achieved if the nominal angle of the lower joint of SAM should be 90 degrees to the upper link of RALF, and the angle of the upper joint of SAM should be 90 degrees to the lower link of RALF. Hence a control law has the terms which force SAM to keep these nominal angles.

3) In order to suppress the vibrations of RALF, the angles of SAM should oscillate around the nominal angles and the oscillation should generate D or PD actions in response to the vibrations. The amplitudes of the oscillation need to be reasonably small for not disturbing the stability and nominal configuration of SAM. Total control forces must require less than the peak torque of a joint motor. Up to now the effects of D and PD control have been found; D control suppresses the vibrations at nearly same rate as PD

control, and needs less torque than PD control. PD control is more effective than D control in keeping nominal angles.

PUBLICATIONS

Book, W. J. and Soo-Han Lee, "Vibration Control of a Large Flexible Manipulator by a Small Robotic Arm," Proceedings, 1989 American Control Conference, Pittsburgh, PA, July , pp.

Lee, Soo-Han, Wayne J. Book, "Control of a Small Working Robot on a Large Flexible Manipulator for Suppressing Vibrations," Submitted to 1990 American Control Conference, May 23-25, 1990, San Diego, CA.

Book, W. J., Soon-Han Lee, "Robot Vibration Control Using Inertial Damping Forces," submitted to 1990 CISM-IFTOMM Symposium on Theory and Practice of Robotic Manipulators, Cracow, Poland, July 2-6, 1990.

RESEARCH TOPIC: Control Strategy for Cooperating Disparate Manipulators

RESEARCH ASSISTANT: Jae Young Lew

Jae Lew's research seeks higher performance manipulators in large workspace, particularly for those that require precise positioning and mating relatively massive payloads. Demand for these manipulators can be found in some of the common space maintenance and construction scenarios. As a solution, the concept of a small arm mounted on the end of a large arm is introduced to provide precise motion as well as large workspace. From a real world experience with crane-human coordination, when a heavy payload is unloaded, we know that we can obtain precise positioning and high payload capacity. This crane-human configuration may be analogous to the topology of bracing at the tip of the small arm and having an end effector at the middle of the chain. Since contact with the environment occurs at a bracing point on the small arm, similarity to a dual arm topology exists. However, this topology is different than dual arm in some ways. For example, the large arm (crane) is powerful and the small one (human) is capable of precise positioning. To take full advantage of such disparate features, several control strategies have been studied.

The short term objective is to investigate and identify the theory and the related problem behind the disparate large/small arms coordination. The research activities during the last 6 months have included the following. First, related literatures were briefly reviewed. Second, the kinematic topology was synthesized in various combinations of the large/small arms for the planar motion. Third, the kinematics for the large/small arms was studied when they are constrained by a closed chair, and the advantage of the proposed configuration was analytically proven. Finally, with the master/slave approach, the control strategy for the two arms was considered, and the typical force control problem of a flexible arm, so called, "non-colocated control" was examined.

PUBLICATION

Lew, Jae Y. "Control Strategy for Cooperating Disparate Manipulators", (Draft) Ph.D. thesis proposal, Department of Mechanical Engineering, Georgia Institute of Technology, Atlanta, Georgia, Fall Quarter 1989.

RESEARCH TOPIC: Dynamics of Cooperating Robots

RESEARCH ASSISTANT: Jonathan M. Cameron

SHORT TERM OBJECTIVE: Assist in various research-related activities and prepare for Ph.D. qualifying exams.

Mr. Cameron worked as a graduate research assistant for one month of this reporting period. During that time, he assisted with several research-related activities in the ME Research building. Also, he helped in the system management of several computers related to this research. Much of his time was spent in preparing for his Ph.D. qualifying exams which he took in the beginning of November and passed.

In relation to this research, he prepared to write a robot simulation program that will be useful in this research as well as a useful tool in the ME research building. He also investigated several research ideas in preparation to forming a dissertation proposal.

RESEARCH TOPIC: Control of a Large Flexible Arm

RESEARCH ASSISTANT: Bau-San Yuan (previously supported)

PUBLICATIONS:

Yuan, B-S, J. D. Huggins, and W. J. Book, "Small Motion Experiments on a Large Flexible Arm with Strain Feedback," Proceedings, 1989 American Control Conference, June 21-23, 1989, Pittsburgh, PA, pp 2091-2095.

Yuan, B-S, W. J. Book and J. D. Huggins, "Decentralized Adaptive Control of a Two Degree of Freedom Flexible Arm," to be presented, 1989 ASME Winter Annual Meeting, December 10-15, 1989, San Francisco, CA.

Yuan, B-S, Wayne J. Book and Bruno Siciliano, "Direct Adaptive Control of a One-Link Flexible Arm with Tracking," to appear J. of Robotic Systems, December 1989.

Yuan, B-S, W. J. Book and J. D. Huggins, "Control of a Multi-Link Flexible Manipulator with a Decentralized Approach," submitted to the 11th IFAC World Confress, 13-17 August, 1990, Tallinn, USSR.

RESEARCH TOPIC: Characterization of the Limits of Control of Flexible Arms

RESEARCH ASSISTANT: Sabri Cetinkunt

PUBLICATIONS:

Cetinkunt, Sabri and Wayne Book, "Performance Limitations of Joint Variable Feedback Controllers Due to Manipulator Structural Flexibility," submitted to IEEE Transactions on Robotics and Automation, June, 1989.

Cetinkunt, Sabri and Wayne J. Book, "Symbolic Modeling and Dynamic Simulation of Robotic Manipulators with Compliant Links and Joints," Robotics and Computer Integrated Manufacturing, Vol. 5, No. 4, pp. 301-310, 1989.

APPENDIX

The abstract of the paper "A Causal Approach to The Inverse Dynamics of a Flexible Link Arm" was submitted to the 90' American Control Conference.

Book, W. J. and Soo-Han Lee, "Vibration Control of a Large Flexible Manipulator by a Small Robotic Arm," Proceedings, 1989 American Control Conference, Pittsburgh, PA, July 1989.

Book, W. J., Soon-Han Lee, "Robot Vibration Control Using Inertial Damping Forces," submitted to 1990 CISM-IFTOMM Symposium on Theory and Practice of Robotic Manipulators, Cracow, Poland, July 2-6, 1990.

Cetinkunt, Sabri and Wayne Book, "Performance Limitations of Joint Variable Feedback Controllers Due to Manipulator Structural Flexibility," submitted to IEEE Transactions on Robotics and Automation, June, 1989.

Cetinkunt, Sabri and Wayne J. Book, "Symbolic Modeling and Dynamic Simulation of Robotic Manipulators with Compliant Links and Joints," Robotics and Computer Integrated Manufacturing, Vol. 5, No. 4, pp. 301-310, 1989.

Lee, Jeh-Won and Wayne J. Book, "Efficient Dynamic Models for Flexible Robots," submitted to 1990 IEEE Robotics and Automation Conference, May 13-18, Cincinnati, OH.

Lee, Soo-Han, Wayne J. Book, "Control of a Small Working Robot on a Large Flexible Manipulator for Suppressing Vibrations," Submitted to 1990 American Control Conference, May 23-25, 1990, San Diego, CA.

Yuan, B-S, J. D. Huggins, and W. J. Book, "Small Motion Experiments on a Large Flexible Arm with Strain Feedback," Proceedings, 1989 American Control Conference, June 21-23, 1989, Pittsburgh, PA, pp 2091-2095.

Yuan, B-S, W. J. Book and J. D. Huggins, "Decentralized Adaptive Control of a Two Degree of Freedom Flexible Arm," to be presented, 1989 ASME Winter Annual Meeting, December 10-15, 1989, San Francisco, CA.

Yuan, B-S, Wayne J. Book and Bruno Siciliano, "Direct Adaptive Control of a One-Link Flexible Arm with Tracking," to appear J. of Robotic Systems, December 1989.

Yuan, B-S, W. J. Book and J. D. Huggins, "Control of a Multi-Link Flexible Manipulator with a Decentralized Approach," submitted to the 11th IFAC World Confress, 13-17 August, 1990, Tallinn, USSR.

Submitted to 1990 American Control Conference, May 23-25, 1990,
San Diego, Ca.

A CAUSAL APPROACH TO THE INVERSE DYNAMICS OF A FLEXIBLE LINK ARM

Dong-Soo Kwon and Wayne J. Book
The George W. Woodruff School of Mechanical Engineering
Georgia Institute of Technology
Atlanta, Georgia 30332

ABSTRACT

An inverse dynamic equation which gives a causal solution for certain desired end point trajectories is derived from a flexible arm by using model. The model uses assumed modes to represent arm bending. The torque which is calculated from the inverse dynamics is applied to the arm as an open loop control. However, the friction at the joint and unmodelled dynamics causes tracking error and final positioning error. To compensate for these errors, feedback control is added to the nominal joint position and strain commands which are obtained from the forward dynamics model upon applying the torque calculated from the desired end point trajectory. The results of open loop control and the combination of open loop control and feedback control are shown in simulation and experiment. Also, preliminary results for control of a flexible link arm as it contacts a rigid surface to initiate a bracing action are presented.

To appear in Proceedings, 1989 American Control Conference, June 1989, Pittsburgh, PA.

VIBRATION CONTROL OF A LARGE FLEXIBLE MANIPULATOR BY A SMALL ROBOTIC ARM[1]

Wayne J. Book and Soo Han Lee
George W. Woodruff School of Mechanical Engineering
Georgia Institute of Technology

ABSTRACT

The vibration of a large flexible manipulator is suppressed by inertial forces induced by the joint torques of a small arm which is located at the tip of the large manipulator. The control of the small arm is studied based on a slow and fast submodel which are derived by applying the singular perturbation technique. A composite controller is designed to control the slow and fast motion.

I. Introduction

A large, two degree of freedom flexible manipulator which has a small arm at one end has been constructed in the Flexible Automation Laboratory at Georgia Institute of Technology as shown in Figure 1. The large manipulator is designated RALF (Robotic Arm, Large and Flexible) and the small arm is designated SAM (Small Articulated Manipulator). The large flexible manipulator is for gross motions, and the small arm is for fine motions. The large manipulator consists of two ten foot long links made of aluminum tubing actuated hydraulically through a parallel link drive. The small arm is actuated by three brushless D.C. motors through harmonic drives at each joint. The small arm could be used as a fast wrist or braced robot. In this research, however, the small arm is used as an inertial force generator for suppressing flexible vibrations of the large manipulator. This is consistent with many applications where the small arm has little to do during large arm motion.

To control the vibration of a light weight manipulator, most researchers have used the joint actuators of that manipulator. The joint actuator also controls rigid body motion. A few researchers have studied using additional actuators which control flexible motions. Zalucky, and Hardt [1] designed two parallel beams with a hydraulic actuator mounted at one end. This arrangement was used to compensate deflection and to improve dynamic response. A similar configuration was applied to tracking control [2]. Singh and Schy [3] studied control of the vibraton by external forces acting at one end. Their approach required separate actuators solely for vibration damping.

When the RALF changes configuration, the vibration modes of the manipulator change. SAM also can change its configuration to increase the ability to suppress vibrations of RALF.

In order to study the effectiveness of the inertial force of SAM, the dynamics of the manipulator is decomposed into a slow and a fast submodel by applying the singular perturbation technique [4]. A composite controller is designed based on the submodels.

Two Time Scale Control

The dynamics of a flexible manipulator is viewed as coupled rigid and flexible motion which, under certain conditions, can

[1] This work was partially supported by NEC Corporation and the Computer Integrated Manufacturing Systems Program at Georgia Tech.

be also classified as slow and fast motion. In this case, the system dynamics can be analyzed by a two time scale model [4]. Several researchers have applied singular perturbation theory to the control of manipulators with flexible joints [5,6]. One of the authors has studied the control of flexible manipulators based on two time scale models [7,8]. In this study, the effectiveness of inertial forces of the small arm for suppression of vibrations is studied by two time scale model.

For initial understanding the large flexible arm is considered with joints locked. The deflection of each link is modeled with one assumed mode. Based on analysis by Tsujisawa [9] this is adequate to represent the most important dynamic behavior. Applying Lagrange's equations to this configuration the general form resulting is:

$$M(\theta,q)\begin{bmatrix}\ddot{\theta}\\ \ddot{q}\end{bmatrix}+\begin{bmatrix}0\\ kq\end{bmatrix}+\begin{bmatrix}N_1(\theta,\dot{\theta},q,\dot{q})\\ N_2(\theta,\dot{\theta},q,\dot{q})\end{bmatrix}=\begin{bmatrix}u\\ 0\end{bmatrix} \quad (1)$$

where,

$M(\theta,q)$ is the inertia matrix,

$N(\theta,\dot{\theta},q,\dot{q})$ contains nonlinear and gravity terms,

K is the stiffness matrix, of RALF

θ is the vector of joint angles of SAM

q is the vector of deflection amplitudes and

u is the control torque vector.

This equation can be expressed as,

$$\begin{aligned}\ddot{\theta} &= -H_{12}Kq - H_{11}N_1 - H_{12}N_2 + H_{11}u\\ \ddot{q} &= -H_{22}Kq - H_{21}N_1 - H_{22}N_2 + H_{21}u\end{aligned} \quad (2)$$

where, $[H_{ij}]$ is the inverse matrix of matrix M.

By taking $\mu = 1/k_{22}$ as a perturbation parameter, we can rearrange equation (2) as follows;

$$\ddot{\theta} = -H_{12}z - H_{11}N_1 - H_{12}N_2 + H_{11}u \quad (3a)$$

$$\mu\ddot{z} = -\bar{K}H_{22}z - \bar{K}H_{21}N_1 - \bar{K}H_{22}N_2 + \bar{K}H_{21}u \quad (3b)$$

where, $\bar{K} = \mu K$, and $z = kq$.

When we set $M = 0$, we can obtain the quasi-steady-state z as,

$$\bar{z} = H_{22}^{-1}(-H_{21}N_1 - H_{22}N_2 + H_{21}u), \quad (4)$$

where the over-bars are used for denoting the terms when $\mu = 0$. By substituting (4) into (3-a), we can obtain the slow submodel, that is, the rigid model of a manipulator as,

$$\ddot{\theta} = \bar{M}^{-1}{}_{11}(-\bar{N}_1 + \bar{u}) \quad (5)$$

To derive the fast submodel, we assume that the slow variables θ, are fixed during the fast transient. By introducing the fast time scale, we can obtain the fast submodel as,

$$\tau = t/\sqrt{\mu}$$

$$\eta'' - \bar{K}H_{22}\eta + \bar{K}H_{21}u_f \quad (6)$$

where, $\eta = z - \bar{z}$

$$u_f = u = \bar{u}$$

and " indicates diferentiation with respect to τ.

In order to guarantee that the fast variables z follow the slow manifold, we need to use a composite control law [4] as,

$$u = \bar{u}(\theta) + u_f(\eta)$$

In this research, a nonlinear feedback control law like the computed torque method is used for controlling the slow motion. A pole assignment control algorithm is used for the fast motion. If the number of actuators and modes included in modeling are the same enabling the neceesary matrix inverse, the slow control law, $\bar{u}$, and the fast control law, u_f, are given as

$$\bar{u} = \bar{N}_1 + \bar{M}_{11}\left\{\ddot{\theta}_d - \Lambda_{1s}\left[\dot{\theta} - \dot{\theta}_d\right] - \Lambda_{2s}\left[\theta - \theta_d\right] - \Lambda_{3s}\int\left[\theta - \theta_d\right]dt\right\}$$

$$u_f = \left[\bar{K}\bar{H}_{21}\right]^{-1}\left\{\bar{K}\bar{H}_{22}\eta - \Lambda_{1f}\eta' - \Lambda_{2f}\eta\right\},$$

where, Λ_1, Λ_2 and Λ_3 are diagonal gain matrices and the subscript s denotes the slow motion control, and f denotes the fast motion.

II. DISCUSSION

The application of the two time scale control has verified the simplification possible with this approach. The two control laws must each control a 4th order system as opposed to one 8th order system. This will make real time implementation easier.

The advantage of simplification is obtained at the price of limited performance. The fast system variables η are controlled relative to the slow manifold $\bar{Z}$. Thus when $\eta=0$ the deflections q might not be zero.

Based on preliminary studies of a one link flexible arm with a one link rigid arm on its tip, we expect effective vibration dampening. When compared to joint motions of the flexible arm, several other parameters must be considered, such as the nominal joint angles, initial conditions, and which mode is to be damped.

While the fast control algorithm described above requires equal numbers of actuators and modes, this is not a general limitation for other possible algorithms.

Further work on these issues is underway.

REFERENCES

1. Zalucky, A. and Hardt, D.E., "Active Control of Robot Structure Deflections," ASME J. of Dynamic Systems Measurement and Control, Vol. 106, March 1984, pp. 63-69.
2. David, J.H. and Hirschorn, R.M., "Tracking Control of a Flexible Robot Link," IEEE Trans. on Automatic Control, Vol. 33, No. 3, March 1988, pp. 238-248.
3. Singh, S.N. and Schy, A.A., "Control of Elastic Robotic Systems by Nonlinear Inversion and Modal Damping," ASME J. of Dynamic Systems Measurement and Control, Vol. 108, Sept. 1986, pp. 180-189.
4. Koktovic, P.V., "Applications of Singular Perturbation Techniques to Control Problems," SIAM Review, Vol. 26, No. 4, 1984, pp. 501-550.
5. Marino, R. and Spong, M.W., "Nonlinear Control Techniques for Flexible Joint Manipulators: A Single Link Case Study," Proc. IEEE Int. Conf. on Robotics and Automation, 1986, pp. 1030-1036.
6. Khorasani, K. and Spong, M.W. "Invariant Manifolds and Their Application to Robot Manipulators with Flexible Joints," Proc. IEEE International Conference on Robotics and Automation, 1985.
7. Siciliano, B. and Book, W.J., "A Singular Perturbation Approach to Control of

Lightweight Flexible Manipulators," International Journal of Robotics Research, Jan., 1988.

8. Siciliano, B., Book, W.J., and Maria, D.G., "An Integral Manifold Approach to Control of a One Link Flexible Arm," Proc. 25th IEEE Conference on Decision and Control, Athens, Greece, 1986, pp. 10-12.
9. Tsujisawa, T. and Book, W.J., "A Reduced Order Model Derivation for Light Weight Arms with a Parallel Mechanism," to appear, Proc., 1989 IEEE International Conference on Robotics and Automation, May 14-19, Scottsdale, AZ.

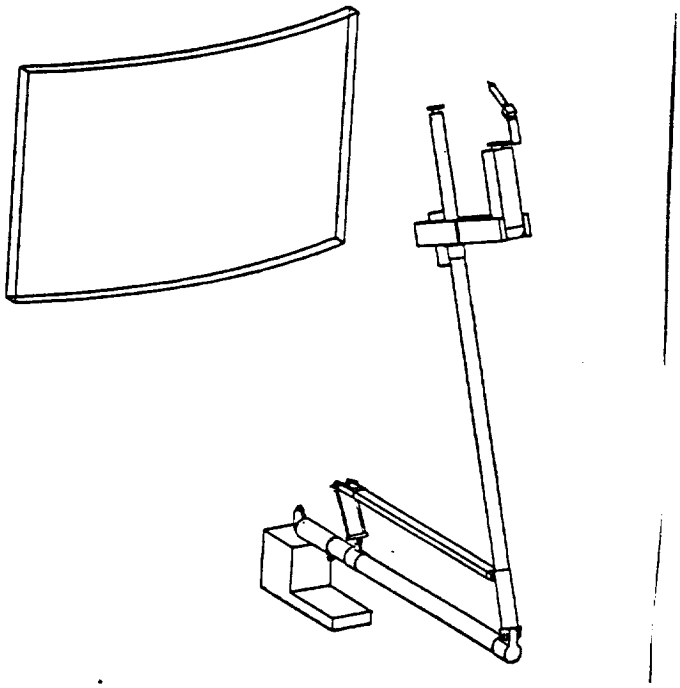

Figure 1: The system of interest: RALF (Robotic Arm, Large and Flexible) carrying SAM (Small Articulated Manipulator).

Submitted to 1990 CISM0TFT.MM Symposium on Theory and Practice of Robotics and Manipulators, Cracow, Poland, July 2-6, 1990.

Robot Vibration Control Using Inertial Damping Forces

Wayne J. Book
Soo-Han Lee
School of Mechanical Engineering
Georgia Institute of Technology
Atlanta, GA 30332, U.S.A.
Tel. 404-894-3247

Lightweight manipulators are subject to vibrations that reduce their performance. Active means to damp these vibrations are of significant research interest. Joint actuators of the arm can perform this task very effectively as has been shown in theory and experiment by several researchers. These actuators must respond at the bandwidth of the vibration they are to damp. If the manipulator and/or the payload is large the actuators are correspondingly large. The bandwidth requirement is a serious impediment to practical implementation of the active vibration damping scheme. An alternative under exploration is vibration damping through inertial forces. Inertial forces are commonly used for active vibration control in large space structures. Reaction wheels and linear momentum exchange devices are placed on the structure specifically for this purpose. This paper will explore the use of the existing degrees of freedom at the end of a large arm to damp vibrations during gross motions when they are not otherwise employed. These smaller actuators can have a higher bandwidth and more precise control than the joints used to reconfigure the arm. The smaller actuators could be actuating the wrist of a manipulator in a traditional industrial manipulator.

The system used in the analysis and experiments of this paper is actually two arms. (See Figure 1.) The large arm is designated RALF (Robotic Arm Large and Flexible). It consists of two, 3 meter beams and two rotary joints actuated by hydraulic cylinders and controlled by a MicroVAX II computer. The moving structure weighs only 32 kg (70 pounds) and has natural frequencies under 9 Hz when no payload is present. A small arm with three electrically actuated degrees of freedom has two links of about .5 meter each. Each joint is controlled by a Motorola 68000 microprocessor supervise by a common IBM PC. It is designated SAM (Small Articulated Manipulator). Its links are essentially rigid. SAM is designed to be carried by RALF. These robots are test beds for control algorithms and operating strategies appropriate to flexible arms. In this paper we consider the use of SAM to generate inertial forces for damping the vibrations of RALF. Motions in a plane are our initial consideration.

The effectiveness of the inertial forces in damping vibrations depend on the nominal configuration of both arms. At this time we are not considering the problem of moving the small arm to the configuration that will be required for the manipulator task. As a useful strategy the center of mass of the small arm and its motion are moved as required for inertial force generation on the tip of the large arm. The moments produced are of less significance on the motion of the large arm. The large arm is modeled by an assumed modes method.

This model can be linearized when the motions are relatively slow. The mode shapes of the arm change when the arm changes configuration, and this is accounted for in determining the appropriate small arm nominal configuration ang the appropriate small arm nominal configuration and motions.

SAM is significantly affected by the nonlinear terms in the dynamics. Its controller must allow for these terms. The control explored strives to maintain the simplicity of a decoupled motion. In other words, the large and small arm are controlled separately, not as a single kinematic chain.

Conclusions on the most effective configurations for SAM for various configurations of RALF are presented. The effectiveness inertial forces in active damping is compared to the use of the large arm's joints for active damping. Inertial forces do not appear to be as effective as joint motion for the test system. The approach is relevant to cases where the joint control is not possible, however. The approach seems particularly relevant to space manipulators proposed for the space station, where a small manipulator is carried by a "space crane." It also holds advantages for use in combination with a bracing strategy, since after bracing the small arm can be moved to perform its manipulation task without significantly exciting the large arm's vibration.

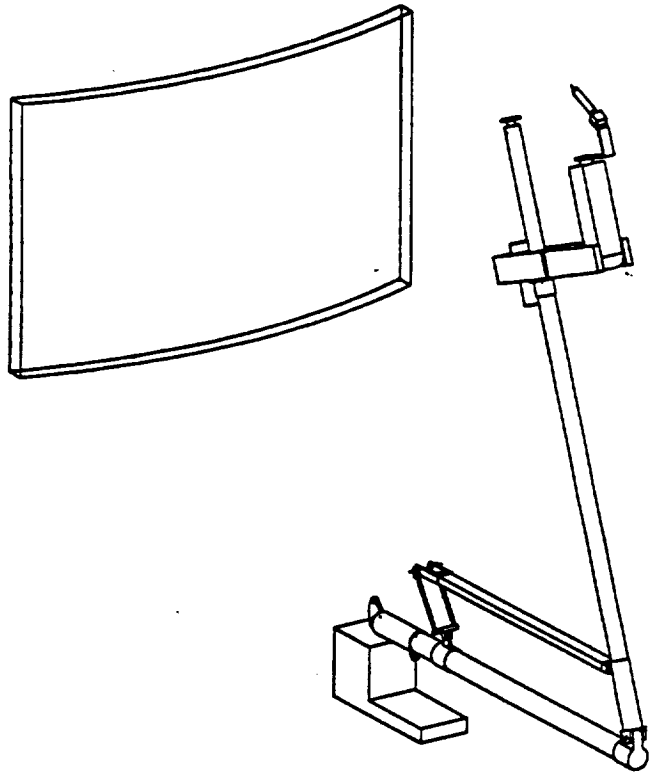

FIGURE 1. The Test Case: Robotic Arm Large and Flexible (RALF) and Small Articulated Manipulator (SAM).

Submitted to the IEEE Transactions on Robotics and Automation, June, 12, 1989.

PERFORMANCE LIMITATIONS OF JOINT VARIABLE FEEDBACK CONTROLLERS DUE TO MANIPULATOR STRUCTURAL FLEXIBILITY

Dr. Sabri Cetinkunt
Assistant Professor
Dept. of Mechanical Engineering
University of Illinois at Chicago
Chicago, IL 60680

Dr. Wayne J. Book
Professor
The George W. Woodruff School of Mechanical Engineering
Georgia Institute of Technology
Atlanta, GA 30332

Abstract

The performance limitations of manipulators under joint variable feedback control are studied as function of the mechanical flexibility inherent in the manipulator structure. A finite dimensional time domain dynamic model of a two link, two joint planar manipulator is used in the study. Emphasis is placed on determining the limitations of control algorithms that use only joint variable feedback information in calculations of control decision, since most motion control systems in practice are of this kind. Both fine and gross motion cases are studied. Fine motion results agree well with previously reported results in the literature, and are also helpful in explaining the performance limitations in fast gross motions.

Nomenclature

$w_i(x_i,t)$: elastic deformation of link i, at location x_i and time t.

$\underline{\theta}$: vector of joint angles ($[\theta_1, \ \theta_2\ ]$)

$\underline{\delta}$: vector of flexible mode generalized coordinates

$\underline{u}$: vector of effective torque at joints

$\underline{x}_\theta$: $\left[\underline{\theta}, \underline{\dot{\theta}}\right]$

$\underline{x}_p$: plant full state vector

$\underline{x}_m$: reference model state vector ($[\ \underline{\theta}, \underline{\dot{\theta}}\ ]_{desired}$)

$\underline{x}$: $\left[\underline{\theta}, \underline{\delta}, \underline{\dot{\theta}}, \underline{\dot{\delta}}\right]$

$\underline{u}_m$: commanded input vector to the reference model

$\underline{e}$: error state vector ($\underline{x}_m - \underline{x}_\theta$)

$\underline{\nu}$: filtered error state

$\underline{z}$: output vector of the nonlinear time varying feedback block of the standard hyperstability problem

k_{ij} : ij component of joint angle feedback gain matrix

c_{ij} : ij component joint velocity feedback gain matrix

K_{pn} : nominal joint variable (position and velocity) feedback gain matrix

K_{un} : nominal feedforward gain matrix

ΔK_p : adaptive state feedback gain matrix

ΔK_u : adaptive feedforward gain matrix

p_{pi}, p_{ui} : positive scalar constants of integral gain adaptation algorithm.

w_{st}^* : the lowest natural frequency of the arm with all joints clamped.

w_{bw} : closed loop bandwidth of the feedback controlled flexible arm

w_{rl} : closed loop bandwidth of the feedback controlled equivalent rigid arm

w_{mi} : desired motion bandwidth (the natural frequency of the reference model which has step command input)

ξ_i : damping ratio of mode i

R^n : n dimensional real vector space

$\in$: *belongs to* symbol

$\exists$: *there exists* symbol

$\{P\}$: dynamic systems defined by Popov class

$\rightarrow$: *approaches* symbol

LTI : linear time invariant

NLTV : nonlinear time varying

FFB : feedforward block

FBB : feedback block

AMFC : adaptive model following control

CLS : closed loop system

I. Introduction

Robotic manipulators have compliance that are inherent in their links and joints. The compliance becomes significant especially at high manipulation speeds and/or large payload conditions. Today, there is an increasing demand for manipulators with high speed, precision and payload handling capabilities as a result of higher productivity needs. Hence, the manipulator flexibility and control of it has become an important problem. In some cases, structural flexibility in manipulators may be desirable. For instance, a manipulator cleaning delicate surfaces, handling household jobs, is desired to have significant structural flexibility so that errors in position control do not generate large forces that may damage the surface, or become dangerous for the people in the house in case of accidents.

Regardless of the reason that the flexibility becomes significant (i.e. due to high speeds, large payloads, inherently very soft links for household services), precision control of the manipulator tip is necessary to accomplish the desired task. Manipulator motions may be divided into two groups in terms of the range of motion: 1. fine motion, 2. gross motion. In fine motion, the manipulator tip moves in a small region of workspace. Despite high closed loop bandwidth, absolute velocities do not become very large since the motion occurs in a small region. Therefore, the nonlinear dynamic forces (coriolis and centrifugal) are generally negligible. In gross motion, the manipulator tip makes large rotational maneuvers in workspace. The large rotations of joints relative to each other are the main source of complicated nonlinear dynamic coupling between the generalized coordinates [Shabana and Wehage 83, Sunada and Dubowsky 82]. Absolute velocities may become large during the fast, large maneuvers to the point that the nonlinear dynamic forces become very dominant [Luh 83].

I.1 Review of the State of Art

The majority of work in control of robotic manipulators ignores the flexibility of the manipulator in the analysis. Therefore, no reference is made to the effect and/or limitations of flexibility in control system performance [Dubowsky and DesForges 78, Balestrino et. al. 87, Hsia 86, Craig et. al. 86, Slotine 87]. In order to avoid the flexibility problem, very conservative controller design rules are suggested [Paul 83, Luh 83]. At a time when researchers are striving to design high performance controllers, it is logical to explicitly study the limitations imposed by the manipulator flexibility, instead of taking conservative design measures. Closed loop bandwidth limitations of non-adaptive joint variable feedback controllers were studied explicitly as function of arm flexibility in fine motion [Book et. al. 75]. However, the results can not be generalized to fast gross motions where dynamic nonlinear effects become significant. The dynamics of flexible manipulators are described by infinite dimensional mathematical models due to their distributed flexibility [Book 84, Low and Vidyasagar 87], yet the controllers are designed based on truncated finite dimensional models. The discrepancy between the designed performance and the actual performance achieved as a result of model truncation for the purpose of controller design is studied and an iterative design procedure is suggested in [Book and Majette 85].

The class of control algorithms studied here, that is algorithms that use only joint variable measurements, are particularly important since most industrial robots and mechanisms are controlled that way. Tip position measurements [Cannon and Schmitz 84, Shung and Vidyasagar 87], strain measurements along the flexible link [Hastings and Book 86], tip acceleration measurements [Kotnic, Yuckovitch, Özgüner 88] are examples of attempts to design so called *noncolocated* controllers that would achieve performance beyond the traditional limitations of *colocated* controllers. A major problem associated with noncolocated control is the destabilizing effect of observation and control spillover

[Gevarter 69, Balas 78]. Independent joint variable control of multi-link manipulators, that is each joint control action is based on the local measurement information of that joint only (colocated control), does not have this problem since spillover never drives the system unstable in colocated control [Gevarter 69]. This conclusion, however, cannot be extended to the class of joint variable controllers where intra-joint feedback is used to achieve decoupled joint response [Book et. al. 75].

In short, joint variable feedback controllers require fewer sensors, have better stability robustness against spillover and unmodelled dynamics, and widely used in practice. Therefore, it is worthwhile to study their potential use in fine and gross motion control of flexible manipulators, even though their upper limit of closed loop bandwidth is in general considerably smaller than that of noncolocated controllers. In particular, the adaptive joint variable feedback controllers should be analyzed since they receive increasing interest due to the adaptability of feedback gains as a function of the changing task conditions.

I.2 Characterization of the Problem and Definitions

The signficance of structural flexibility in motion control of a manipulator is a function of the task conditions. Any given manipulator can be moved *slowly enough* that the structural flexibility will not cause any significant deviation from the intended motion. Similarly, it can also be moved *fast enough* such that the structural flexibility will become very apparent in the response of the manipulator (presuming the availability of actuators that can deliver sufficiently high torque/force levels).

Physically, every robotic manipulator has structural flexibility. The question of whether the controller needs to be concerned with it or not varies from task to task. At this point, one must quantify the term *slow enough* motions such that flexibility does not present any problem, as well as the *fast enough* motions where the flexibility

does present a problem.

The speed of motion is quantified as slow or fast (low, medium, or high speed) with respect to the structural flexibility of a manipulator using the lowest structural frequency of the manipulator when all joints are locked (w_{st}^*) as the reference.

[Book et. al. 75] quantified the speed of a given fine motion relative to the structural flexibility using the ratio of necessary closed loop bandwidth (w_{bw}) to the lowest structural frequency of the system (w_{bw}/w_{st}^*). Given a manipulator, and a desired fine motion, one can easily predict whether the structural flexibility will be significant or not during that motion using the ratio of (w_{bw}/w_{st}^*).

In fast gross motion, where dynamic nonlinearities are dominant due to high joint speeds and large angular rotations, the notion of bandwidth is no longer a well defined characteristic of the control system. However, in the context of model reference control, the speed of gross motion may be quantified using the bandwidth of the reference model, (w_m), with a step input. Here, the (w_m/w_{st}) ratio is proposed to quantify the speed of gross motions relative to the structural flexibility.

The essential difference between this work and other works in control of single link flexible arm is that, in case of multiple joints (two joint two link example used in this study) there are many nonlinear couplings between the generalized coordinates of different links as a result of large angular rotations of joints. Most of these couplings do not exist in single link case. [Book et. al. 75, Book and Majette 85] studied the control aspects of two link two joint flexible manipulator example in fine motion using infinite dimensional linear frequency domain models based on transfer matrices. Here both fine and gross motion control aspects are studied using a finite dimensional nonlinear time domain model.

The remainder of this paper is organized as follows: The mathematical model of

a two-link, two joint flexible manipulator is briefly described in Section II. Fine and gross motion control under joint variable feedback controllers are analyzed in Section III, results are discussed in Section IV. The conclusions of this work are summarized in Section V. Design details of the proposed adaptive model following controller are presented in the Appendix.

II. Dynamic Model of a Two Link Flexible Manipulator

Symbolic derivation details of dynamic models for flexible manipulators are described in [Cetinkunt and Book 89]. The differences between different Lagrangian-assumed modes based modeling approaches come from the kinematic descriptions. Here the kinematic description will be summarized, and derivation using Lagrangian-assumed modes approach will be skipped since it is a well known standard procedure.

Let $(O_o X_o Y_o)$ be the inertial coordinate frame (Fig. 1). Assign two coordinates for each flexible link; one is fixed to the base (e.g. $O_1 X_1 Y_1$), the other is fixed to the tip of the link (e.g. $O_2 X_1' Y_1'$). In order to describe the absolute position of any differential element on the links, let θ_1 and θ_2 describe the joint angles, and $w_1(x_1, t)$, $w_2(x_2, t)$ describe the elastic deformations of links from the undeformed positions.

The spatial variable dependence of the deformation coordinates leads to a mathematical dynamic model that is of partial integro-differential equation form [Low and Vidyasagar 87]. In order to simplify the model, the deformation coordinates are approximated by a finite series which consists of shape functions multiplied by time dependent generalized coordinates.

$$w_i(x_i, t) = \sum_{j=1}^{n_i} \phi_{ij}(x_i)\,\delta_{ij}(t) \quad ; \quad i = 1, 2$$

$$j = 1, \ldots, n_i$$

where n_i is the number of mode shapes considered in the approximation in describing

the elastic deformation of link i.

This results in a finite order dynamic model. Since the spatial variable dependence is already specified through the shape functions, the mathematical model is of ordinary differential equation form. Let us order the generalized coordinates as $\underline{q} = [\underline{\theta}, \underline{\delta}]$, where $\underline{\theta} = [\theta_1, \theta_2]$, the joint coordinates, and $\underline{\delta} = [(\delta_{11}, \ldots, \delta_{1n_1})], (\delta_{21}, \ldots, \delta_{2n_2})]$, the deformation coordinates. Having uniquely established the kinematic description of the manipulator, the derivation steps of the equations of motion via Lagrangian formulation is straight forward [Book 84, Cetinkunt and Book 89]. The dynamic model of a flexible manipulator may be expressed in the form

$$\begin{bmatrix} m_r(\theta, \delta) & m_{rf}(\theta, \delta) \\ m_{rf}^T(\theta, \delta) & m_f(\theta, \delta) \end{bmatrix} \begin{bmatrix} \ddot{\theta} \\ \ddot{\delta} \end{bmatrix} + \begin{bmatrix} \underline{f}_r \\ \underline{f}_f \end{bmatrix} + \begin{bmatrix} \underline{0} \\ [K]\underline{\delta} \end{bmatrix} + \begin{bmatrix} \underline{g}_r \\ \underline{g}_f \end{bmatrix} = \begin{bmatrix} I \\ B_m \end{bmatrix} \underline{u} \qquad (2.1)$$

where $m_r(\theta, \delta)$, $m_{rf}(\theta, \delta)$, $m_f(\theta, \delta)$ are partitioned elements of generalized inertia matrix which is always positive definite, and symmetric, $\underline{f}_r(\theta, \dot{\theta}, \delta, \dot{\delta})$, $\underline{f}_f(\theta, \dot{\theta}, \delta, \dot{\delta})$ are coriolis and centrifugal terms which are quadratic in the generalized coordinate velocities $(\dot{\underline{\theta}}, \dot{\underline{\delta}})$; $\underline{g}_r(\theta, \delta)$, $\underline{g}_f(\theta, \delta)$ are gravitational terms; and $[K]$ is the structural stiffness matrix associated with arm flexibility and mode shape functions, $\underline{u}$ represents the effective torque (or force) vector at the joints. For the two link arm example considered here $\underline{\theta} = [\theta_1, \theta_2]$, and since two mode shapes are used per link, $\underline{\delta} = [(\delta_{11}, \delta_{12}), (\delta_{21}, \delta_{22})]$.

The equation (2.1) is a highly nonlinear and coupled ordinary differential equation set. This makes the controller synthesis and design a problem difficult. Furthermore, experiments [Hastings and Book 86] and analytical studies [Cetinkunt and Yu 89] indicates that the mode shapes of the links quickly converge to the mode shapes of clamped-base beam under joint variable feedback control for even low values of feedback gains of interest. All mode shapes of a clamped-base beam have zero slope at the base, therefore $B_m = 0$ for the dynamics of flexible manipulators under feedback control. That means the joint variable controller effects the flexible variables through coupling from

joint variables, but not directly through the input matrix. The dynamic model of a rigid manipulator, in general, has the form

$$[M(\theta)]\ddot{\underline{\theta}} + \underline{f}(\theta, \dot{\theta}) + \underline{g}(\theta) = \underline{u} \tag{2.2}$$

The structural difference between the dynamics of rigid and flexible manipulator is displayed by equations (2.1) and (2.2).

III. Fine and Gross Motion Control with Joint Variable Feedback

The question of when the arm flexibility becomes significant and what limitations it imposes on the performance of joint variable controllers are studied first in fine motion. The results are valid only when the dynamic nonlinearities are negligible. In order to determine the effect of dynamic nonlinearities, the linear and nonlinear control algorithms are simulated on the nonlinear model (2.1).

III.1 Fine Motion Control

The nonlinear model (2.1) is linearized about a nominal configuration, $\underline{x}_n = [\underline{\theta}, \underline{\delta}, \dot{\underline{\theta}}, \dot{\underline{\delta}}] = [\underline{\theta}_{nominal}, \underline{0}, \underline{0}, \underline{0}]$ and nominal input $u_{nominal}$ which compensates for the nominal gravitational loading. Since nonlinear coriolis and centrifugal terms are quadratic in $\dot{\underline{\theta}}, \dot{\underline{\delta}}$, they have no contribution to the model that is obtained by linearizing about a nominal configuration where nominal values of velocities are zero ($\dot{\underline{\theta}} = \dot{\underline{\delta}} = \underline{0}$). Let $\underline{\theta} = \underline{\theta}_{nominal} + \Delta\underline{\theta}$, $\underline{\delta} = \underline{\delta}_{nominal} + \Delta\underline{\delta}$, and $\underline{u} = \underline{u}_{nominal} + \Delta\underline{u}$, then the linear dynamic model about the nominal configuration $\underline{x}_{nominal} = [\underline{\theta}_{nominal}, \underline{0}, \underline{0}, \underline{0}]$ is given by (3.1),

$$\underbrace{\begin{bmatrix} m_r & m_{rf} \\ m_{rf} & m_f \end{bmatrix}}_{M_{eff}} \begin{Bmatrix} \Delta\ddot{\underline{\theta}} \\ \Delta\ddot{\underline{\delta}} \end{Bmatrix} + \underbrace{\begin{bmatrix} \partial\underline{g}_r/\partial\theta & \partial\underline{g}_r/\partial\delta \\ \partial\underline{g}_f/\partial\theta & \partial\underline{g}_f/\partial\delta + [K] \end{bmatrix}}_{K_{eff}} \begin{Bmatrix} \Delta\underline{\theta} \\ \Delta\underline{\delta} \end{Bmatrix} = \begin{Bmatrix} \Delta\underline{u} \\ \underline{0} \end{Bmatrix} \tag{3.1}$$

In compact form, let $\Delta\underline{x} = [\Delta\underline{\theta}, \Delta\underline{\delta}, \Delta\dot{\underline{\theta}}, \Delta\dot{\underline{\delta}}]$, the linear dynamic model about the given

nominal configuration can be expressed as,

$$\Delta \dot{\underline{x}} = A\Delta \underline{x} + B\Delta \underline{u} \tag{3.2}$$

where

$$A = \begin{bmatrix} 0 & I \\ -M_{eff}^{-1}K_{eff} & 0 \end{bmatrix}, \qquad B = \begin{bmatrix} 0 \\ M_{eff}^{-1}\begin{pmatrix} I \\ \underline{0} \end{pmatrix} \end{bmatrix} \tag{3.3}$$

The closed loop eigenstructure of the linear model under linear joint variable feedback controllers is studied as a function the feedback gains. The linear joint variable feedback control has the general form

$$\Delta \underline{u} = -[K_{ij}]\Delta \underline{\theta} - [C_{ij}]\Delta \dot{\underline{\theta}} \tag{3.4}$$

For independent joint control;

$$[K_{ij}] = diag\{k_{ii}\}$$

$$[C_{ij}] = diag\{c_{ii}\}$$

For decoupled joint control;

$$[K_{ij}] = m_r(\theta_{nominal}, 0)\, diag\{k_{ii}\}$$

$$[C_{ij}] = m_r(\theta_{nominal}, 0)\, diag\{c_{ii}\}$$

Independent joint control results are presented here in order to compare with the previously reported ones. Position and velocity feedback gains of joint 1, (k_{11}, c_{11}), are set to very high values in order to force the joint 1 behave like a clamped base. The locus of closed loop eigenvalues are studied as a function of joint 2 feedback gains, k_{22}, c_{22}. The finite dimensional linear model should be able to predict at least the dominant behavior of the closed loop dynamics of the infinite dimensional actual system, despite the errors introduced due to truncated dynamics. Otherwise the truncated finite dimensional model would not be of any value.

By comparing the root locus behavior of a given flexible manipulator with that of an equivalent rigid manipulator, the conditions at which flexibility becomes significant

and the range of conditions where the flexibility can be ignored can be determined and compared with reported results. The study of dominant behavior of closed loop eigenvalues will determine the best possible performance in fine motion.

III.2 Gross Motion - Adaptive Model Following Control

The fundamental challenge in the control of industrial and space robots is to provide high speed, high precision motions despite large variations in payload, and other task conditions. Extensive research in the past decade has shown that adaptive control methods are potentially more promising to meet that change than non-adaptive control methods. It is desirable to have an adaptive controller that would achieve the following performance criteria:

1. Good transient and steady state tracking of desired motion trajectory.
2. High speed and precision manipulation in gross and fine motion (high closed loop bandwidth) relative to the structural flexibility.
3. Good performance and stability robustness against unknown task condition variations.

An adaptive model following control (AMFC) algorithm is developed based on the hyperstablity approach [Cetinkunt 87]. The design details are presented in the Appendix in order to keep the essential points of this paper in focus. Let us call $\underline{x}_\theta = [\underline{\theta}, \underline{\dot{\theta}}]$. The adaptive control algorithm is given by, (Fig. 2)

$$\underline{u} = -K_{pn}\underline{x}_\theta + K_{un}\underline{u}_m + \Delta K_p(\underline{e}, t)\,\underline{x}_\theta + \Delta K_u(\underline{e}, t)\,\underline{u}_m \tag{3.5}$$

where

$$K_{pn} = m_r(\theta, \delta_{st})\Big[[k_{ii}], [c_{ii}]\Big] \tag{3.6.a}$$

$$K_{un} = m_r(\theta, \delta_{st}) \tag{3.6.b}$$

$$\Delta K_p = \int_o^t p_{pi}\, m_r(\theta_o, \delta_{st})\, \underline{\nu}\, \underline{x}_\theta^T\, d\tau \tag{3.6.c}$$

$$\Delta K_u = \int_o^t p_{ui}\, m_r(\theta_o, \delta_{st})\, \underline{\nu}\, \underline{u}_m^T\, d\tau \qquad (3.6.d)$$

$[k_{ii}]$, and $[c_{ii}]$ are the reference model dynamic components chosen by the designer, $\underline{\delta}_{st}$ is the static deflection values of flexible modes. Here, the reference model is chosen as a decoupled linear system of the form

$$\begin{bmatrix} \dot{\underline{\theta}}_m \\ \ddot{\underline{\theta}}_m \end{bmatrix} = \begin{bmatrix} \underline{0} & I \\ [-k_{ii}] & [-c_{ii}] \end{bmatrix} \begin{bmatrix} \underline{\theta}_m \\ \dot{\underline{\theta}}_m \end{bmatrix} + \begin{bmatrix} \underline{0} \\ I \end{bmatrix} \underline{u}_m \qquad (3.7)$$

The response of the reference model, $\underline{\theta}_m(t)$, to the commanded input, $\underline{u}_m(t)$, is the desired joint response. The reference model dynamics affects the control through equations (3.6.a, c, d). Using δ_{st} in the control algorithm does not require real-time feedback information about the flexible states. Therefore, the controller is still a joint variable feedback control algorithm. The use of $\underline{\delta}_{st}$ as opposed to $\underline{0}$ (zero) for the flexible modes is more accurate and improves the decoupled control of the flexible manipulator without imposing any significant implementation difficulty. The $\underline{\nu}$ is the filtered tracking error $\underline{e}$ (Fig. 2). p_{pi} and p_{ui} are arbitrary positive scalar adaptive controller design parameters effecting the convergence rate of the adaptive control system and the transient response of the closed loop system.

The specific dynamic characteristics of manipulators are utilized in the general context of hyperstability based design so that the resultant controller is particularly suitable in control of manipulators exploiting their specific dynamic characteristics as opposed to treating them as a *black box* dynamic system. Following that philosophy, the generalized inertia matrix plays a significant role in the adaptation algorithm (eqn. 3.6.c-d), and in the nominal control (eqn. 3.6.a-d). First, the feedback gains are naturally adapted in a manner to preserve the decoupled joint control. Secondly, arbitrary parameter selection that is generally required in Lyapunov and hyperstability based designs, is reduced to the selection of only *two scalar parameters* no matter how many joints the manipulator has, as opposed to the usual requirement for selection of two arbitrary positive definite

matrices [Hsia 87]. Notice that the gain adaptation is of integral type (eqn. 3.6.c-d), which is a commonly used adaptation type in model reference adaptive control.

IV. Results and Discussion

IV.1 Fine Motion Control Results and Discussion

Let w_{st}^* be the lowest structural frequency of the manipulator when both joints are clamped and extended (k_{11} and $k_{22} \rightarrow \infty$, c_{11} and $c_{22} = 0$, Fig. 3). Consider an equivalent rigid manipulator with the same inertial and geometric properties of the flexible manipulator. The rigid system with first joint clamped ($k_{11} \rightarrow \infty$) will be a second order mass-spring system with feedback gains ($k_{22}, c_{22} \neq 0$). Let w_{r1} be the undamped natural frequency of the rigid system for a set of feedback gains k_{22} and c_{22}.

In fine motion, the w_{r1}/w_{st}^* ratio determines the significance of flexibility and the dominant behavior of the closed loop system. In the rigid manipulator case, it is possible to achieve arbitrarily large closed loop bandwidth by increasing k_{22} and c_{22}, for $w_{r1} = \sqrt{k_{22}/(J_{02})_{eff}}$, and damping ratio $\xi_{r1} = c_{22}/(2.0 \times \sqrt{(J_{02})_{eff} \times k_{22}})$, where $(J_{02})_{eff}$ is the effective moment of inertia of link 2 and payload about joint 2 axis of rotation.

However, when the same controller is applied to the flexibile manipulator, the closed loop bandwidth, w_{bw} will definitely be smaller than w_{st}^*, for the fact that as $k_{22} \rightarrow \infty$, $| w_{bw} | \rightarrow w_{st}^*$ with very little damping ratio (Fig. 3). If the servo stiffness is low relative to the structural flexibility, that is $w_{r1}/w_{st}^* \ll 1/2$, the locus of closed loop eigenvalues is indistinguishable from those of rigid case as c_{22} increases. However, if the velocity feedback gain, c_{22}, is further increased to large values, the effective result is to stiffen the joint. One dominant eigenvalue meets with another on the negative real axis, and breaks away from the real axis converging to the w_{st}^* magnitude on the imaginary axis as c_{22} increases (Fig. 3, curve a, Fig. 4.a). In the rigid case, this phenomenon does not exist for any value of feedback gains. The root locus analysis of fine motion is

done as function of c_{22} for many other values of w_{r1}/w_{st}^*. The basic outcome of this analysis is illustrated in (Fig. 3 and 4, only dominant regions of root locus are shown in the figures). It is seen from (Fig. 4.b-c) that above certain values of w_{r1}/w_{st}^* ratio, the dominant eigenvalues are no longer able to reach the real axis. Physically that means, if joint position control is too stiff relative to the arm flexibility, it is not possible to provide well damped dominant modes no matter how large the velocity feedback gain is.

For a given manipulator and payload, w_{st}^* is determined by the geometric, inertial and structural flexibility properties of the manipulator. If a joint variable controller attempts closed loop bandwidth larger than $(1/2)w_{st}^*$, then the flexibility of the manipulator will be a significant factor during the fine motions. Otherwise, the structural flexibility may be ignored, and controller may be designed based on rigid manipulator assumptions (Fig. 3, curve a, Fig. 4.a). The best performance of a joint variable feedback controller is defined here as the highest possible closed loop bandwidth (that is the largest dominant eigenvalue magnitudes with sufficient damping ratios; i.e. 0.707 or more). As shown in figure 4.b, approximately $(2/3)\,w_{st}^*$ closed loop bandwidth can be achieved by appropriate choice of feedback gains. It is equally important, however, to note that the dominant eigenvalues are very sensitive to the variations in feedback gains in the best performance region (Fig. 4.b, locations 8,9,10, between each point the velocity feedback gain is incremented by a constant amount). In practice it may not be easy to realize that performance due to modeling errors.

The results concerning the effects of structural flexibility in closed loop performance agree very well with the previously reported results based on infinite dimensional frequency domain results [Book et. al. 75, Book and Majette 85].

IV.2 Gross Motion Control Results and Discussion

In order to see the effect of dynamic nonlinearities, the closed loop system is simulated for two classes of motions: first, slow motions where nonlinear forces are small (Fig. 5a-b, curves (a)), and secondly, fast motions where nonlinear forces are significantly larger or of same magnitude with the other dynamic forces (Fig. 5a-b, curves (b)).

Fig. 6 shows the response of the manipulator with adaptive controller to the desired slow motion. Two different adaptive control results are shown for slow and fast adaption, refering to small and large values of the adaption parameters p_{pi} and p_{ui}. The appropriate values for these parameters are found by trial and error. This motion has two properties: 1. dynamic nonlinearities are not significantly large (Fig. 5, curve (a)), 2. the bandwidth of the desired motion is about 1/4 of the lowest natural frequency of the arm. The bandwidth of the desired motion, w_{mi}, is defined as the bandwidth of the reference model which generates the desired motion in response to a step input command (Fig. 2).

Since the adaptive controller essentially tries to make the closed loop dynamic behavior match to that of the reference model, the function of w_{mi} in the nonlinear analysis content is similar to the function of the w_{r1} in the linear analysis. Clearly, figures 6.a-e show that flexibility of the arm is not significant in terms of joint tracking and setting time of flexible vibrations at the end of motion, which is in agreement with the linear analysis results. When the same system is simulated for motion (b) where $w_{mi}/w_{cc1} = 1/2$ and nonlinearities are significant (Fig. 5a-b, curves (b)), the response deteriorates. Persistent, lightly damped oscillations occur in joint and flexible mode variables (Fig. 7.a-e). The difference between the two simulations (Fig. 6 and 7) is the magnitude of nonlinear forces (Fig. 5, curve (a) and (b)). When the nonlinear forces are significant compared

to other dynamic forces, the performance is unacceptably poor. Therefore, the nonlinear effects during fast gross motions impose further restrictions on the performance of adaptive joint variable feedback controllers with integral gain adaptation.

The mechanism through which the nonlinear forces affects the joint controller performance can be desribed as follows with the help of the insights gained from the fine motion analysis. If the nonlinearities are significant, the adaptive controller automatically adjusts its feedback gains through integral adaptation (eqn. 4.6.c-d) to compensate for the tracking errors caused by the nonlinear forces. Increasing the controller gains through the adaptation rule eventually leads to very stiff joints. Linear analysis has shown that very high joint stiffness relative to the flexibility of a given arm results in very lightly damped dominant modes (Fig.3 curve (c), Fig.4.c). Thus, lightly damped dominant modes are generated by the adaptive controller, while it is trying to compensate for the joint tracking errors caused by the large nonlinear forces. It is important to note that this mechanism is valid for the class of adaptive controllers that use *integral type gain adaptation.*

V. Conclusion

In fine and slow gross motions where coriolis and centrifugal nonlinear forces are negligible, a given manipulator can be considered as rigid if the controller does not attempt to reach closed loop bandwidth more than 1/2 of the lowest structural frequency of the manipulator when all joints are locked (w_{st}^*). In fine motion, the best possible performance of joint variable feedback controllers may be up to 2/3 of w_{st} with damping ratios greater than 0.707. However, it is equally important to note that the sensitivity of the dominant eigenvalues to the variations of joint feedback gains are highest in the best performance region (Fig. 4.b, locations 8,9,10). Therefore, it may be difficult to achieve $(2/3)\,w_{st}^*$ closed loop bandwidth in a practical situation due to the modeling errors. The fine motion analysis results obtained here based on a finite dimensional time domain model agree very well with the previously reported results based on infinite dimensional frequency domain models [Book et al. 75, Book and Majette 85].

The performance of an adaptive controller with integral gain adaptation is also shown to be limited by the structural flexibility. While the adaptation algorithm increases the feedback gains to provide good tracking in joint variables against the large nonlinear forces (Fig. 5, curve b), the same increase in feedback gains will result in very stiff joint hence persistent structural vibrations. Through that mechanism, the manipulator flexibility presents a potential problem and limitations to the utilization of adaptive controllers with *integral type gain adaptation.*

Acknowledgments

This work was supported in part by the National Aeronautics and Space Administration under grant NAG-1-623, and the National Science Foundation under grant MEA-8303539, and the Campus Research Board of University of Illinois at Chicago.

Reference

Balas, M.J., "Active Control of Flexible Systems", *Journal of Optimization Theory and Applications*, Vol. 25, No. 3, July 1978, pp. 415-436.

Balestrino, A., De Maria, G., Sciavicco, L., "An Adaptive Model Following Control for Robotic Manipulators", *Journal of Dynamic Systems, Measurement and Control*, Sep. 1983, Vol. 105, pp. 143-151.

Barbieri, E., Özgüner, Ü., "Unconstrained and Constrained Mode Expansions for a Flexible Slewing Link", *Journal of Dynamic Systems, Measurement, and Control*, Vol. 110, Dec. 1988, pp. 416-421.

Book, W.J., "Recursive Lagrangian Dynamics of Flexible Manipulator Arms", *International Journal of Robotic Research*, Vol. 3, No. 3, Fall 1984, pp. 87-101.

Book, W.J., Maizza-Netto, O., Whitney, D.E., "Feedback Control of Two Beam, Two Joint Systems with Distributed Flexibility", *Journal of Dynamics Systems, Measurement, and Control*, 97G, Dec. 1975.

Book, W.J., Majette, M., "Controller Design for Flexible, Distributed Parameter Mechanical Arms Via Combined State Space and Frequency Domain Techniques", *Journal of Dynamic Systems, Measurement, and Control*, Vol. 105, Dec. 1985, pp. 245-254.

Cannon, R.J., Jr., Schmitz, E., "Initial Experiments on the End-Point Control of a Flexible One-Link Robot", *International Journal of Robotics Research*, Vol. 3, No. 3, Fall 1984, pp. 62-75.

Cetinkunt, S., "On Motion Planning and Control of Multi-Link Lightweight Robotic Manipulators", Ph.D. Thesis, The George W. Woodruff School of Mechanical Engineering, Georgia Institute of Technology, 1987.

Cetinkunt, S., Book, W.J., "Symbolic Modeling and Dynamic Simulation of Robotic Manipulators with Compliant Links and Joints", *Int. J. of Robotics and Computer-Integrated Manufacturing*, Vol. 5, No. 4, 1989, pp. 301-310.

Cetinkunt, S., Book, W.J., "Symbolic Modeling of Flexible Manipulators", *Proc. of 1987 IEEE International Conf. on Robotics and Automation*, March 31- April 3, 1987, Raleigh, NC., Vol. 3, pp. 2074-2080.

Cetinkunt, S., Yu, W.L., "Closed Loop Behavior of a Feedback Controlled Flexible Beam: A Comperative Study", *International Journal of Robotics Research*, submitted, February 1989.

Chalboub, N.G., Ulsoy, G., "Dynamic Simulation of a Leadscrew Driven Flexible Robot Arm and Controller", *ASME J. of Dynamic Systems, Measurment, and Control*, June 1986, Vol. 108, pp. 119-126.

Chang, C.W., Shabana, A.A., "Hybrid Control of Flexible Multi-Body Systems", *Computers and Structures* , Vol. 25, No. 6, 1987, pp. 831-844.

Craig, J.J., Hsu, P., Sastry,S.S., "Adaptive Control of Mechanical Manipulators", *IEEE Robotics and Automation Conference*, San Fransisco, CA, 1986, pp. 190-195.

Dubowsky, S., DesForges, D.E., "The Application of Model- Refernce Adaptive Control to Robotic Manipulators", *Journal of Dynamic Systems, Measurement, and Control*, Sept. 1979, Vol. 101, pp. 193-200.

Gevarter, W.B., "Basic Relations for Control of Flexible Vehicles", *AIAA Journal*, Vol. 8, No. 4, April 1970, pp. 666-672.

Hastings, G.G., Book, W.J., "Verification of a Linear Dynamic Model for Flexible Robotic Manipulators", *IEEE Control Systems Magazine*, IEEE Control Systems Society, April, 1987.

Horowitz, R., Tomizuka, M., "An Adaptive Control Scheme for Mechanical Manipulators - Compensation of Nonlinearity and Decoupling Control", *ASME J. of Dynamic Systems, Measurement and Control*, 1985.

Hsia, T.C., "Adaptive Control of Robot Manipulators - A Review", *IEEE Robotics and Automation Conference*, San Fransisco, CA, 1986, pp. 183-189.

Kotnic, P.T., Yurkovich, S., Özgüner, Ü., "Acceleration Feedback for Control of a Flexible Arm", *J. of Robotic Systems*, 5(3), pp. 181-196, 1988.

Landau, Y.D., *Adaptive Control*, Marcer Dekker, Inc. 1979.

Lim., K.L., Eslami, M., "Robust Adaptive Controller Design for Robot Manipulator Systems", *IEEE Trans. on Auto. Control*, Vol. AC-30, No. 12, Dec. 1985, pp. 1229-1233.

Low, K.H., Vidyasagar, M., "A Lagrangian Formulation of the Dynamic Model for Flexible Manipulator Systems", *J. of Dyn. Syst. Meas. and Control*, June 1988, Vol. 110, pp. 175-181.

Luh, J.Y.S., "Conventional Controller Design for Industrial Robots - A Tutorial", *IEEE Trans. on Systems, Man and Cybernetics*, Vol. SMC-12, No. 3 May/June 1983, pp. 298-316.

Luh, J.Y.S., Walker, M.W., Paul, R.P.C., "Resolved- Acceleration Control of Mechanical Manipulators", *IEEE Trans. on Auto. Control*, Vol. AC-25, 1980, pp. 468-474.

Matsuno, F., Fukushima, S., Ohsawa, Y., Kiyohara, M., Sakawa, Y., "Feedback Control of a Flexible Manipulator with Parallel Drive Mechanism", *Int. J. of Robotic Research*, Vol. 6, No. 4, Winter 1987, pp. 76-84.

Meldrum, D.R., Balas, M.J., "Direct Adaptive Control of a Remote Manipulator Arm", *In Robotics, Manufac. Auto.*, eds. Donath Max and Ming Leu, ASME Winter Annual Meeting 1985, pp. 115-119.

Naganathan, G., Soni, A.H., " Coupling Effects of Kinematics and Flexibility in Manipulators", *The International Journal of Robotics Research*, Vol. 6, No. 1, Spring 1987, pp. 75-84.

Oakley, C.M., Cannon, R.H. Jr., "Initial Experiments on the Control of a Two-link Manipulator with a Very Flexible Forearm", *1988 American Control Conference*, Atlanta, GA, pp. 996-1002.

Paul, R.P., *Robot Manipulators: Mathematics, Programming, and Control*, The MIT Press, 1983.

Piedboeuf, J.C., Hurteau, R., "Modeling and Identification of Parameters of a Flexible One-Link Arm Using Visual Feedback", *Presented at the 1987 IEEE Int. Conf. on Robotics and Automation*, March 30-April 3, 1987, Raleigh, NC.

Seraji, H., "A New Approach to Adaptive Control of Manipulators" *Journal of Dynamic Systems, Measurement, and Control*, Sept. 1987, Vol. 109, pp. 193-202.

Shabana, A.A., Wehage, R.A., "A coordinate Reduction Technique for Dynamic Analysis of Spatial Substructures with Large Angular Rotations", *J. Struct. Mech.*, 1983, pp. 401-431.

Shahinpoor, M., Meghdari, A., "Combined flexural-joint stiffness matrix and elastic deformation of a servo-controlled two-link robot manipulator", *Robotica*, Vol. 4, 1986, pp. 237-242.

Shung, I.Y., Vidyasagar, M., "Control of a Flexible Robot Arm with Bounded Input: Optimum Step responses", *1987 IEEE Int. Conf. on Robotics and Automation*, Raleigh, NC. , pp. 916-922.

Siciliano, B., Yuan, B., Book, W.J., "Model Reference Adaptive Control of a One Link Flexible Arm", *25th IEEE Conference on Decision and Control*, Athens, Greece, December 10-12, 1986.

Spong, M.W., "Modeling and Control of Elastic Joint Robots", *Trans. of ASME, J. of Dyn. Sys. Mea. and Control*, Vol. 109, Dec. 1987, pp. 310-319.

Sunada, W., Dubowsky, S., "The Application of Finite Element Methods to the Dynamic Analysis of Flexible Linkage Systems", *Journal of Mechanical Design*, Vol. 103, 1983, pp. 643-651.

Sunada, W., Dubowsky, S., "On the Dynamic Analysis and Behavior of Industrial Robotic Manipulators with Elastic Members", *Transactions of ASME, J. Mech.,Trans., Automation and Design*, Vol 105, 1983, pp. 42-51.

Usoro, P.B., Nadira, R., Mahil, S.S., "A Finite Element/Lagrangian Approach to Modeling Lightweight Flexible

Manipulators", *J. Dyn. Syst. Meas. and Control*, Sept. 1986, Vol. 108, pp. 198-205.

Wang, D., Vidyasagar, M., "Control of a Flexible Beam fro Optimum Step Response", *1987 IEEE Int. Conf. on Robotics and Automation*, Raleigh, NC., pp. 1567-1572.

Whitney, D.E., "The Mathematics of Coordinated Control of Prosthetic Arms and Manipulators", *Journal of Dynamic System, Meas. and Control*, Dec. 1972, pp. 188-194.

Appendix

A.1 AMFC-Hyperstability Based Design

The basic idea of AMFC comes from the linear perfect model following control (LPMFC) problem of [Erzberger 69]. AMFC attempts to asymptotically realize the same objective of LPMFC for time varing systems.

Let the reference model be

$$\dot{\underline{x}}_m = A_m \underline{x}_m + B_m \underline{u}_m \tag{A.1}$$

and the plant dynamics be in time varing (quasi-linear) form

$$\dot{\underline{x}}_p = A_p(\underline{x}_p, t)\,\underline{x}_p + B_p(\underline{x}_p, t)\,\underline{u}_p \tag{A.2}$$

with the control algorithm of the form,

$$\underline{u}_p = -K_p \underline{x}_p + K_u \underline{u}_m + K_m \underline{x}_m \tag{A.3}$$

Clearly, as the plant dynamics ($A_p(\underline{x}_p, t)$, $B_p(\underline{x}_p, t)$) varies, the feedback gains must also vary in order to match the dynamics of the plant to that of the reference model.

There are two basic assumptions associated with the current AMFC designs [Landau 1979]:

1. There exist K_p, K_u, K_m for every ($A_p(\underline{x}_p, t)$, $B_p(\underline{x}_p, t)$) and the given (A_m, B_m) so that at any instant LPMFC conditions of Erzberger are satisfied.

2. Variations of $A_p(\underline{x}_p, t)$, $B_p(\underline{x}_p, t)$ are slower than the speed of adaptation.

Assumption # 1 is an expected existence condition. AMFC attempts to converge to the ideally correct values of feedback gains through adaptation as the plant dynamics vary. Existence of such limit values is the first requirement for the convergence, let alone whether the adaptation algorithm will converge or not.

Assumption # 2 is commonly made in most AMFC design methods. During adap-

tation intervals, it is assumed that time invariant approximations of plant model is accurate enough. Therefore, robot motions must be slow compared to the adaptation speed of adaptive controller. Let us look at the origin of this assumption by going through the derivation steps of hyperstability based AMFC design.

Letting $K_m = 0$, without loss of generality [Landau 79], the error dynamics is described by

$$\begin{aligned}\dot{\underline{e}} = A_m \underline{e} + [A_m - A_p(\underline{x}_p, t) + B_p(\underline{x}_p, t) K_p] \underline{x}_p \\ + [B_m - B_p(\underline{x}_p, t) K_u] \underline{u}_m\end{aligned} \tag{A.4}$$

For $\underline{e}(t) \rightarrow 0$ as $t \rightarrow \infty$ for all $\underline{x}_p$, $\underline{u}_m$ that belong to a piecewise continuous, bounded class of functions, the coefficients of $\underline{x}_p$, $\underline{u}_m$ must be zero. By assumption # 1, there exist K_p^*, K_u^* such that

$$A_p(\underline{x}_p, t) - A_m = B_p(\underline{x}_p, t) K_p^* \tag{A.5.a}$$

$$B_m = B_p(\underline{x}_p, t) K_u^* \tag{A.5.b}$$

The goal is to develop adaptive control algorithms for K_p, K_u such that K_p, K_u converge to K_p^*, K_u^*. Convergence must be fast enough for the assumption # 2 to hold.

Let the feedback gains be

$$K_p = K_{pn} - \Delta K_p(\underline{e}, t) \tag{A.6.a}$$

$$K_u = K_{un} + \Delta K_u(\underline{e}, t) \tag{A.6.b}$$

where K_{pn}, K_{un} are nominal, and ΔK_p, ΔK_u are adaptive feedback gain matrices. Following the standard steps of hyperstability based design [Landau 79], it can be shown that the equivalent hyperstable closed loop system representation of the error dynamics can be expressed as (Fig. A.1)

$$\dot{\underline{e}} = A_m \underline{e} + B_p(\underline{x}_p, t) \underline{z}_1 \tag{A.7.a}$$

$$\underline{v} = D\underline{e} \tag{A.7.b}$$

$$\underline{z} = -\underline{z}_1 = [K_p^* - K_{pn} + \Delta K_p]\,\underline{x}_p + [K_{un} + \Delta K_u - K_u^*]\,\underline{u}_m \qquad (A.7.c)$$

where D is determined by using Kalman-Yakubovich-Popov lemma. In order to guarentee the hyperstability of the closed loop system (CLS), the ΔK_p, ΔK_u selection as follows is sufficient (not necessary):

$$\Delta K_p(\underline{e}, t) = \int_0^t \phi_1(\underline{v}, t, \tau)\, d\tau + \phi_2(\underline{v}, t) + \Delta K_p(0) \qquad (A.8.a)$$

$$\Delta K_u(\underline{e}, t) = \int_0^t \psi_1(\underline{v}, t, \tau)\, d\tau + \psi_2(\underline{v}, t) + \Delta K_u(0) \qquad (A.8.b)$$

where the most general conditions on ϕ_1, ϕ_2, ψ_1, ψ_2 are discussed in [Landau 79], and more specific forms are discussed in section A.2. $\Delta K_p(0)$, $\Delta K_u(0)$ can be chosen as zeros without loss of generality since any nonzero values of them can be included in K_{pn}, K_{un} nominal gains. Substituting (A.8) into (A.7.c)

$$\begin{aligned} \underline{z} = -\underline{z}_1 = &[\int_0^t \phi_1(\underline{v}, t, \tau)\, d\tau + \phi_2(\underline{v}, t) + \Delta K_p^0]\,\underline{x}_p \\ &+ [\int_0^t \psi_1(\underline{v}, t, \tau)\, d\tau + \psi_2(\underline{v}, t) + \Delta K_u^0]\,\underline{u}_m \end{aligned} \qquad (A.9)$$

where

$$\Delta K_p^0 = K_p^* - K_{pn} \qquad (A.10.a)$$

$$\Delta K_u^0 = -K_u^* + K_{un} \qquad (A.10.b)$$

The hyperstability of the feedback block (hence the CLS using Kalman-Yakubovich-Popov lemma) is proven for ΔK_p^0, ΔK_u^0 constant case. That is where the assumption # 2 comes from.

ΔK_p^0, ΔK_u^0 constant requirement implies that ($K_p^* - K_{pn}$), and ($K_u^* - K_{un}$) are constants. If K_{pn}, K_{un} are chosen to be constant nominal gains, then K_p^*, K_u^* must be constant at least during the adaptation intervals. From eqn. (A.5), this implies that ($A_p(\underline{x}_p, t)$, $B_p(\underline{x}_p, t)$) must be constant during the adaptation process. Equivalently,

($A_p(\underline{x}_p, t)$, $B_p(\underline{x}_p, t)$) must vary slower than the speed of adaptation (which is the assumption # 2).

Notice that the condition imposed by the hyperstability is not that K_p^*, K_u^* should be constant, but ($K_p^* - K_{pn}$), and ($K_u^* - K_{un}$). If nominal feedback gains are not constant, but somewhat better in keeping the plant track the reference model, then assumption # 2 would not have been so restrictive. Choosing variable K_{pn}, K_{un} nominal gains based on the decoupled joint control algorithm [Whitney 72] where generalized inertia matrix plays a significant role, assumption #2 may be *relaxed* as follows:

The previous assumption # 2 was:

> The difference between the reference model and the closed loop plant dynamics under *constant linear nominal control* should vary slower than the speed of adaptation.

The new assumption # 2 is:

> The difference between the reference model and the closed loop plant dynamics under *variable nonlinear nominal control* should vary slower than the speed of adaptation.

A.2 Generalized Inertia Matrix Based AMFC: Application to Flexible manipulators

Consider the flexible manipulator model

$$\begin{bmatrix} m_r(\theta,\delta) & m_{rf}(\theta,\delta) \\ m_{rf}^T(\theta,\delta) & m_f(\theta,\delta) \end{bmatrix} \begin{bmatrix} \ddot{\underline{\theta}} \\ \ddot{\underline{\delta}} \end{bmatrix} + \begin{bmatrix} \underline{f}_r \\ \underline{f}_f \end{bmatrix} + \begin{bmatrix} \underline{0} \\ [K]\underline{\delta} \end{bmatrix} + \begin{bmatrix} \underline{g}_r \\ \underline{g}_f \end{bmatrix} = \begin{bmatrix} \underline{u} \\ \underline{0} \end{bmatrix} \tag{A.11}$$

$$m_r(\theta,\delta)\ddot{\underline{\theta}} = \underline{u} - [m_{rf}\ddot{\underline{\delta}} + \underline{f}_r + \underline{g}_r] \tag{A.12}$$

$$\underline{u} = \hat{\underline{g}}_r + \underline{u}_p \tag{A.13}$$

$$m_r(\theta,\delta)\ddot{\underline{\theta}} = \underline{u}_p + [m_{rf}\ddot{\underline{\delta}} + \underline{f}_r + (\underline{g}_r - \hat{\underline{g}}_r)] \tag{A.14}$$

where $\hat{g}_r$ is gravity compensation (feedforward). During the gross motion, nonlinear terms and coupling from the flexible modes to the joint variable dynamics are treated as a disturbance and to be taken care of by the closed loop system robustness.

Under the influence of a gravitational field, a flexible arm will deflect. Designing a control system which uses the static deflections as the nominal value for flexible states as opposed to zero would be more accurate.

Let the desired reference model be

$$\begin{bmatrix} \dot{\underline{\theta}}_m \\ \underline{\theta}_m \end{bmatrix} = \begin{bmatrix} 0 & I \\ -\Lambda_o & -\Lambda_1 \end{bmatrix} \begin{bmatrix} \underline{\theta}_m \\ \dot{\underline{\theta}}_m \end{bmatrix} + \begin{bmatrix} 0 \\ I \end{bmatrix} \underline{u}_m \tag{A.15}$$

and the control law

$$\begin{aligned} \underline{u}_p &= -K_p \underline{x}_p + K_u \underline{u}_m + \overbrace{K_m \underline{x}_m}^{0} \\ &= \underbrace{-K_{pn} \underline{x}_p + K_{un} \underline{u}_m}_{\textit{Nominal control}} + \underbrace{\Delta K_p(\underline{e}, t)\, \underline{x}_p + \Delta K_u(\underline{e}, t)\, \underline{u}_m}_{\textit{Adaptation algorithm control action}} \end{aligned} \tag{A.16}$$

The nominal control can be chosen in the form (as used by the computed torque method), [Luh et. al. 80, Cetinkunt 87].

$$\begin{aligned} \underline{u}_{pn} = {} & \hat{m}_r(\underline{\theta}, \underline{\delta}_{st})\, \underline{u}_m + \hat{m}_r(\underline{\theta}, \underline{\delta}_{st}) \left[[c_{ii} - \Lambda_1] \dot{\underline{\theta}}_m + [k_{ii} - \Lambda_0] \underline{\theta}_m + [k_{ii}] \underline{\theta}_0 \right] \\ & - \hat{m}_r(\theta, \delta_{st}) \left[[c_{ii}] \dot{\underline{\theta}} + [k_{ii}] \underline{\theta} \right] \end{aligned} \tag{A.17}$$

The nominal gains for the adaptive model following control algorithm based on the generalized inertia matrix is given by

$$K_{un} = \hat{m}_r(\underline{\theta}, \underline{\delta}_{st}) \tag{A.18.a}$$

$$K_{pn} = \hat{m}_r(\underline{\theta}, \underline{\delta}_{st}) \left[[k_{ii}], [c_{ii}] \right] \tag{A.18.b}$$

$$K_{mn} = \hat{m}_r(\underline{\theta}, \underline{\delta}_{st}) \left[[k_{ii}] - \Lambda_0], [c_{ii}] - \Lambda_1] \right] \tag{A.18.c}$$

If error dynamics eigenvalues are equal to those of the reference model, then $k_{ii} = \Lambda_0$, $c_{ii} = \Lambda_1 \Rightarrow K_{mn} = 0$. The $\hat{m}_r(\theta, \delta_{st})$ term in the control algorithm is the key for

decoupled control of joints. The adaptation algorithm should be designed such that when added to the nominal control vector $\underline{u}_{pn}$, the decoupled nature of the control is preserved. The adaptive part of the control is:

$$\Delta K_p = \underbrace{\int_0^t F_{p1}\,\underline{v}[G_{p1}\underline{x}_p]^T d\tau}_{Integral\ adaptation;\Delta K_{pi}} + \underbrace{F_{p2}\,\underline{v}[G_{p2}\underline{x}_p]^T}_{Proportional\ Adaptation;\Delta K_{pp}} \qquad (A.19.a)$$

$$\Delta K_u = \underbrace{\int_0^t F_{u1}\,\underline{v}[G_{u1}\underline{u}_m]^T d\tau}_{Integral\ adaptation;\Delta K_{ui}} + \underbrace{F_{u2}\,\underline{v}[G_{u2}\underline{u}_m]^T}_{Proportional\ Adaptation;\Delta K_{up}} \qquad (A.19.b)$$

Any positive definite matrix of appropriate dimension for F_{p1}, F_{p2}, G_{p1}, G_{p2}, F_{u1}, F_{u2}, G_{u1}, G_{u2} would be sufficient (but is not necessary) to guarantee the global asymptotic stability of the control system with an appropriate output filter. For an n-degree of freedom system with m number of inputs; F_{p1}, F_{p2}, F_{u1}, F_{u2}, G_{u1}, $G_{u2} \in R^{m\times m}$, and G_{p1}, $G_{p2} \in R^{n\times n}$. There are too many design parameters which can be chosen arbitrarily from a large admissible class. Neither the hyperstability based design nor Lyapunov methods give any guidelines for the selection of the elements of these matrices. As the system dimension increases, finding appropriate adaptation algorithm parameters becomes a more serious design problem.

The proposed AMFC design method solves that problem to a great extent. Since decoupled control calls for the use of the generalized inertia matrix, one should utilize this fact in the adaptation algorithm to direct the adaptation algorithm in the right direction. The following adaptation algorithm, which uses the generalized inertia matrix, will guarantee the global asymptotic stability of the closed loop system.

$$\begin{aligned}\Delta K_p &= \Delta K_{pi} + \Delta K_{pp} \\ &= \int_o^t p_{pi}\,\hat{m}_r(\underline{\theta}_o, \underline{\delta}_{st})\,\underline{v}\,\underline{x}_p^T\,d\tau + p_{pp}\hat{m}_r(\underline{\theta}_o, \underline{\delta}_{st})\,\underline{v}\,\underline{x}_p^T\end{aligned} \qquad (A.20.a)$$

$$\Delta K_u = \Delta K_{ui} + \Delta K_{up}$$
$$= \int_o^t p_{ui}\, \hat{m}_r(\underline{\theta}_o, \underline{\delta}_{st})\, \underline{v}\, \underline{u}_m^T\, d\tau + p_{up} \hat{m}_r(\underline{\theta}_o, \underline{\delta}_{st})\, \underline{v}\, \underline{u}_m^T \qquad (A.20.b)$$

The generalized inertia matrix based AMFC algorithm described by (A.16), (A.18) and (A.20) has the following advantages over previous algorithms:

1. The use of the generalized inertia matrix immediately solves the magnitude selection problem of the adaptation algorithm, for it is naturally compatible with the problem in the sense that it preserves the decoupled joint control.

2. The number of design parameters for integral adaptation is only 2, for integral plus proportional adaptation is 4, no matter how many degrees of freedom the system has. Thus the design problem of finding the good adaptation parameters becomes much simpler.

3. Utilizing the generalized inertia matrix as an integral part of adaptation improves the decoupled response of joint variables.

4 The use of variable nominal gains results in less restrictive conditions on the applications of AMFC to nonlinear systems.

List of Figures

Fig.1 - Two link flexible manipulator kinematic description.

Fig.2 - Generalized inertia matrix based AMFC.

Fig.3 - Illustration of performance limitations of joint varible feedback controller due to arm structural flexibility.

Fig.4 - Locus of closed loop eigenvalues as function of joint 2 velocity position and velocity feedback gains.

Fig.5 - Relative importance of nonlinear (coriolis and cenrifugal) forces and gravitational forces along different speed of motions.

Fig.6 - Joint and flexible mode responses along the motion (a) of figure 5, under the AMFC controller.

Fig.7 - Joint and flexible mode responses along the motion (b) of figure 5, under the AMFC controller.

Fig. A.1 - The problem of hyperstability.

List of Tables

Table 1: Manipulator dynamic model parameters used in the analysis.

Table 1

Manipulator model parameters	Value
Geometric properties of uniform, slender links	
(link 1 and 2 are identical)	
Length of link i (l_i)	2.0 m.
Cross-section area of link i (A_i)	7.224x10^{-4} m^2
Cross-section area moment of inertia about z-axis (I_{zi})	7.6190x10^{-9} m^4
Link material properties (Aluminum)	
Mass density (ρ_i)	2768.8 kg/m^3
Young's modulus of elasticity (E_i)	7.0x10^{+10} Nt/m^2
Resultant link inertial and structural properties	
Mass per unit length ($\rho_i A_i$)	2.0 kg/m
Mass of link i	4.0 kg
Flexural rigidity of link i ($E_i I_{zi}$)	533.33 and 5333.33 $Nt.m^2$
Lowest natural frequency of the arm (w_{cc1})	3.59 and 11.35 rad/sec
(both joint are locked, and $\theta_2 = 0$)	
Joint inertial parameters	
Joint 1 and 2 masses (m_{j1}, m_{j2})	0.0
Joint 1 and 2 mass moment of inertia about the joint center of mass (J_{j1}, J_{j2})	0.0
Payload inertial properties	
Mass (m_p)	0.0 to 2.0 kg.
Mass moment of inertia about the center of mass (J_p)	0.0

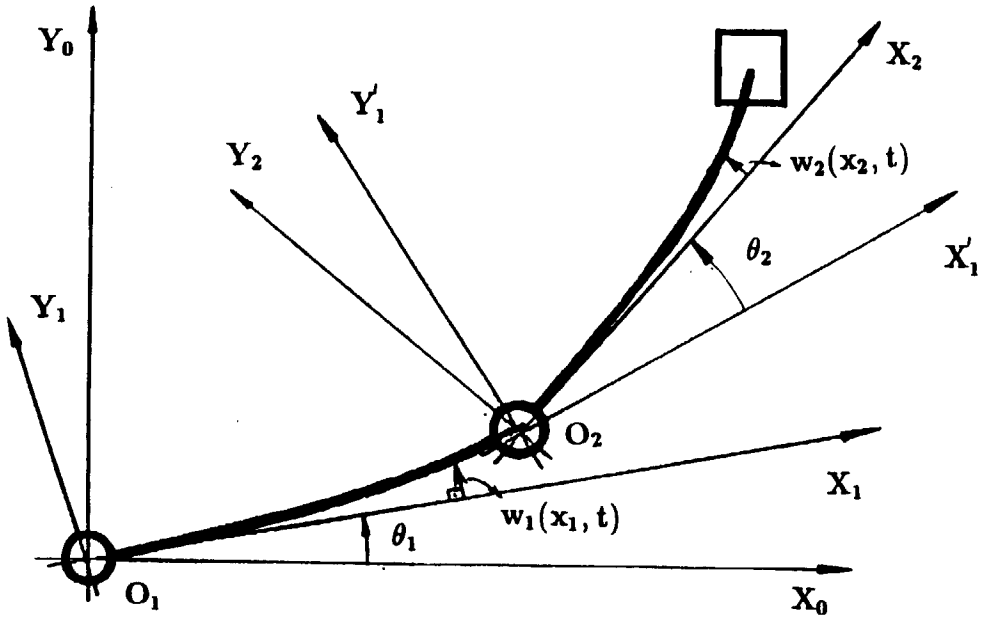

Fig. 1

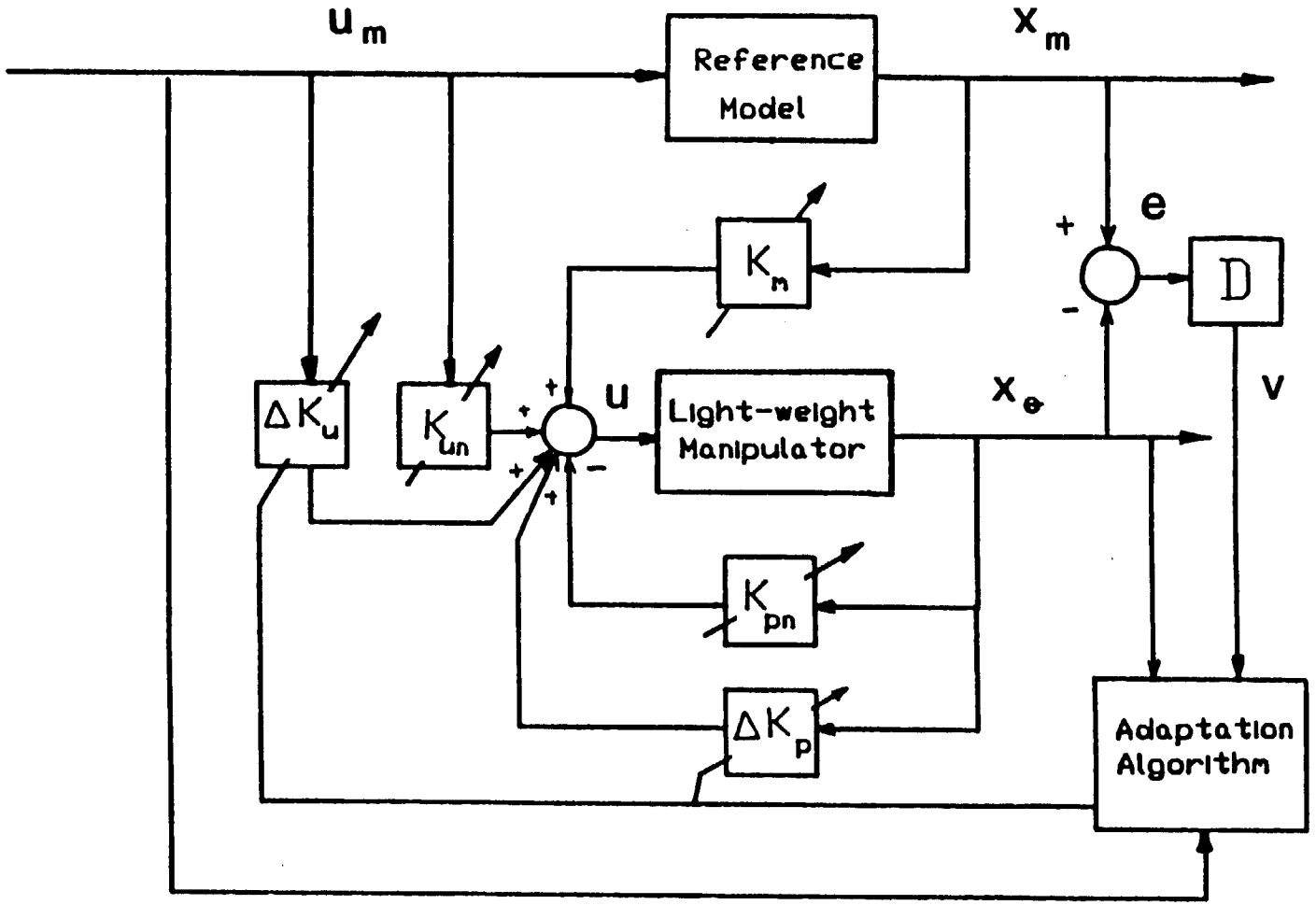
u_m
Reference Model
x_m
K_m
e
+
-
D
v
ΔK_u
K_{un}
+
+
+
-
u
Light-weight Manipulator
x_e
K_{pn}
ΔK_p
Adaptation Algorithm

Fig. 2

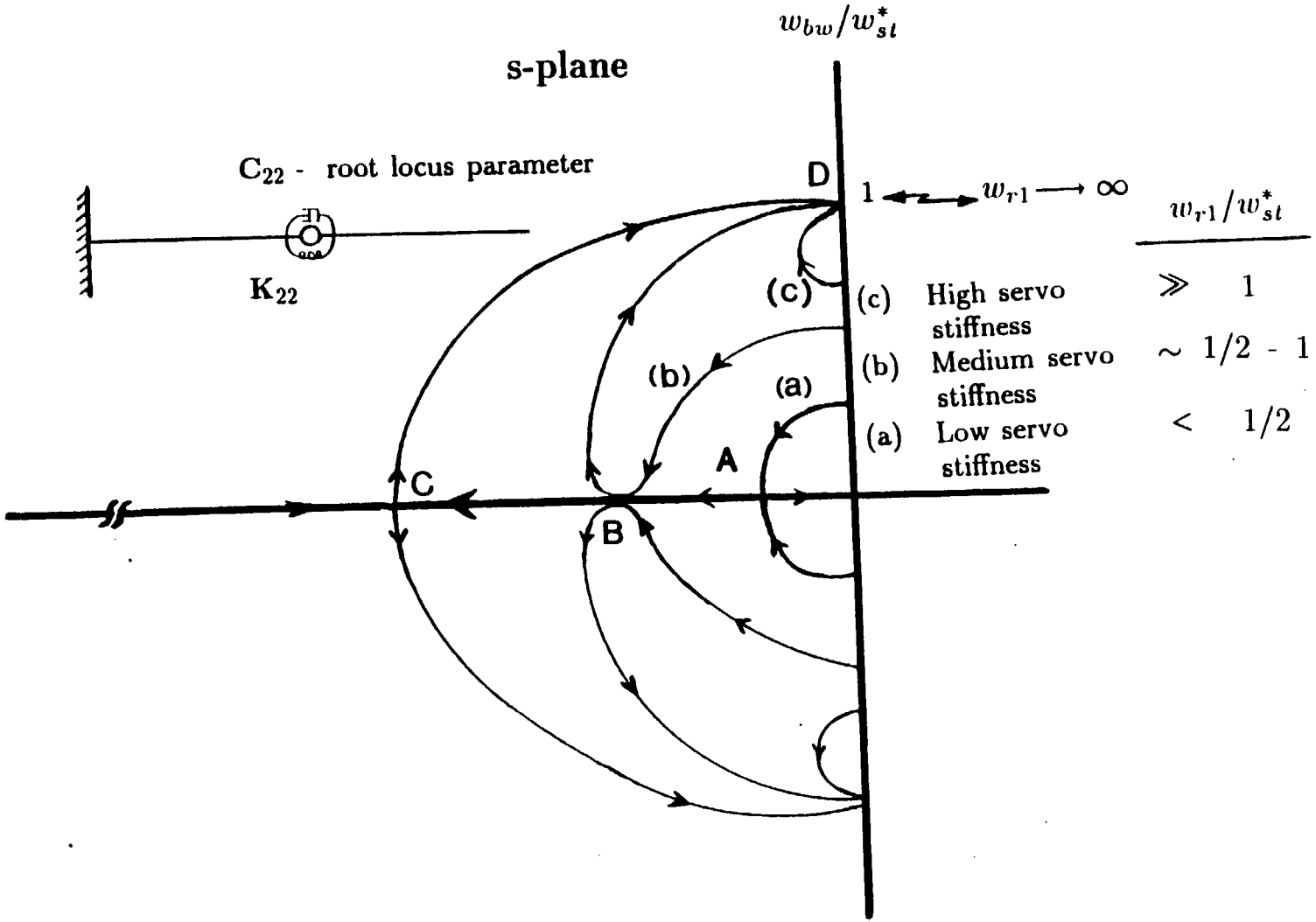
w_{bw}/w^*_{st}
s-plane
C_{22} - root locus parameter
K_{22}
D
1 ⟷ $w_{r1} \longrightarrow \infty$
(c)
(b)
(a)
A
B
C
(c) High servo stiffness
(b) Medium servo stiffness
(a) Low servo stiffness
w_{r1}/w^*_{st}
$\gg$ 1
$\sim$ 1/2 - 1
< 1/2

Fig. 3

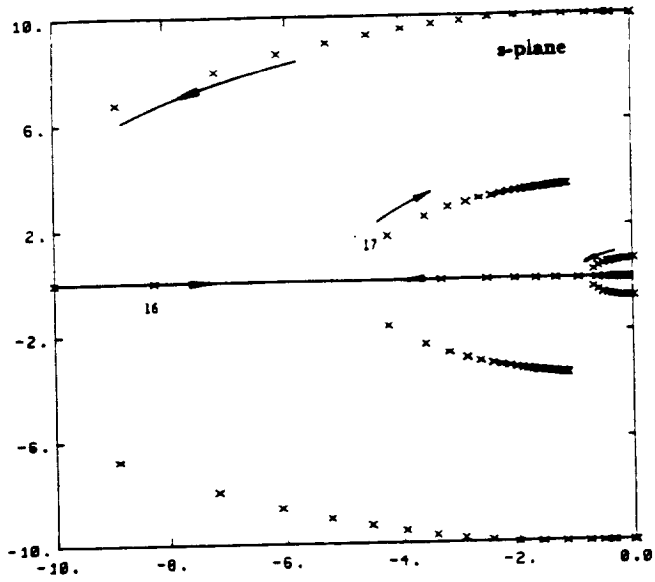

a) Low servo stiffness case.

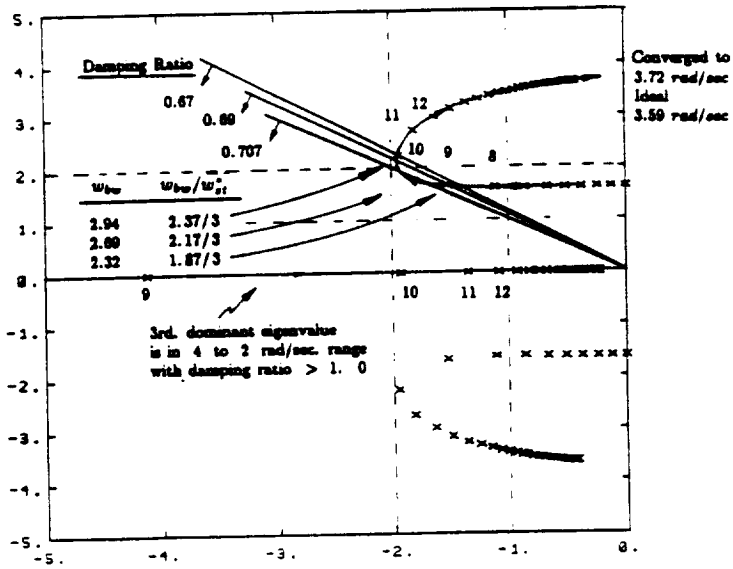

b) Meduim servo stiffness case.

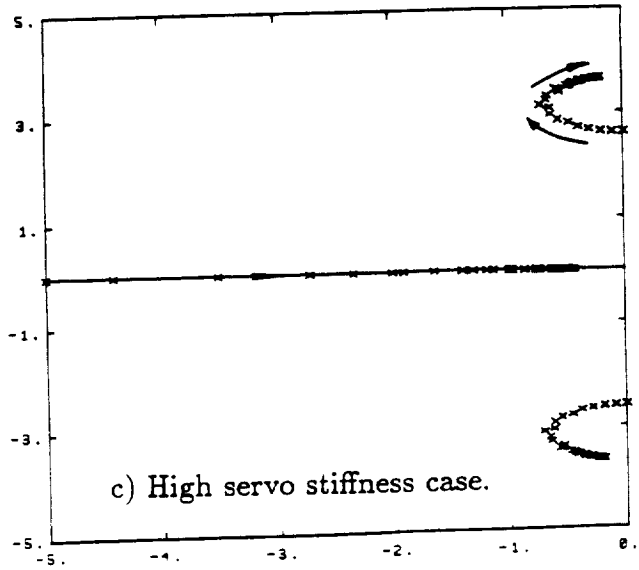

c) High servo stiffness case.

ORIGINAL PAGE IS
OF POOR QUALITY

Fig. 4

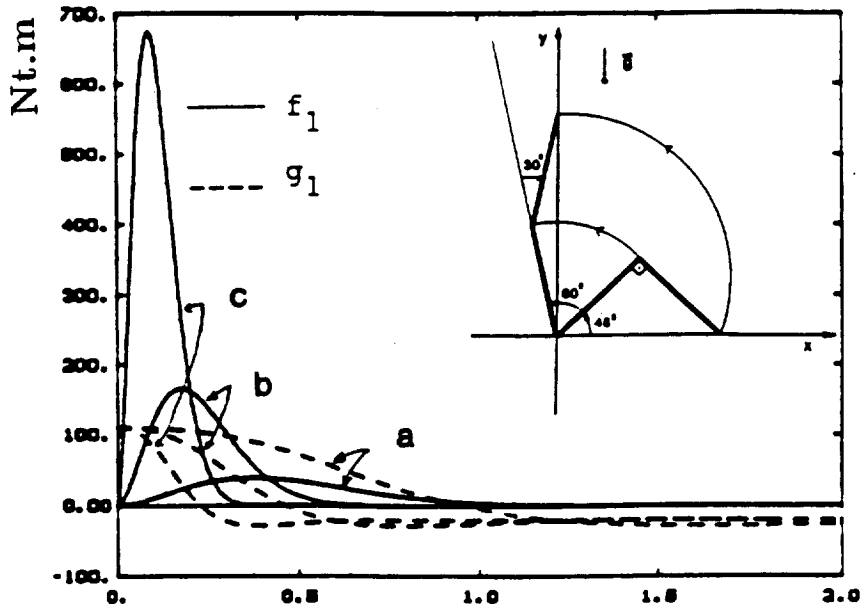

(a) time(sec.)

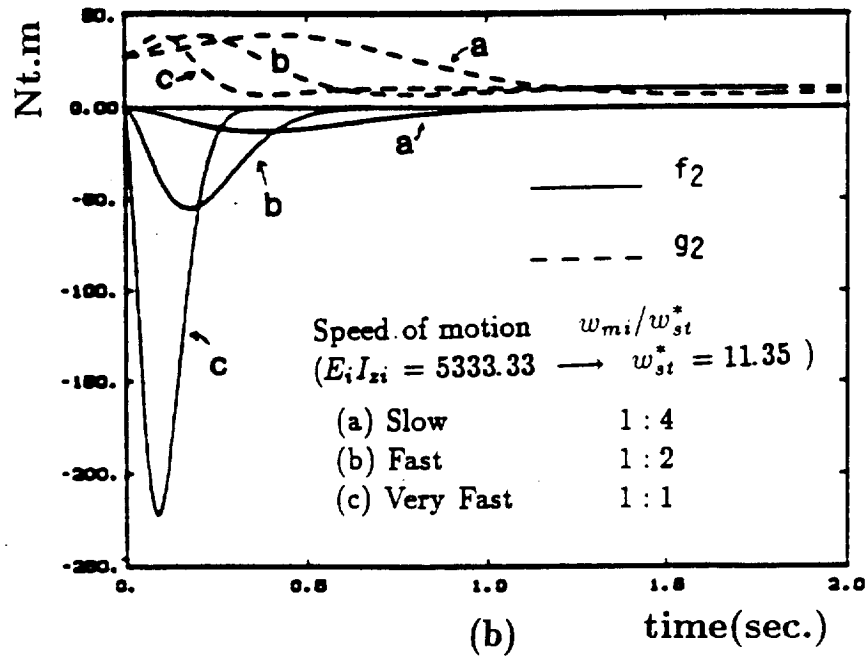

(b) time(sec.)

Fig. 5

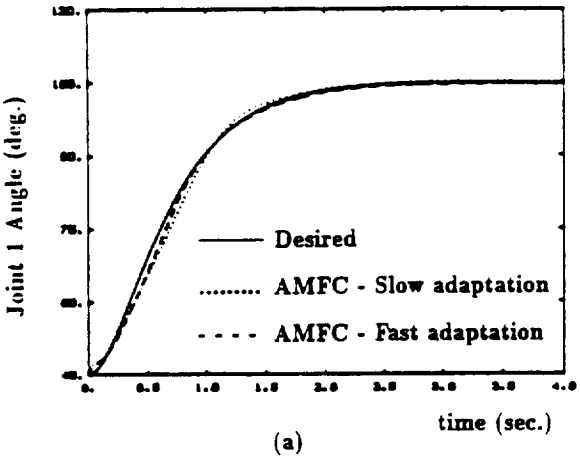
Joint 1 Angle (deg.)
Desired
AMFC - Slow adaptation
AMFC - Fast adaptation
time (sec.)

(a)

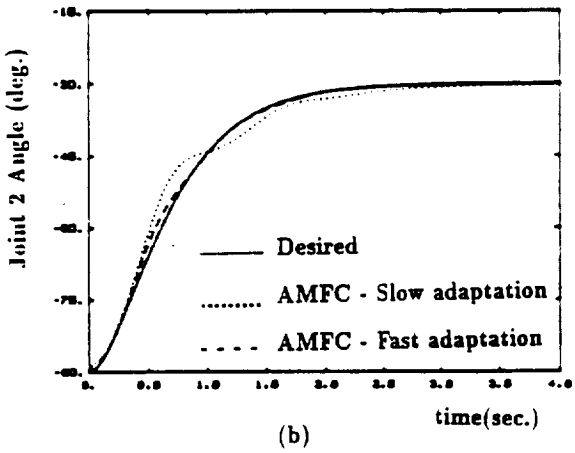
Joint 2 Angle (deg.)
Desired
AMFC - Slow adaptation
AMFC - Fast adaptation
time(sec.)

(b)

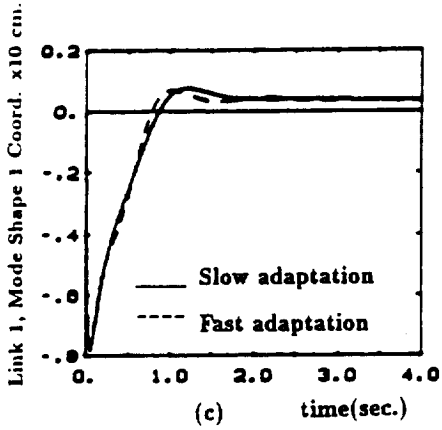
Link 1, Mode Shape 1 Coord. x10 cm.
0.2
0.
-.2
-.4
-.6
-.8
Slow adaptation
Fast adaptation
0.
1.0
2.0
3.0
4.0
time(sec.)

(c)

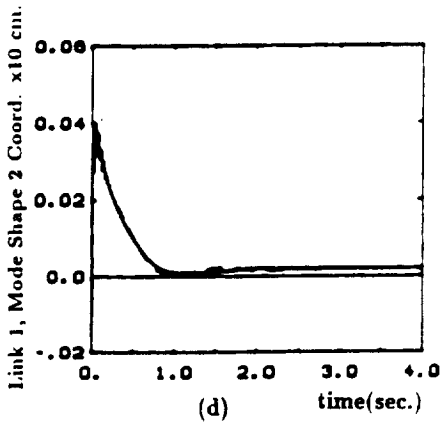
Link 1, Mode Shape 2 Coord. x10 cm.
0.06
0.04
0.02
0.0
-.02
0.
1.0
2.0
3.0
4.0
time(sec.)

(d)

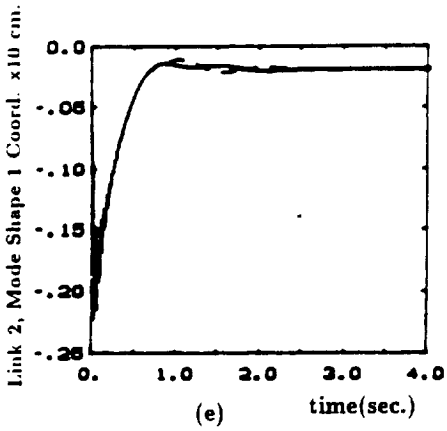
Link 2, Mode Shape 1 Coord. x10 cm.
0.0
-.05
-.10
-.15
-.20
-.25
0.
1.0
2.0
3.0
4.0
time(sec.)

(e)

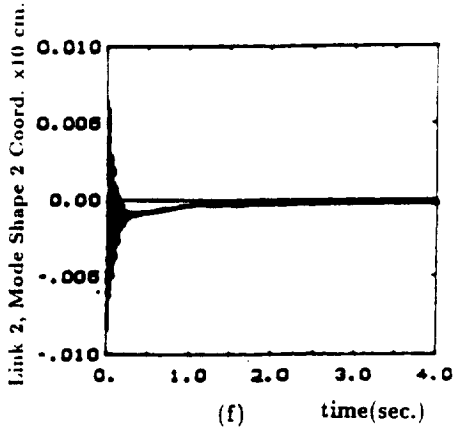
Link 2, Mode Shape 2 Coord. x10 cm.
0.010
0.005
0.00
-.005
-.010
0.
1.0
2.0
3.0
4.0
time(sec.)

(f)

Fig. 6

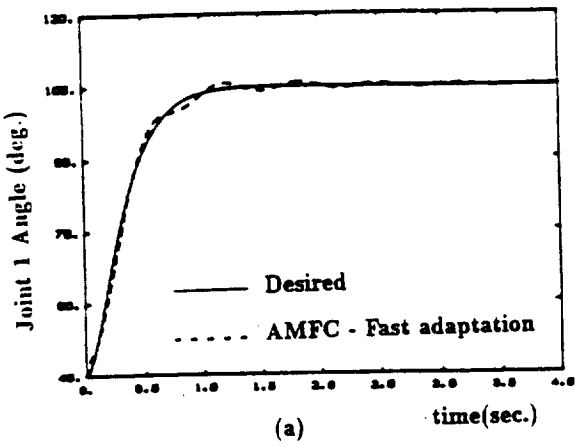
Joint 1 Angle (deg.)
Desired
AMFC - Fast adaptation
time(sec.)

(a)

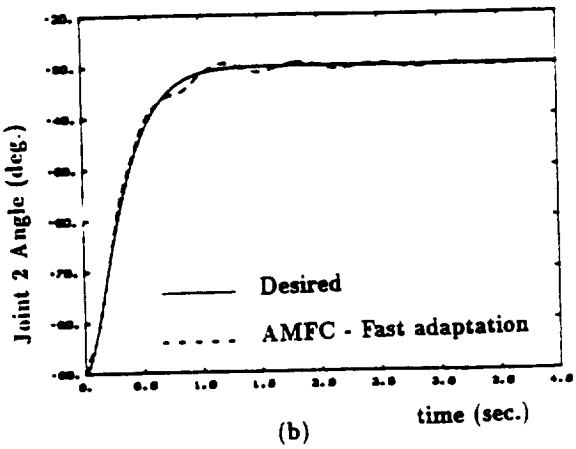
Joint 2 Angle (deg.)
Desired
AMFC - Fast adaptation
time (sec.)

(b)

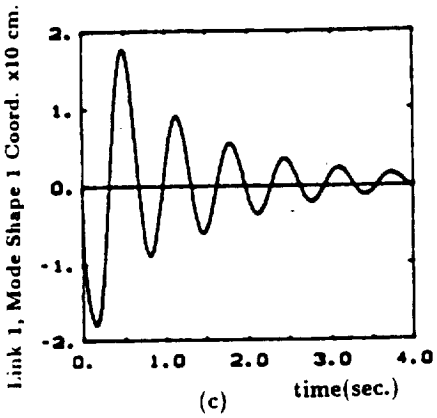
Link 1, Mode Shape 1 Coord. x10 cm.
2.
1.
0.
-1.
-2.
0.
1.0
2.0
3.0
4.0
time(sec.)

(c)

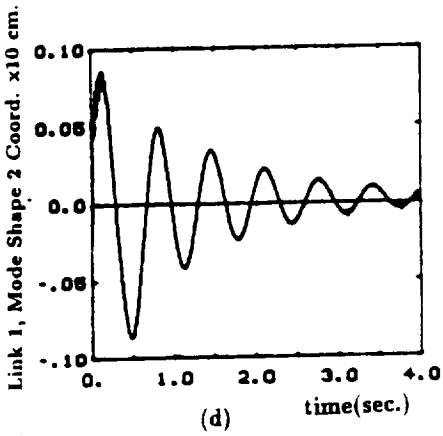
Link 1, Mode Shape 2 Coord. x10 cm.
0.10
0.05
0.0
-.05
-.10
0.
1.0
2.0
3.0
4.0
time(sec.)

(d)

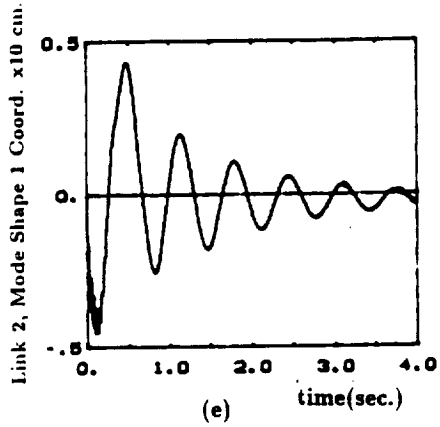
Link 2, Mode Shape 1 Coord. x10 cm.
0.5
0.
-.5
0.
1.0
2.0
3.0
4.0
time(sec.)

(e)

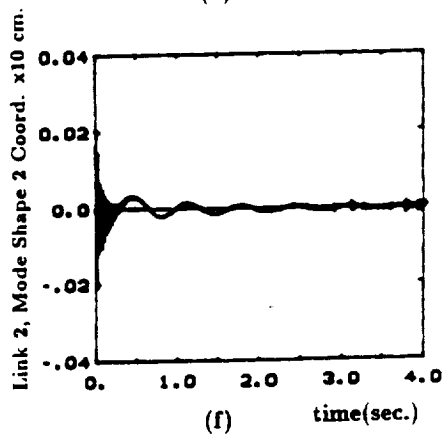
Link 2, Mode Shape 2 Coord. x10 cm.
0.04
0.02
0.0
-.02
-.04
0.
1.0
2.0
3.0
4.0
time(sec.)

(f)

Fig. 7

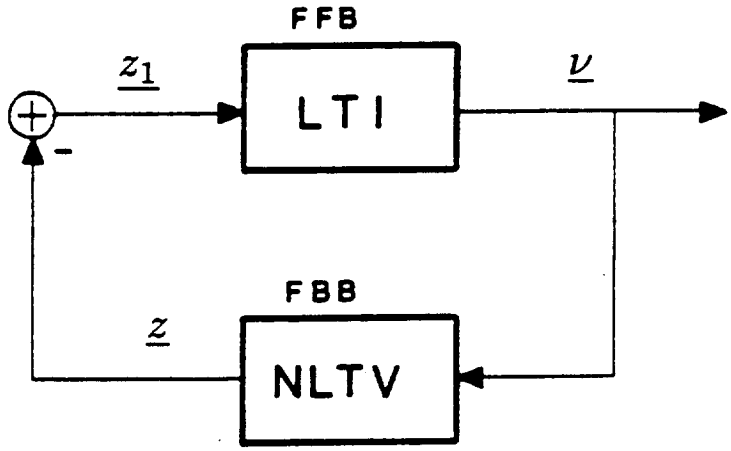

$$\{ \mathbf{P} \} = \{ \int_{t_0}^{t_1} \underline{\nu}^T \, \underline{z} \; dt \geq -\gamma_0^2 \quad , \forall \; t_1 \geq t_0 \}$$

Fig. A.1

Robotics & Computer-Integrated Manufacturing, Vol. 5, No. 4, pp. 301–310, 1989
Printed in Great Britain.

0736-5845/89 $3.00 + 0.00

● *Paper*

SYMBOLIC MODELING AND DYNAMIC SIMULATION OF ROBOTIC MANIPULATORS WITH COMPLIANT LINKS AND JOINTS

SABRI CETINKUNT* and WAYNE J. BOOK†

*Department of Mechanical Engineering, University of Illinois at Chicago, Chicago, IL 60680, U.S.A. and †The George W. Woodruff School of Mechanical Engineering, Georgia Institute of Technology, Atlanta, GA 30332, U.S.A.

The explicit, non-recursive symbolic form of the dynamic model of robotic manipulators with compliant links and joints are developed based on a Lagrangian-assumed mode of formulation. This form of dynamic model is suitable for controller synthesis, as well as accurate simulations of robotic applications. The final form of the equations is organized in a form similar to rigid manipulator equations. This allows one to identify the differences between rigid and flexible manipulator dynamics explicitly. Therefore, current knowledge on control of rigid manipulators is likely to be utilized in a maximum way in developing new control algorithms for flexible manipulators.

Computer automated symbolic expansion of the dynamic model equations for any desired manipulator is accomplished with programs written based on commercial symbolic manipulation programs (SMP, MACSYMA, REDUCE). A two-link manipulator is used as an example. Computational complexity involved in real-time control, using the explicit, non-recursive form of equations, is studied on single CPU and multi-CPU parallel computation processors.

NOMENCLATURE

$q_{2i,j}$	jth generalized coordinate associated with element $2i$
n_{2i}	number of generalized coordinates associated with element $2i$
N	total number of links
$x_{2i,j}$, $y_{2i,j}$, $z_{2i,j}$	jth mode shapes for the deflections of element $2i$ in the x_{2i}, y_{2i}, z_{2i} axes directions, respectively.
W_{2i-1}	homogeneous transformation matrix from coordinate frame $2i$ to inertial coordinate frame
A_{2i}	homogeneous transformation matrix from coordinate frame $(2i+1)$ to coordinate frame $(2i)$
K	kinetic energy of the system
P_g	gravitational potential energy
P_e	elastic potential energy
η_{2i}	spatial variable along element $2i$
$\mu(\eta_{2i})$	mass distribution of element
μ_0	uniform mass distribution value
$\mathbf{q}_1$	generalized coordinates associated with joint angles between links
$\mathbf{q}_2$	generalized coordinates associated with link flexibilities
$\mathbf{q}_3$	generalized coordinates associated with joint flexibilities
m_{2i}	mass of element $2i$ (link i)
E	Young's modulus of elasticity of the material
G	shear modulus of elasticity
$(I_x)_{2i}$, $(I_y)_{2i}$, $(I_z)_{2i}$	area moment of inertia of element $2i$ cross section about x_{2i}, y_{2i}, z_{2i} axes, respectively.
$(A_x)_{2i}$	cross section area of element $2i$.
intm	maximum rounded integer, e.g. *intm*(5.2, 6.3) = 7
m_{2i-1}	mass element $2i-1$ (link i)
I_{2i-1}	inertia tensor of element $2i-1$ with respect to a coordinate frame fixed at its center of mass
$[J]$	generalized inertia matrix of all joints
g	gravity vector, $[g_x, g_y, g_z, 0]^T$
$m_{(p,r),(s,t)}$	generalized mass matrix element with row index (p, r), and column index (s, t)
(p, r)	row index: $\sum_{i=1}^{p-1} n_i + r$
(s, t)	column index: $\sum_{i=1}^{s-1} n_i + t$

Acknowledgements—This work was supported in part by the National Aeronautics and Space Administration under grant NAG-1-623, and the National Science Foundation under grant MEA-8303539.

1. INTRODUCTION

1.1 *Motivation for the work*

Computer controlled robotic manipulators are very versatile elements of modern flexible manufacturing systems. Their versatility stems from two main characteristics: (1) mechanical reconfigurability, (2) reprogrammability with the control computer. There is an increasing demand for the utilization of robotic manipulators in many manufacturing operations such as milling, grinding, drilling, and deburring. Furthermore, manipulators are required to complete their part of a job in shorter times, in order to reduce the cycle time and thus improve productivity. This requires manipulators to move faster and faster.

The compliance of manipulators due to links and joints becomes a significant factor affecting the precision of manipulation as the manipulators move at high speeds and/or interact with large contact forces. In order to operate within a desired precision range, the computer control algorithms must account for previously neglected manipulator compliance. Understanding and appropriately accounting for the compliance in control is a prerequisite for the utilization of manipulators in the forementioned high-performance tasks. Therefore, effective means of modeling the dynamics of manipulators, including the link and joint compliance, is needed.

In general, there are two different reasons for mathematical modeling of any dynamic system, and for that matter, compliant manipulators.

1. Study and simulate a system before it is actually built. For that purpose, the model should be as accurate and detailed as possible to closely represent (*model*) the actual system, so that the predicted behavior will be close to the actual behavior of the real system.
2. Model only the major characteristics of the system so that it is simple enough to synthesize an appropriate control algorithm, and implement it in real-time. Explicit, symbolic form of the flexible manipulator dynamics presented in this paper offers important insights to the dynamic characteristics, which is crucial for the development of an appropriate controller.

1.2 *Literature review*

Dyamics and control studies of flexible manipulators have concentrated on a single joint-single link example.[1-3] The single flexible beam is modeled as a Bernoulli–Euler beam and infinite dimensional vibration coordinates are truncated to a finite number of modal coordinates. Joint flexibility is considered as a torsional spring coupling the actuator rotor/gear assembly to the link.

Previous work on the Lagrangian formulation based dynamic modeling of multi-link flexible manipulators can be classified into two groups:

1. Lagrangian—finite element based methods,
2. Lagrangian—assumed modes based methods.

The small vibration dynamic models of flexible mechanisms and manipulators are developed about known nominal joint variable trajectories.[4] The coupling effects of deformation coordinates on the joint motions were neglected. This assumption is removed in Ref. 5. Static deflection modes are included in the model in addition to dynamic deflection modes, thus improving the accuracy of model.[6] A two-link flexible arm is modeled with a Lagrange-finite element based method, and the performance of linear quadratic regulators (LQR) with prescribed degree of stability is studied.[7] In a recent work, a Newton–Euler formulation and Timoshenko beam theory are used.[8] Stiffness matrix accounting for combined flexibility of joints and links is derived again for a two-link example.[9] The main advantage of finite element based methods is that they can be applied to complex shaped systems, covering a wide class of problems. However, the main disadvantage is that they do not give much insight to the dynamic structure of the system.

A general Lagrangian-assumed modes based method is presented in Ref. 10. The equations of motion are developed in recursive form to reduce the real-time computation in inverse dynamic control. A symbolic modeling method based on Ref. 10 is developed in Ref. 11. Transfer matrices are used to develop linear frequency domain model of servo controlled manipulators.[12] The method of 10 is attractive for the following reasons:

1. It is an easy-to-understand conceptual approach: therefore, utilization of the results by other researchers in the robotics field will be at a maximum.
2. As a result of using an independent set of relative coordinates in the kinematic description, the dynamic model has a form similar to the rigid manipulator models. Therefore, it provides more insight to the dynamics of the system and may suggest modifications of rigid manipulator control algorithms for use on flexible manipulators by exploiting the differences between rigid and flexible manipulator dynamics.

2. PROBLEM STATEMENT

Explicit, non-recursive, symbolic modeling of robotic manipulators with compliant links and joints is the problem dealt with in this work. In order to accurately study and simulate the behavior of the system, the

modeling method should yield accurate models. Yet simpler models conveying only dominant characteristics of the dynamics are needed for successful controller design. The Lagrangian-assumed modes based method described in Ref. 10 fulfill these requirements. A recursive formulation is useful and critically important in computed-torque control. However, the *non-recursive*, direct dynamic form of equations is needed for more general simulation and controller synthesis studies. If the multi-cpu parallel computation is needed in order to implement a detailed dynamic model based controller in real-time, the recursive form of equations is not suitable, rather, the explicit, non-recursive form is desirable.

3. SYMBOLIC MODELING OF FLEXIBLE MANIPULATORS

1. *Flexible-arm kinematic description*

Consider the kinematic structure shown in Fig. 1 representing a manipulator with serial links connected by revolute joints. The elements of the manipulator are numbered, and body fixed moving coordinates are assigned as shown, where O_0XYZ is the inertial coordinate frame. 4 × 4 homogeneous transformation matrices are used to describe the position and orientation of one coordinate frame with respect to another. Let $\mathbf{q}_{k,j}^T = (q_{k,1}, q_{k,2}, \ldots, q_{k,m_k})$ be the generalized coordinates associated with the degrees of freedom (d.o.f.) of element k. For instance, if element k is a single d.o.f. revolute joint, then $\mathbf{q}_{k,j} = q_{k,1}$, if it is a two d.o.f. revolute joint, then $\mathbf{q}_{k,j} = (q_{k,1}, q_{k,2})^T$. If element k is a flexible link, $\mathbf{q}_{k,j}$ is a vector of modal coordinates, if the link is rigid (zero d.o.f.), $\mathbf{q}_{k,j}$ is a null vector.

The position vector of a differential element along link i (element $2i$) with respect to coordinate frame $2i$ is given by (Fig. 1)

$$^{2i}h_{2i} = [\eta_{2i}, 0, 0, 1]^T + \sum_{j=1}^{n_{2i}} q_{2i,j}[x_{2i,j}, y_{2i,j}, z_{2i,j}, 0]^T. \quad (1)$$

The second summation term in (Eq. 1) describes the deflection of the element $2i$ at that point in terms of modal coordinates approximately. The $x_{2i,j}, y_{2i,j}, z_{2i,j}$ are the jth mode shape functions of the element in x_{2i}, y_{2i}, z_{2i} directions, respectively, $q_{2i,j}$ is the generalized modal coordinate, n_{2i} is the number of modes used to describe the deflection of element $2i$. The absolute position of this point with respect to the inertial frame O_0XYZ is given by

$$^0h_{2i}(\eta) = {}^0W_{2i-1} \cdot {}^{2i}h_{2i}(\eta) \quad (2)$$

where $^0W_{2i-1}$ is the 4 × 4 homogeneous transformation matrix from coordinate frame $2i$ to the inertial coordinate frame (Fig. 1)†

$$W_{2i-1} = A_1 \cdot A_2 \cdots A_{2i-1}. \quad (3)$$

†Preceding superscript^0 will be dropped for notational simplicity.

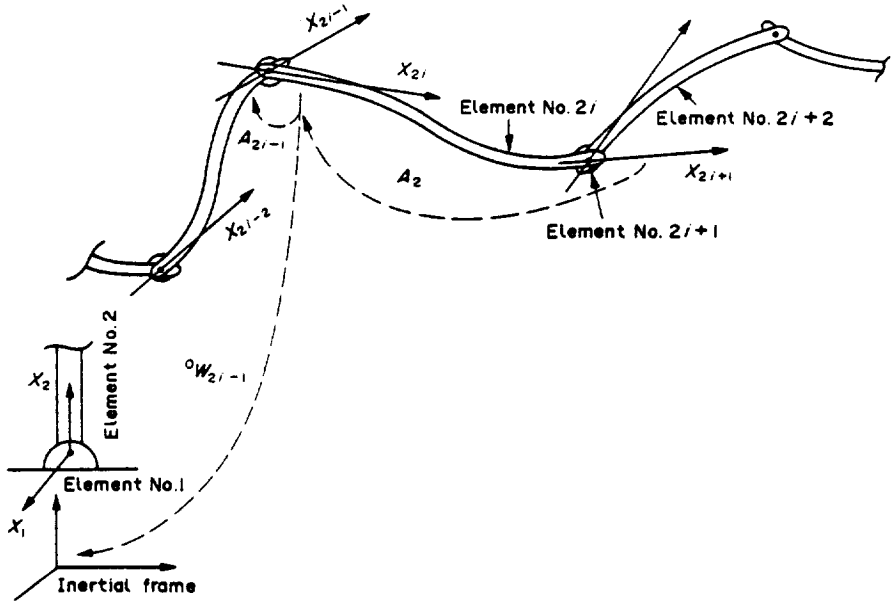

Fig. 1. Kinematic description of serial link flexible manipulators.

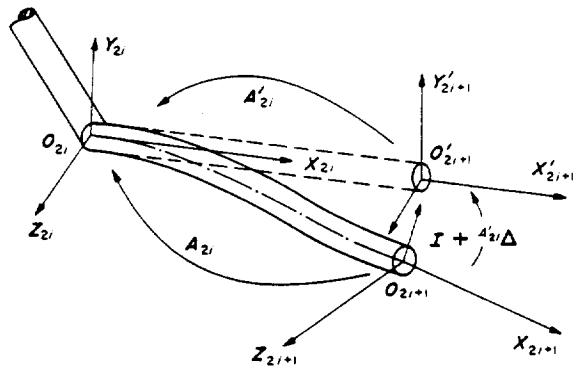

Fig. 2. Illustration of flexible link transformation.

Note that if a link is considered rigid, the corresponding link transformation will be a constant matrix. Approximations are involved in the definition of link transformation, A_{2i}, as described below. If link i (element $2i$) was a rigid, slender beam, A_{2i} would be (Fig. 2)

$$A_{2i} = \begin{bmatrix} 1 & 0 & 0 & l_{2i} \\ 0 & 1 & 0 & 0 \\ 0 & 0 & 1 & 0 \\ 0 & 0 & 0 & 1 \end{bmatrix} \tag{4}$$

The change in the position and orientation of the $(2i+1)$th coordinate frame due to the flexible deflection of link i is described by a differential coordinate transformation (Fig. 2). This is an approximation in the kinematic description. The approximation is valid to the extent that the orientation change of coordinate frame $(2i+1)$ due to deflections is small enough to justify the following approximation:

$$\sin\theta^*_{2i} \simeq \theta^*_{2i}, \cos\theta^*_{2i} \simeq 1. \tag{5}$$

where θ^*_{2i} is the equivalent rotation angle about an axis of rotation to transform the orientation of $(2i+1)$ to that of the $(2i+1)$ th coordinate frame. This approximation is well satisfied in robotic applications. Finally, the link transformation A_{2i},

$$A_{2i} = A'_{2i} + dA'_{2i} \tag{6}$$

$$dA'_{2i} = A'_{2i} \cdot {}^{A'_{2i}}\Delta. \tag{7}$$

Invoking the modal approximation for the deflections

$${}^{A'_{2i}}\Delta = \begin{bmatrix} 0 & -(\theta_z)_{2i} & (\theta_y)_{2i} & x_{2i} \\ (\theta_z)_{2i} & 0 & -(\theta_x)_{2i} & y_{2i} \\ -(\theta_y)_{2i} & (\theta_x)_{2i} & 0 & z_{2i} \\ 0 & 0 & 0 & 0 \end{bmatrix}$$

$$= \sum_{j=1}^{n_{2i}} q_{2i,j} \begin{bmatrix} 0 & -(\theta_z)_{2i,j} & (\theta_y)_{2i,j} & x_{2i,j} \\ (\theta_z)_{2i,j} & 0 & -(\theta_x)_{2i,j} & y_{2i,j} \\ -(\theta_y)_{2i,j} & (\theta_x)_{2i,j} & 0 & z_{2i,j} \\ 0 & 0 & 0 & 0 \end{bmatrix} \tag{8}$$

Hence

$$A_{2i} = \begin{bmatrix} 1 & 0 & 0 & l_{2i} \\ 0 & 1 & 0 & 0 \\ 0 & 0 & 1 & 0 \\ 0 & 0 & 0 & 1 \end{bmatrix}$$

$$+ \sum_{j=1}^{n_{2i}} q_{2i,j} \begin{bmatrix} 0 & -(\theta_z)_{2i,j} & (\theta_y)_{2i,j} & x_{2i,j} \\ (\theta_z)_{2i,j} & 0 & -(\theta_x)_{2i,j} & y_{2i,j} \\ -(\theta_y)_{2i,j} & (\theta_x)_{2i,j} & 0 & z_{2i,j} \\ 0 & 0 & 0 & 0 \end{bmatrix} \tag{9}$$

A_{2i-1} (for $i = 1, \ldots, N$), are joint transformations and no approximations involved in their description.

3.2 *Flexible-arm kinetics: Lagrangian-assumed modes formulation*

Once the kinematic description of the system is set up, the next step in Lagrangian formulation is to form the kinetic and potential energies and take the necessary derivatives of the equations of motion:

$$\frac{d}{dt}\left(\frac{\partial K}{\partial \dot{q}_{p,r}}\right) - \frac{\partial K}{\partial q_{p,r}} + \frac{\partial P}{\partial q_{p,r}} = Q_{p,r}; \{p = 1, \ldots, 2N; \{r = 1, \ldots, n_p\}\} \tag{10}$$

where

$$K = \sum_{i=1}^{N} K_{2i} - \text{total kinetic energy} \tag{11}$$

$$P = \sum_{i=1}^{N} P_{2i} - \text{total potential energy} \tag{12}$$

$$Q_{p,r} - \text{the generalized force vector.} \tag{13}$$

Here only the link dynamics are considered. Inclusion of the joint dynamics into the model will be discussed in Section 3.4. Kinetic energy of element $2i$ (link i)

$$K_{2i} = 1/2 \int_0^{l_{2i}} Tr\{{}^0h_{2i} \cdot {}^0h_{2i}^T\}\mu(\eta)d\eta \tag{14}$$

$${}^0h_{2i}(\eta) = W_{2i-1} \cdot {}^{2i}h_{2i}(\eta) \tag{15}$$

$${}^0\dot{h}_{2i}(\eta) = \dot{W}_{2i-1} \cdot {}^{2i}h_{2i}(\eta) + W_{2i-1} \cdot {}^{2i}\dot{h}_{2i}(\eta) \tag{16}$$

where

$$\dot{W}_{2i-1} = \sum_{j=1}^{2i-1} \left[A_1 A_2 \ldots \left(\sum_{k=1}^{n_j} \frac{\partial A_j}{\partial q_{j,k}}\right) \ldots A_{2i-1}\right]\dot{q}_{j,k}$$

$$= \sum_{j=1}^{2i-1} \sum_{k=1}^{n_j} \left(\frac{\partial W_{2i-1}}{\partial q_{j,k}}\right)\dot{q}_{j,k} \tag{17}$$

$${}^{2i}\dot{h}_{2i} = \sum_{j=1}^{n_{2i}} \dot{q}_{2i,j}[x_{2i,j}, y_{2i,j}, z_{2ij}, 0]^T. \tag{18}$$

Substituting Eqs (15) to (18) into (14) and summing over i as in (11) yields the kinetic energy of the

manipulator links

$$K = 1/2 \sum_{i=1}^{N} \sum_{s=1}^{2i-1} \sum_{u=1}^{2i-1} \sum_{t=1}^{n_s} \sum_{v=1}^{n_u} Tr\left(\frac{\partial W_{2i-1}}{\partial q_{s,t}} \left[C_{2i} + \sum_{j=1}^{n_{2i}} [C_{2i,j} + C_{2i,j}^T] q_{2i,j} + \sum_{j=1}^{n_{2i}} \sum_{k=1}^{n_{2i}} C_{2i,j,k} q_{2i,j} q_{2i,k} \right] \frac{\partial W_{2i-1}^T}{\partial q_{u,v}} \dot{q}_{s,t} \dot{q}_{u,v}\right)$$
$$+ \sum_{i=1}^{N} \sum_{s=1}^{2i-1} \sum_{t=1}^{n_s} Tr\left(\frac{\partial W_{2i-1}}{\partial q_{s,t}} \left[\sum_{j=1}^{n_{2i}} C_{2i,j} \dot{q}_{2i,j} + \sum_{j=1}^{n_{2i}} \sum_{k=1}^{n_{2i}} C_{2i,j,k} q_{2i,k} \dot{q}_{2i,j} \right] W_{2i-1}^T \dot{q}_{s,t}\right)$$
$$+ 1/2 \sum_{i=1}^{N} Tr\left(W_{2i-1} \left[\sum_{j=1}^{n_{2i}} \sum_{k=1}^{n_{2i}} C_{2i,j,k} \dot{q}_{2i,j} \dot{q}_{2i,k} \right] W_{2i-1}^T\right) \quad (19)$$

where

$$C_{2i} = \int_0^{l_{2i}} [\eta_{2i}, 0, 0, 1]^T [\eta_{2i}, 0, 0, 1] \mu(\eta) d\eta \quad (20a)$$

$$C_{2i,j} = \int_0^{l_{2i}} [\eta_{2i}, 0, 0, 1]^T [x_{2i,j}, y_{2i,j}, z_{2i,j}, 0] \mu(\eta) d\eta \quad (20b)$$

$$C_{2i,j,k} = \int_0^{l_{2i}} [x_{2i,j}, y_{2i,j}, z_{2i,j}, 0]^T [x_{2i,j}, y_{2i,j}, z_{2i,j}, 0] \mu(\eta) d\eta. \quad (20c)$$

The potential energy of the system is given by

$$P = P_g + P_e = \sum_{i=1}^{N} [(P_g)_{2i} + (P_e)_{2i}]. \quad (21)$$

The gravitational potential energy, P_g,

$$P_g = \sum_{i=1}^{N} \int_0^{l_{2i}} g^T W_{2i-1}\, {}^{2i}h_{2i}(\eta) \mu(\eta) d\eta \quad (22)$$

Substituting ${}^{2i}h_{2i}$ from (1) into (22)

$$P_g = \sum_{i=1}^{N} g^T W_{2i-1} \left[m g_{2i} + \sum_{j=1}^{n_{2i}} q_{2i,j} m e_{2i,j} \right] \quad (23)$$

where

$$g^T = [g_x, g_y, g_z, 0] = [0, 0, -9.81, 0] \quad (24)$$

$$m g_{2i} = \int_0^{l_{2i}} [\eta_{2i}, 0, 0, 1]^T \mu(\eta) d\eta \quad (25)$$

$$m e_{2i,j} = \int_0^{l_{2i}} [x_{2i,j}, y_{2i,j}, z_{2i,j}, 0]^T \mu(\eta) d\eta. \quad (26)$$

Incidentally, $me_{2i,j}$ is same as the bottom row of $C_{2i,j}$ in (20b).

The elastic potential energy expression, considering bending in the y, z, extension in the x, and torsion about the x directions, is given by

$$P_e = \sum_{i=1}^{N} 1/2 \int_0^{l_{2i}} \left\{ E\left[(I_z)_{2i} \left(\frac{\partial^2 z_{2i}}{\partial \eta^2}\right)^2 + (I_y)_{2i} \left(\frac{\partial^2 y_{2i}}{\partial \eta^2}\right)^2 + (A_x)_{2i} \left(\frac{\partial x_{2i}}{\partial \eta}\right)^2 \right] + G(I_x)_{2i} \left(\frac{\partial (\theta_x)_{2i}}{\partial \eta}\right)^2 \right\} d\eta. \quad (27)$$

Noting the truncated modal approximations for the deformation coordinates of the links [Eqs (1) and (9)]

$$P_e = 1/2 \sum_{i=1}^{N} \sum_{j=1}^{n_{2i}} \sum_{k=1}^{n_{2i}} k_{2i,j,k} q_{2i,j} q_{2i,k} \quad (28)$$

where

$$k_{2i,j,k} = (k_x)_{2i,j,k} + (k_y)_{2i,j,k} + (k_z)_{2i,j,k} + (k_t)_{2i,j,k} \quad (29)$$

$$(k_x)_{2i,j,k} = \int_0^{l_{2i}} E(A_x)_{2i} \left(\frac{\partial x_{2i,j}}{\partial \eta}\right) \left(\frac{\partial x_{2i,k}}{\partial \eta}\right) d\eta \quad (29a)$$

$$(k_y)_{2i,j,k} = \int_0^{l_{2i}} E(I_y)_{2i} \left(\frac{\partial^2 y_{2i,j}}{\partial \eta^2}\right) \left(\frac{\partial^2 y_{2i,k}}{\partial \eta^2}\right) d\eta \delta \quad (29b)$$

$$(k_z)_{2i,j,k} = \int_0^{l_{2i}} E(I_z)_{2i} \left(\frac{\partial^2 z_{2i,j}}{\partial \eta^2}\right) \left(\frac{\partial^2 z_{2i,k}}{\partial \eta^2}\right) d\eta \quad (29c)$$

$$(k_t)_{2i,j,k} = \int_0^{l_{2i}} G(I_x)_{2i} \left(\frac{\partial (\theta_x)_{2i,j}}{\partial \eta}\right) \left(\frac{\partial (\theta_x)_{2i,k}}{\partial \eta}\right) d\eta \quad (29d)$$

Note that the $k_{2i,j,k}$ term is the same structural stiffness value that would be obtained numerically from finite element methods.

3.3. *Dynamic model: non-recursive form*

For general purposes, such as simulation and controller synthesis studies, the non-recursive dynamic form of the model is needed. For computed-torque (inverse dynamic) control, which is a specific control algorithm, the recursive form is desirable.[10] The components of the dynamic model should be explicitly separated out into inertial, centrifugal and Coriolis, gravitational, and structural stiffness terms, so that this information can be embedded in the structure of the real-time control algorithm. For instance, the generalized inertia matrix plays a critical role in decoupled joint control of robotic manipulators. In order to implement a real-time decoupled joint controller for a given manipulator, the generalized inertia matrix must be known explicitly so that it can be used in control action calculations. In contrast, the recursive formulation avoids such separations to reduce the number of operations needed for inverse dynamic calculations. The non-recursive explicit form of the dynamic model is presented below. If the

necessary derivatives are taken, and the terms generated by $\frac{d}{dt}(\partial K/\partial \dot{q}_{p,r})$ and $(\partial K/\partial q_{p,r})$ in Eq (10) are cancelled, the resultant system of equations can be organized in matrix form,

$$[M(\mathbf{q})]\ddot{\mathbf{q}} + C(\mathbf{q}, \dot{\mathbf{q}}) + G(\mathbf{q}) + [K]\mathbf{q} = Q \tag{30}$$

where

$$\mathbf{q}^T = [(q_{1,1}, q_{1,2}, \ldots, q_{1,n_1}), (q_{2,1}, \ldots, q_{2,n_2}), \ldots, (q_{2N,1}, \ldots, q_{2N,n_{2N}})]$$

One row of this matrix Eq. (30) corresponding to $q_{p,r}$ may be written as

$$\sum_{s=1}^{2N} \sum_{t=1}^{n_s} m_{(p,r),(s,t)} \ddot{q}_{s,t} + C_{(p,r)}(\mathbf{q}, \dot{\mathbf{q}}) + G_{(p,r)}(\mathbf{q}) + \sum_{s=1}^{2N} \sum_{t=1}^{n_s} k_{(p,r),(s,t)} q_{s,t} = Q_{(p,r)} \tag{31}$$

where

$\sum_{i=1}^{p-1} n_i + r =$ row index (p, r).

$\sum_{i=1}^{s-1} n_i + t =$ column index (s, t) in Eq. (30).

Elements of the generalized inertia matrix:

$$m_{(p,r),(s,t)} = m^{(1)}_{(p,r),(s,t)} + m^{(2)}_{(p,r),(s,t)} + m^{(3)}_{(p,r),(s,t)} \tag{32}$$

$$m^{(1)}_{(p,r),(s,t)} = \sum_{i=intm\left(\frac{p+1}{2},\frac{s+1}{2}\right)}^{N} Tr\left(\frac{\partial W_{2i-1}}{\partial q_{s,t}} \left[C_{2i} + \sum_{j=1}^{n_{2i}} [C_{2i,j} + C^T_{2i,j}] q_{2i,j} + \sum_{j=1}^{n_{2i}} \sum_{k=1}^{n_{2i}} C_{2i,j,k} q_{2i,j} q_{2i,k}\right] \frac{\partial W^T_{2i-1}}{\partial q_{p,r}}\right) \tag{32a}$$

$$m^{(2)}_{(p,r),(s,t)} = Tr\left(\frac{\partial W_{s-1}}{\partial q_{p,r}} \left[C_{s,t} + \sum_{k=1}^{n_s} C_{s,t,k} q_{s,k}\right] W^T_{s-1}\right) \tag{32b}$$

$$m^{(3)}_{(p,r),(s,t)} = \begin{cases} W_{p-1} C_{p,r,t} W^T_{p-1}; & s = p \\ 0 & ; \ s \neq p. \end{cases} \tag{32c}$$

Elements of the nonlinear centrifugal and Coriolis terms vector:

$$\begin{aligned} C_{(p,r)}(\mathbf{q}, \dot{\mathbf{q}}) = & \sum_{i=intm\left(\frac{p+1}{2},\frac{s+1}{2}\right)}^{N} \sum_{s=1}^{2i-1} \sum_{u=1}^{2i-1} \sum_{t=1}^{n_s} \sum_{v=1}^{n_u} Tr\left(\frac{\partial^2 W_{2i-1}}{\partial q_{s,t} \partial q_{u,v}} \times \left[C_{2i} + \sum_{j=1}^{n_{2i}} [C_{2i,j} + C^T_{2i,j}] q_{2i,j} + \sum_{j=1}^{n_{2i}} \sum_{k=1}^{n_{2i}} C_{2i,j,k} q_{2i,j} q_{2i,k}\right] \times \frac{\partial W^T_{2i-1}}{\partial q_{p,r}} \dot{q}_{s,t} \dot{q}_{u,v}\right) \\ & + \sum_{i=intm\left(\frac{p+1}{2},\frac{s+1}{2}\right)}^{N} \sum_{s=1}^{2i-1} \sum_{t=1}^{n_s} Tr\left(\frac{\partial W_{2i-1}}{\partial q_{p,r}} \times \left[2 \sum_{j=1}^{n_{2i}} C_{2i,j} \dot{q}_{2i,j} + 2 \sum_{j=1}^{n_{2i}} \sum_{k=1}^{n_{2i}} C_{2i,j,k} q_{2i,k} \dot{q}_{2i,j}\right] \times \frac{\partial W^T_{2i-1}}{\partial q_{s,t}} \dot{q}_{s,t}\right) \\ & + \sum_{s=1}^{p-1} \sum_{t=1}^{n_s} \sum_{u=1}^{p-1} \sum_{v=1}^{n_u} Tr \left(\frac{\partial^2 W_{2i-1}}{\partial q_{s,t} \partial q_{u,v}} \left[C_{p,r} + \sum_{k=1}^{n_p} C_{p,r,k} q_{p,k}\right] \times W^T_{p-1} \dot{q}_{s,t} \dot{q}_{u,v}\right) \\ & + \sum_{s=1}^{p-1} \sum_{t=1}^{n_s} Tr\left(\frac{\partial W_{p-1}}{\partial q_{s,t}} \times \left[2 \sum_{k=1}^{n_p} C_{p,r,k} \dot{q}_{p,k}\right] W^T_{p-1} \dot{q}_{s,t}\right). \end{aligned} \tag{33}$$

Elements of the gravity vector

$$G_{(p,r)}(\mathbf{q}) = \sum_{i=intm}^{N} g^T \frac{\partial W_{2i-1}}{\partial q_{p,r}} \left[m g_{2i} + \sum_{j=1}^{n_{2i}} m e_{2i,j} q_{2i,j}\right] + g^T W_{p-1} m e_{p,r}. \tag{34}$$

Elements of the structural stiffness matrix

$$k_{(p,r),(s,t)} = \begin{cases} k_{p,r,t} & \text{for } p = s \\ 0 & \text{for } p \neq s. \end{cases} \tag{35}$$

Note some simplifying facts as follows

$$C_{p,r}, C_{p,r,k}, k_{p,r,t} = 0 \qquad \text{for } p \text{ odd} \tag{36a}$$

$$\frac{\partial W_{s-1}}{\partial q_{p,r}} = 0 \qquad \text{for } s - 1 < p \tag{36b}$$

In symbolic expansion of Eqs (32) to (35) for a manipulator, these facts (36a), (36b) will be automatically utilized and will cancel out the terms that are already known to be zero. Such capabilities are conveniently provided by commercial manipulation programs (SMP, MACSYMA, REDUCE).

Considering (35) and (36), and rearranging generalized coordinate vector into two groups associated with joint and link flexibility

$$[\mathbf{q}_1^T, \mathbf{q}_2^T] = [(q_{1,j}, q_{3,j}, \ldots)^T, (q_{2,j}, q_{4,j}, \ldots)^T]. \tag{37}$$

The equations of motion (30) can be shown to have the following form:

$$\begin{bmatrix} m_r & m_{rf} \\ m^T_{rf} & m_f \end{bmatrix} \begin{Bmatrix} \ddot{\mathbf{q}}_1 \\ \ddot{\mathbf{q}}_2 \end{Bmatrix} + \begin{Bmatrix} C_r(\mathbf{q}_1, \mathbf{q}_2, \dot{\mathbf{q}}_1, \dot{\mathbf{q}}_2) \\ C_f(\mathbf{q}_1, \mathbf{q}_2, \dot{\mathbf{q}}_1, \dot{\mathbf{q}}_2) \end{Bmatrix} + \begin{Bmatrix} G_r(\mathbf{q}_1, \mathbf{q}_2) \\ G_f(\mathbf{q}_1, \mathbf{q}_2) \end{Bmatrix} + \begin{bmatrix} 0 & 0 \\ 0 & K_f \end{bmatrix} \begin{Bmatrix} \mathbf{q}_1 \\ \mathbf{q}_2 \end{Bmatrix} = \begin{Bmatrix} \mathbf{u} \\ 0 \end{Bmatrix}. \tag{38}$$

3.4 *Inclusion of joint dynamics*

Inclusion of joint dynamics into model involves

1. modifications of Eqs (20a–c), (25), and (26) by redefining mass distribution of links,
2. augmenting a set of second order equations to (38) as a result of joint flexibility and inertia.

DC motor-driven revolute joints whose rotor/gear arrangement is elastically coupled to the links will be considered. Joints can have more than one degree of freedom. Elastic mechanical coupling between a joint and link is modeled as a torsional spring. The following assumptions are made regarding the joint assembly mass distribution.

Assumption 1: Rotational kinetic energy of each joint about is own center of mass is only due to its own rotation. Rotational kinetic energy due to rotation of previous joints and links is neglected. This amounts to neglecting terms in the order of gear reduction ratio, which is typically in the order of 1 : 100. Translational kinetic energy due to both previous joints and elastic deformations is taken into account.

Assumption 2: Rotor/gear assembly inertia is symmetric about the rotor axis of rotation such that gravitational potential energy, and translational velocity of joint center of mass are independent of rotor position.[3] This assumption is generally satisfied by joint assemblies of most industrial robots.

Let $\mathbf{q}_3^T = [(q_{1,1}^{(j)}, \ldots, q_{1,n_1}^{(j)}), (q_{3,1}^{(j)}, \ldots, q_{3,n_3}^{(j)}), \cdots (q_{2N-1,1}^{(j)}, \ldots, q_{N-1,n_{2N-1}}^{(j)})]$

be the generalized coordinates associated with joints (Fig. 3). The relative motion between a joint rotor and elastically coupled link is $(q_{2i-1,r} - q_{2i-1,r}^{(j)})$. The contribution of the joint dynamics to the equation of motion will be reflected through kinetic, potential energies and generalized forces. The kinetic energy of joint i (element $2i-1$) is

$$K_{2i-1} = 1/2 m_{2i-1}(V_G)_{2i-1}^T \cdot (V_G)_{2i-1} + 1/2 w_{2i-1}^T [I_{2i-1}] w_{2i-1} \tag{39}$$

where m_{2i-1} is the mass, $(V_G)_{2i_1}$ velocity of center of mass, w_{2i-1} angular velocity vector, $[I_{2i-1}]$ inertia tensor with respect to a coordinate frame fixed at the center of mass of joint. From assumption 2, $(V_G)_{2i-1}$ will be function of the generalized coordinates of proximal elements and will not depend on $q_{2i-1,r}^{(j)}$. Therefore translational kinetic energy of joint i can be included in the formulation by considering its mass as part of the proximal link. This is accomplished by redefining mass distribution of link $(i-1)$ as

$$\mu_{2i-2} = \mu_0 + m_{2i-1}\delta(\eta - l_{2i-2}) \tag{40}$$

where

$$\delta(\eta - l_{2i-2}) = \begin{cases} 1 & \text{for } \eta = l_{2i-2} \\ 0 & \text{for } \eta \neq l_{2i-2} \end{cases} \tag{41}$$

and evaluate Eq. (20a–c) with new definition of μ as in (40).

From assumption 1, $w_{2i-1} \approx \dot{\mathbf{q}}_{2i-1,r}^{(j)}$

$$K_{2i-1} = 1/2(\dot{\mathbf{q}}_{2i-1,r}^{(j)})^T [I_{2i-1}] \dot{\mathbf{q}}_{2i-1,r}^{(j)}. \tag{42}$$

For all joints of the manipulator

$$K^{(j)} = \sum_{\substack{i=\text{inter} \\ \left(\frac{p+1}{2}, \frac{s+1}{2}\right)}}^{N} K_{2i-1} = 1/2 \dot{\mathbf{q}}_3^T [J] \dot{\mathbf{q}}_3. \tag{43}$$

The contribution of joint potential energy to the dynamic model equations is

$$V^{(j)} = V_g^{(j)} + V_e^{(j)} \tag{44}$$

From assumption 2, the gravitational potential energy of joint i may be included in that of link $(i-1)$ by the evaluation of (25) and (26) with $\mu(\eta)$ as defined in Eq. (40). The elastic potential energy stored in elastic coupling between joint and links is

$$V_e^{(j)} = 1/2(\mathbf{q}_1 - \mathbf{q}_3)^T \quad Diag\{K_i\}(\mathbf{q}_1 - \mathbf{q}_3). \tag{45}$$

As a result of the contributions of (43) and (45) equations of motion (38) is modified to the following form:

$$\begin{bmatrix} m_r & m_{rf} \\ m_{rf}^T & m_f \end{bmatrix} \begin{Bmatrix} \ddot{\mathbf{q}}_1 \\ \ddot{\mathbf{q}}_2 \end{Bmatrix} + \begin{Bmatrix} C_r(\mathbf{q}_1, \mathbf{q}_2, \dot{\mathbf{q}}_1, \dot{\mathbf{q}}_2) \\ C_f(\mathbf{q}_1, \mathbf{q}_2, \dot{\mathbf{q}}_1, \dot{\mathbf{q}}_2) \end{Bmatrix} + \begin{Bmatrix} G_r(\mathbf{q}_1, \mathbf{q}_2) \\ G_f(\mathbf{q}_1, \mathbf{q}_2) \end{Bmatrix} + \begin{bmatrix} 0 & 0 \\ 0 & K_f \end{bmatrix} \begin{Bmatrix} \mathbf{q}_1 \\ \mathbf{q}_2 \end{Bmatrix} = \begin{bmatrix} K_i & 0 \\ 0 & 0 \end{bmatrix} \begin{Bmatrix} \mathbf{q}_1 - \mathbf{q}_3 \\ \mathbf{q}_2 \end{Bmatrix}$$

$$[J]\{\ddot{\mathbf{q}}_3\} + [K_i]\{\mathbf{q}_3 - \mathbf{q}_1\} = \{\mathbf{u}\}. \tag{46a, b}$$

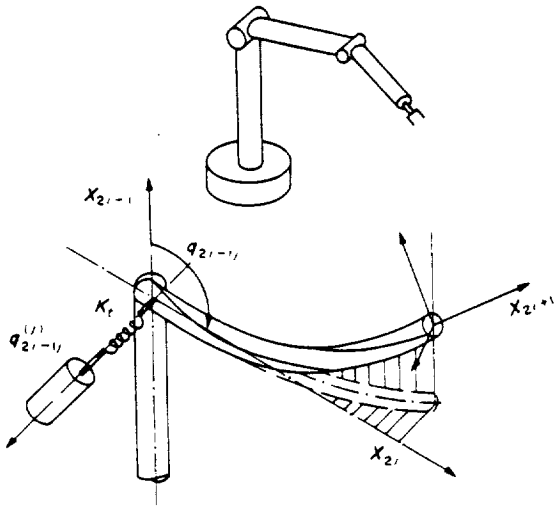

Fig. 3. Flexible joint-link assembly.

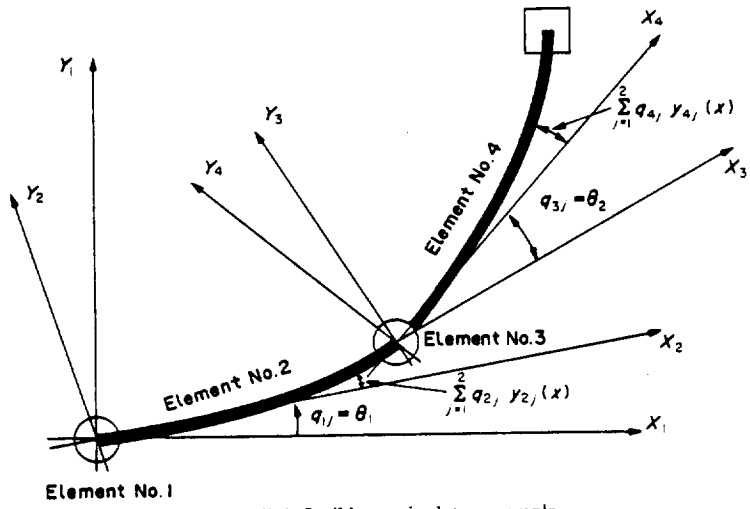

Fig. 4. Two-link flexible manipulator example.

4. A CASE STUDY

The described modeling method has been applied to a two-link planar flexible arm, with single d.o.f revolute joints (Fig. 4). In this case study, only the link flexibilities are considered, the joint flexibilities are not included. The bending deflections of links are approximated with two assumed mode shapes for each link. Mode shapes are chosen from the analytical solution of a Euler–Bernoulli beam eigenfunction analysis but, of course, could also be otained using a finite element analysis program. The mathematical model is symbolically obtained using SMP symbolic manipulation program and simulated with a VAX-11/750 microcomputer with the following objectives:

1. Verify that the model generated by the above algorithm is correct,
2. Demonstrate the ease of changing mode shapes for the given example manipulator, and study the effect of using different mode shapes on the predicted dynamic response of the system.

Model verification is supported by comparing the response of the flexible arm model with that of rigid arm model. Clearly, as the flexural rigidity, EI_z, of the links increase, joint angle response of the flexible model should converge to that of rigid model. This is observed as shown in Figs 5 and 6a, b. In the simulations of Fig. 6, mode shapes corresponding to clamped–free boundary conditions of a beam were used in the model. Now, let us consider the case that one would like to use a different set of mode shapes. The necessary change required in the model is to re-evaluate the following terms with new mode shapes (considering the fact that selected mode shapes form an orthogonal set): $\{C_{2i,j}, C_{2i,j,k}$, for $i = 1, 2$ and $j = k = 1, 2$: $(C_{2,1}, C_{2,2}, C_{4,1}, C_{4,2})$, $(C_{2,1,1}, C_{2,2,2}, C_{4,1,1}, C_{4,2,2})$, $(K_{2,1,1}, K_{2,2,2}, K_{4,1,1}, K_{4,2,2})\}$, $me_{2i,j}$ must be updated with the new values of the fourth row of $C_{2i,j}$. Figure 7a–b shows the same simulation case results of flexible model with clamped– clamped mode shapes. The reason for the faster convergence of joint angle responses compared with those of the rigid model is that clamped–clamped mode shapes results in a stiffer model than clamped–free mode shapes.

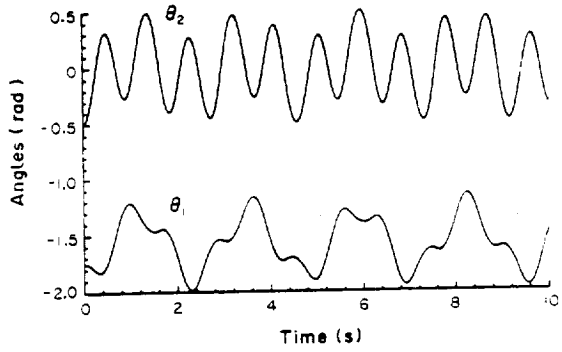

Fig. 5. Two-link rigid model joint angle responses.

Computational, complexity of the resultant model is studied for real-time dynamic control of flexible manipulators. These computational results give us an idea about the algebraic complexity of the explicitly symbolic model and the computational power need for real-time control. Since we have obtained the equations in explicit, symbolic form, we could simply equally distribute the computational load over a multi-CPU architecture where each processor could work independent of each other. The computation time

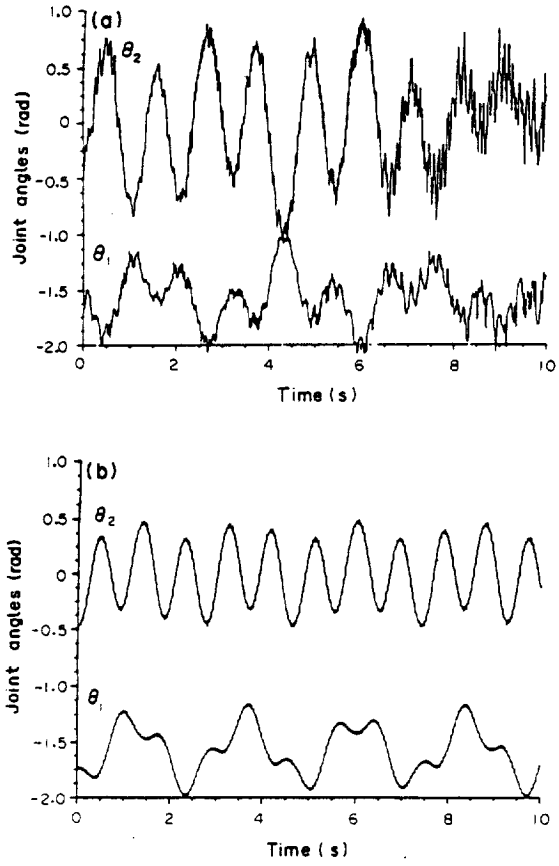

Fig. 6. Two-link flexible model joint angle responses—clamped-free mode shapes: (a) $EI_i = 10\ \text{Nm}^2$ (b) $EI_i = 100\ \text{Nm}^2$.

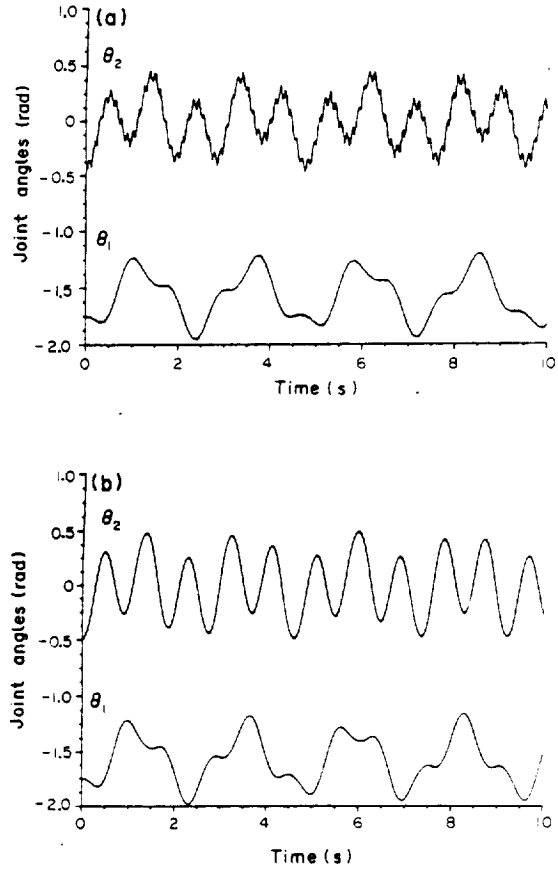

Fig. 7. Two-link flexible model joint angle responses—clamped-clamped mode shapes: (a) $EI_i = 10\ \text{Nm}^2$ (b) $EI_i = 100\ \text{Nm}^2$.

for the inverse dynamics of the example flexible manipulator (Fig. 4) is as follows:

1. Computer: VAX-11/750
   (a) without floating point accelerator: 7 Hz.
   (b) with floating point accelerator: 14 Hz.
2. Computer: 8 transputer (T414) configuration in parallel computation architecture (estimated value, not fully implemented): 80 Hz.

It seems that real-time dynamic control of large dimensional flexible systems can only be realized by distributing the real-time computation load over an array of processors, for the dynamic model equations are, in general, too complicated to be handled by a single processor at a fast enough rate for real-time control. An explicit non-recursive form of equations readily lends itself for multi-CPU implementation. Since the equations are non-recursive, the computational load may be distributed over a multi-CPU system where the computational task of each processor is independent of others. This is not possible using recursive form of model.

5. SUMMARY AND CONCLUSION

The elastic deformations are described by summation of a finite number of mode shapes which may either be assumed or obtained from a finite element analysis program. Link deformations are assumed to be small enough to justify differential coordinate transformation and linear elasticity theory [Eqs (6) to (9), and (27)].

The modeling considers all dynamic couplings (linear and nonlinear) between deflection and joint coordinates. Links are assumed to be slender beams. Revolute joints with multiple degrees of freedom are allowed. Joint flexibility and link flexibility are included.

An explicit symbolic form of the equations is directly useful for simulation and control studies. Computer automated symbolic expansion of Eq. (32) to (35), and (46) to obtain a dynamic model for any desired manipulator structure is studied and an example case is presented. The dynamic model is presented in an analogous way to the dynamic model of rigid

manipulators. This displayed the way link and joint flexibility enter the model, i.e. $C_{2i,j}$, $C_{2i,j,k}$ terms in the elements of generalized inertia matrix. The mode shape dependent model parameters are identified and changing mode shapes for a given model is simplified (only $C_{2i,j}$, $C_{2i,j,k}$, $K_{2i,j,k}$ need to be re-evaluated for new mode shapes).

The explicit symbolic modeling method presented here has the following advantages:

1. improves the insightful understanding of dynamics of flexible manipulators.
2. often equations must be simplified for real-time control implementation. The importance of each term can be determined by simulations, and the unimportant terms can be eliminated from the symbolic equations.
3. equations readily lend themselves to multi-CPU parallel computation for real-time control.
4. changing mode shapes for a given model is very simple.
5. the approach is conceptually easy-to-understand and similar to rigid manipulator formulations.

REFERENCES

1. Hastings, G.G., Book, W.J.: Verification of a linear dynamic model for flexible robotic manipulators. *IEEE Control Syst. Mag. IEEE Control Syst. Soc.* April 1987.
2. Cannon, R.H. Jr., Schmitz, E.: Initial experiments on the end-point control of a flexible one-link robot. *Int. J. Robotics Res.* **3**: 62–75, 1984.
3. Spong, M.W.: Modeling and control of elastic joint robots. *Trans ASME, J. Dyn. Syst. MMT Control* **109**: 310–319, 1987.
4. Sunada, W., Dubowsky, S.: On the dynamic analysis and behavior of industrial robotic manipulators with elastic members. *Trans ASME J. Mech. Trans. Automation Design* **105**: 42–51, 1983.
5. Shabana, A.A., Wehage, R.A.: A coordinate reduction technique for dynamic analysis of spatial substructures with large angular rotations. *J. Struct. Mech.* 401–431, 1983.
6. Yoo, W.S., Haug, E.J.: Dynamics of flexible mechanical systems. *Third Army Conference on Applied Mathematics and Computing*, 13–16 May 1985, Atlanta, Georgia.
7. Usoro, P.B., Nadira, R., Mahil, S.S.: Advanced control of flexible manipulators. Phase 1 Final report, NSF Award Number ECS-8260419, April 1983.
8. Naganathan, G., Soni, A.H.: Coupling effects of kinematics and flexibility in manipulators. *Int. J. Robotics Res.* **6** (1): 75–84, 1987.
9. Shahinpoor, M., Meghdari, A.: Combined flexural-joint stiffness matrix and elastic deformation of a servo-controlled two-link robot manipulator. *Robotica* **4**: 237–242, 1986.
10. Book, W.J.: Recursive Lagrangian dynamics of flexible manipulator arms. *Int. J. Robotic Res.* **3**(3): 87–101, 1984.
11. Book, W.J., Majette, M.: Controller design for flexible, distributed parameter mechanical arms via combined state space and frequency domain techniques. *J. Dyn. Syst. Msmt. Control* **105**: 245–254, 1985.
12. Cetinkunt, S., Book, W.J.: Symbolic modeling of flexible manipulators. *Proceedings of* 1987 *IEEE International Conference on Robotics and Automation*, March 31–April 3 1987, Raleigh, NC, Vol. 3, pp. 2074–2080.
13. Leu, M.C., Hemati, N.: Automated symbolic derivation of dynamic equations of motion for robotic manipulators. *J. Dyn. Syst. Msmt Control.* 108: 172–179, 1986.
14. Neuman, C.P., Murray, J.J.: The complete dynamic model and customized algorithms of the puma robot. *IEEE Trans. Syst Man Cybernetics* SMC-17: (4) 635–644, July/August 1987.

Submitted to 1990 IEEE Robotics and Automation Conference, May 13-18, Cincinnati, OH.

Efficient Dynamic Models for Flexible Robots

Jeh Won Lee
Wayne J. Book

School of Mechanical Engineering
Georgia Institute of Technology, Atlanta, GA 30332

Abstract

Dynamic equations of motion of flexible manipulators are more complicated than those of rigid manipulators. The number of equations of motion increases as the number of modes to be included increases. It is difficult to understand the effect of flexible motion on rigid motion via recursive forms of the equations of motion for multi-link arm even if it were efficient. On the other hand, the closed form of the equations of motion is useful in understanding the characteristics of model parameters. However, the equations resulting from existing closed forms are too complex to serve this purpose. Therefore, a method which is structually well organized and computationally efficient is developed.

1 Introduction

One of the primary concerns in manipulator dynamics is computational efficiency. For the efficient form of the manipulator dynamic equations, various recursive formulations for rigid manipulators using Lagrangian [6], Newton - Euler [10], or Kane's method [4], have been proposed. For flexible manipulators, Book used the method of homogeneous transformation matrices. He first considered small linear motions of a massless elastic chain [2] and later considered distributed mass and elasticity [3]. When the recursive formulation is used, the structure of the dynamic model, which is quite useful in providing insight for designing the controller, is destroyed. To overcome this problem, several programs for rigid manipulators have been developed to derive the equations of motion in symbolic form. Symbolic formulation has the advantage of allowing the identification of the distinct components of the model. Maizza-Neto [11] derived symbolically the equations of motion of a two link flexible manipulator by hand. A systematic method to symbolically derive the nonlinear dynamic equations of multi-link flexible manipulators was presented by Cetinkunt [5]. However, he did not explore the structure of the terms in the flexible manipulator model. The conceptual framework leads to design guidelines for simplifying and reducing the nonlinear kinematic and dynamic coupling of robot dynamics. The physical interpretations and structural characteristics of the Lagrangian dynamic rigid manipulator model was drawn by Tourassis and Neuman [13,14]. The mass matrix is deduced from the masses and center of gravity of links. In turn, the centrifugal and Coriolis coefficients are derived from an inertia matrix through the Christoffel symbol. However, the method of deriving mass matrices is not efficient. Asada [1] presented a method which uses the Jacobian matrix to derive the mass and gravity matrices. This method is found in this paper to be very efficient in the modelling of a flexible manipulator. Low [9] used the Jacobian matrix in deriving the equations of motion of a flexible manipulator. However, the link deformation was not represented in the assumed mode method and the structure of centrifugal and Coriolis force was still complicated and hard to understand.

In this paper, a Lagrangian method is used to derive the equations of motion for a flexible manipulator. The Jacobian matrix is used to derive the mass and gravity matrices. The Coriolis and centrifugal coefficients are derived from the mass matrices using the Christoffel symbol.

2 Derivation of Equations of Motion

The total kinetic energy of an elastic link can be written as

$$T = \frac{1}{2}\sum_{i=1}^{n}\int_0^{l_i} \dot{r}_i^T \dot{r}_j \rho_i A_i dx_i \qquad (1)$$

where $\dot{r}$ is the velocity vector of any point on the elastic link and ρ_i, A_i, l_i are the density, the area, and the length of link i respectively. The velocity vector can be expressed by Jacobian matrix and generalized coordinates.

$$\dot{r}_i = J_i \dot{q}_i \qquad (2)$$

Substitute (2) into (1),

$$\begin{aligned} T &= \frac{1}{2}\sum_{i=1}^{n}\int_0^{l_i}(J_i\dot{q}_i)^T(J_j\dot{q}_j)\rho_i A_i dx_i \\ &= \frac{1}{2}\sum_{i=1}^{n}\dot{q}_i^T(\int_0^{l_i}J_i^T J_j\rho_i A_i dx_i)\dot{q}_j \\ &= \frac{1}{2}\sum_{i=1}^{n}\sum_{j=1}^{n}M_{ij}\dot{q}_i\dot{q}_j \end{aligned} \tag{3}$$

where

$$M_{ij} = \int_0^{l_i} J_i^T J_j \rho_i A_i dx_i \tag{4}$$

The potential energy due to gravity is

$$\begin{aligned} U_g &= \sum_{j=1}\int_0^{l_j} g^T r_j \rho_j A_j dx_j \\ &= \sum_{j=1} m_j g^T r_j \end{aligned} \tag{5}$$

where g is the 3 x 1 gravity vector and

$$m_j = \int_0^{l_j}\rho_j A_j dx_j \tag{6}$$

The potential energy due to elastic deformation is :

$$U_e = \frac{1}{2}\sum_{i=1}^{n}\int_0^{l_i} E_i I_i \frac{\partial^2 u_j}{\partial x_j^2}\frac{\partial^2 u_k}{\partial x_k^2}dx_i \tag{7}$$

where E is Young's modulus of elasticity, and I is the area moment of inertia. u is the elastic deflection which can be expressed as follows.

$$u_i = \sum_{j=1}^{m}\psi_{ij}\delta_{ij} \tag{8}$$

Therefore, the elastic energy can be rewritten as (9)

$$\begin{aligned} U_e &= \frac{1}{2}\sum_{i=1}^{n}\sum_{j=1}^{m}\sum_{k=1}^{m}\int_0^{l_i} E_i I_i \frac{\partial^2\psi_j}{\partial x_j^2}\frac{\partial^2\psi_k}{\partial x_k^2}\delta_{ij}\delta_{ik}dx_i \\ &= \frac{1}{2}\sum_{i=1}^{n}\sum_{j=1}^{m}\sum_{k=1}^{m}K_{ijk}\delta_{ij}\delta_{ik} \end{aligned} \tag{9}$$

where

$$K_{ijk} = \int_0^{l_i} E_i I_i \frac{\partial^2\psi_j}{\partial x_j^2}\frac{\partial^2\psi_k}{\partial x_k^2}dx_i \tag{10}$$

Lagrange's equation is

$$\frac{d}{dt}(\frac{\partial T}{\partial\dot{q}_i}) - \frac{\partial T}{\partial q_i} + \frac{\partial(U_g+U_e)}{\partial q_i} = Q_i \tag{11}$$

Substitute the kinetic energy (3) into (11),

$$\frac{d}{dt}(\frac{\partial T}{\partial\dot{q}_i}) = \frac{d}{dt}(\sum_{j=1}^{n}M_{ij}\dot{q}_j) = \sum_{j=1}^{n}M_{ij}\ddot{q}_j + \sum_{j=1}^{n}\frac{dM_{ij}}{dt}\dot{q}_j \tag{12}$$

where

$$\frac{dM_{ij}}{dt} = \sum_{k=1}^{n}\frac{\partial M_{ij}}{\partial q_k}\frac{dq_k}{dt} = \sum_{k=1}^{n}\frac{\partial M_{ij}}{\partial q_k}\dot{q}_k \tag{13}$$

Therefore,

$$\begin{aligned} \frac{d}{dt}(\frac{\partial T}{\partial\dot{q}_i}) &= \sum_{j=1}^{n}M_{ij}\ddot{q}_j + \sum_{j=1}^{n}\sum_{k=1}^{n}\frac{\partial M_{ij}}{\partial q_k}\dot{q}_j\dot{q}_k \\ &= \sum_{j=1}^{n}M_{ij}\ddot{q}_j + \sum_{j=1}^{n}\sum_{k=1}^{n}\frac{1}{2}(\frac{\partial M_{ij}}{\partial q_k} + \frac{\partial M_{ik}}{\partial q_j})\dot{q}_j\dot{q}_k \end{aligned} \tag{14}$$

$$\begin{aligned} \frac{\partial T}{\partial q_i} &= \frac{\partial}{\partial q_i}(\frac{1}{2}\sum_{j=1}^{n}\sum_{k=1}^{n}M_{jk}\dot{q}_j\dot{q}_k) \\ &= \sum_{j=1}^{n}\sum_{k=1}^{n}\frac{1}{2}\frac{\partial M_{jk}}{\partial q_i}\dot{q}_j\dot{q}_k \end{aligned} \tag{15}$$

Substitute the potential energy (7), (9) to (11),

$$\begin{aligned} \frac{\partial U_g}{\partial q_i} &= \sum_{j=1}^{n}m_j g^T\frac{\partial r_j}{\partial q_i} \\ &= \sum_{j=1}^{n}m_j g^T J_j^{(i)} \end{aligned} \tag{16}$$

where $J_j^{(i)}$ is the i th column of Jacobian matrix J_j.

$$\begin{aligned} \frac{\partial U_e}{\partial q_i} &= \frac{\partial}{\partial\delta_{ij}}(\frac{1}{2}\sum_{i=1}^{n}\sum_{j=1}^{m}\sum_{k=1}^{m}K_{ijk}\delta_{ij}\delta_{ik}) \\ &= \sum_{j=1}^{m}K_{ijj}\delta_{ij} \end{aligned} \tag{17}$$

The Lagrangian equations of motion can be written symbolically as follows.

$$\sum_{j=1}^{n}M_{ij}\ddot{q}_j + \sum_{j=1}^{m}K_{ijj}\delta_{ij} + \tag{18}$$

$$\sum_{j=1}^{n}\sum_{k=1}^{n}\frac{1}{2}(\frac{\partial M_{ij}}{\partial q_k} + \frac{\partial M_{ik}}{\partial q_j} - \frac{\partial M_{jk}}{\partial q_i})\dot{q}_j\dot{q}_k + \sum_{j=1}^{n}m_j g^T J_j^{(i)} = \tau_i$$

or

$$\sum_{j=1}^{n}M_{ij}\ddot{q}_j + \sum_{j=1}^{n}K_{ij}q_j + \sum_{j=1}^{n}\sum_{k=1}^{n}C_{jk}(i)\dot{q}_j\dot{q}_k + G_i g = \tau_i \tag{19}$$

where q is the vector of generalized coordinates, M is the generalized mass matrix, K is the elastic stiffness matrix, C is the coefficient matrix of Coriolis and centrifugal force, G is the gravity force, τ is the vector of generalized forces.

3 Illustraive Example

In this section, equations of motion of a planar two degree of freedom flexible robot are derived as an illustration. In the conventional two serial link robot, there is a difficulty in measuring the end point slope α of link AB as shown in Fig. 1.a. In order to overcome this problem, the flexible robot with a parallel link mechanism is developed as shown in Fig. 1.b. The angles θ_2 and θ_3 are equal because link AD and link BC remain parallel. In this paper, equations of motion of only link AB and link BC are derived because those of the other link can be derived similarly.

3.1 Mass Matrices and Gravity Vectors

Deformed position vectors of each link in Fig. 2.a and 2.b are described as follows:

$$\vec{r}_1 = (x_1 cos\theta_1 - u_1 sin\theta_1)i + (x_1 sin\theta_1 + u_1 cos\theta_1)j \quad (20)$$

$$\vec{r}_2 = [l_1 cos\theta_1 - u_{1e} sin\theta_1 + x_2 cos(\theta_1+\theta_2) - u_2 sin(\theta_1+\theta_2)]i + [l_1 sin\theta_1 + u_{1e} cos\theta_1 + x_2 sin(\theta_1+\theta_2) + u_2 cos(\theta_1+\theta_2)]j \quad (21)$$

where i and j are unit vectors along the inertial frame, X_0 and Y_0. The elastic deformation, u_i, can be expressed by finite series of mode shape functions which satisfy assumed boundary conditions multiplied by time dependent general coordinates. Suppose that the amplitude of the higher modes is relatively small compared with the first mode, two modes per link are considered in this model.

$$u_1(x_1,t) = \psi_{11}(x_1)\xi_{11}(t) + \psi_{12}(x_1)\xi_{12}(t) \quad (22)$$

$$u_2(x_2,t) = \psi_{21}(x_2)\xi_{21}(t) + \psi_{22}(x_2)\xi_{22}(t) \quad (23)$$

The elastic displacement of the end point is

$$u_{1e} = u_1(l_1,t) \quad (24)$$

Velocity vectors are related to general coordinates by the Jacobian matrix [1].

$$\dot{\vec{r}}_1 = J_1 \dot{q}_{12} \quad (25)$$

$$\dot{\vec{r}}_2 = J_2 \dot{q}_{12} \quad (26)$$

where

$$q_{12} = \{\theta_1, \theta_2, \xi_{11}, \xi_{12}, \xi_{21}, \xi_{22}\}^T \quad (27)$$

$$J_1 = \begin{bmatrix} -u_1C_1 - x_1S_1 & 0 & -\psi_{11}S_1 & -\psi_{12}C_1 & 0 & 0 \\ -u_1S_1 - x_1C_1 & 0 & \psi_{11}C_1 & \psi_{12}C_1 & 0 & 0 \end{bmatrix} \quad (28)$$

$$J_2 = \begin{bmatrix} -l_1S_1 - u_{1e}C_1 - u_2C_{12} - x_2S_{12} & -u_2C_{12} - x_2S_{12} & -\psi_{11e}S_1 & -\psi_{12e}S_1 & -\psi_{21}S_{12} & -\psi_{22}S_{12} \\ +l_1C_1 - u_{1e}S_1 - u_2S_{12} + x_2C_{12} & -u_2S_{12} + x_2C_{12} & \psi_{11e}C_1 & \psi_{12e}C_1 & \psi_{21}C_{12} & \psi_{22}C_{12} \end{bmatrix} \quad (29)$$

The Jacobian matrix, J_1 and J_2, can be easily derived by the MJac function of SMP(Symbolic Manipulation Program) [12]. Using the Jacobian matrix, mass matrices and gravity vectors are calculated by the following equations;

$$M_{ij} = \sum_{i=1}^{2} \int_0^{l_i} \rho_i A_i J_i^T J_j dx_i \quad (30)$$

$$\{G_i\} = \sum_{j=i}^{2} \int_0^{l_j} \rho_j A_j J_j[2,i] dx_j \qquad (i = 1,2) \quad (31)$$

The second row of J_i is used in the gravity vector since the gravity is acting in the negative direction of Y_0.

Elements of mass matrices and gravity forces are:

$$\begin{aligned} M_{11} &= \int_0^{l_1} (x_1^2 + u_1^2)\rho_1 A_1 dx_1 \\ &+ \int_0^{l_2} [l_1^2 + u_{1e}^2 + u_2^2 + x_2^2 \\ &+ 2(l_1 x_2 C_2 - l_1 u_2 S_2 \\ &+ u_{1e} u_2 C_2 + u_{1e} x_2 S_2)]\rho_2 A_2 dx_2 \end{aligned}$$

$$M_{12} = \int_0^{l_2} (x_2^2 + u_2^2 + l_1 x_2 C_2 - l_1 u_2 S_2 + u_{1e} u_2 C_2 + u_{1e} x_2 S_2)\rho_2 A_2 dx_2$$

$$M_{13} = \int_0^{l_1} x_1 \psi_{11} \rho_1 A_1 dx_1 + \psi_{11e} \int_0^{l_2} (l_1 + x_2 C_2 - u_2 S_2)\rho_2 A_2 dx_2$$

$$M_{14} = \int_0^{l_1} x_1 \psi_{12} \rho_1 A_1 dx_1 + \psi_{12e} \int_0^{l_2} (l_1 + x_2 C_2 - u_2 S_2)\rho_2 A_2 dx_2$$

$$M_{15} = \int_0^{l_2} \psi_{21}(x_2 + l_1 C_2 + u_{1e} S_2)\rho_2 A_2 dx_2$$

$$M_{16} = \int_0^{l_2} \psi_{22}(x_2 + l_1 C_2 + u_{1e} S_2)\rho_2 A_2 dx_2$$

$$M_{22} = \int_0^{l_2} (x_2^2 + u_2^2)\rho_2 A_2 dx_2$$

$$M_{23} = \psi_{11e} \int_0^{l_2} (x_2 C_2 - u_2 S_2)\rho_2 A_2 dx_2$$

$$M_{24} = \psi_{12e}\int_0^{l_2}(x_2C_2 - u_2S_2)\rho_2 A_2 dx_2$$

$$M_{25} = \int_0^{l_2} x_2\psi_{21}\rho_2 A_2 dx_2$$

$$M_{26} = \int_0^{l_2} x_2\psi_{22}\rho_2 A_2 dx_2 \qquad (32)$$

$$M_{33} = \int_0^{l_1}\psi_{11}^2\rho_1 A_1 dx_1 + \psi_{11e}^2\int_0^{l_2}\rho_2 A_2 dx_2$$

$$M_{34} = \int_0^{l_1}\psi_{11}\psi_{12}\rho_1 A_1 dx_1 + \psi_{11e}\psi_{12e}\int_0^{l_2}\rho_2 A_2 dx_2$$

$$M_{35} = \psi_{11e}C_2\int_0^{l_2}\psi_{21}\rho_2 A_2 dx_2$$

$$M_{36} = \psi_{11e}C_2\int_0^{l_2}\psi_{22}\rho_2 A_2 dx_2$$

$$M_{44} = \int_0^{l_1}\psi_{12}^2\rho_1 A_1 dx_1 + \psi_{12e}^2\int_0^{l_2}\rho_2 A_2 dx_2$$

$$M_{45} = \psi_{12e}C_2\int_0^{l_2}\psi_{21}\rho_2 A_2 dx_2$$

$$M_{46} = \psi_{12e}C_2\int_0^{l_2}\psi_{22}\rho_2 A_2 dx_2$$

$$M_{55} = \int_0^{l_2}\psi_{21}^2\rho_2 A_2 dx_2$$

$$M_{56} = \int_0^{l_2}\psi_{21}\psi_{22}\rho_2 A_2 dx_2$$

$$M_{66} = \int_0^{l_2}\psi_{22}^2\rho_2 A_2 dx_2$$

$$G_1 = \int_0^{l_1}(x_1C_1 - u_1S_1)\rho_1 A_1 dx_1$$

$$+\int_0^{l_2}(l_1C_1 - u_{1e}S_1 + x_2C_{12} - u_2S_{12})\rho_2 A_2 dx_2$$

$$G_2 = \int_0^{l_2}(x_2C_{12} - u_2S_{12})\rho_2 A_2 dx_2 \qquad (33)$$

where

$$\psi_{ije} = \psi_{ij}(l_i)$$

The integrals in equations are labeled as follows.

$$m_i = \int_0^{l_i}\rho_i A_i dx_i \qquad (34)$$

$$m_i l_{ic} = \int_0^{l_i} x_i\rho_i A_i dx_i \qquad (35)$$

$$J_i = \int_0^{l_i} x_i^2\rho_i A_i dx_i \qquad (36)$$

$$LM_{ij} = \int_0^{l_i}\psi_{ij}(x_i)\rho_i A_i dx_i \qquad (37)$$

$$AM_{ij} = \int_0^{l_i} x_i\psi_{ij}(x_i)\rho_i A_i dx_i \qquad (38)$$

$$NM_{ij} = \int_0^{l_i}\psi_{ij}^2(x_i)\rho_i A_i dx_i \qquad (39)$$

where l_{ic} is center of mass of link i.

The first three terms are parameters which are related to a rigid motion. These are called zeroth, first, and second moments of inertia respectively. On the other hand, the last three terms are parameters which are related to a flexible motion. LM_{ij} and AM_{ij} are called the modal momentum coefficients and the modal angular momentum coefficients respectively [7]. The physical meaning of these terms is not easy to explain. However, these are have the following properties [7].

$$\sum_{j=1}^{\infty} LM_j^2 = m \qquad (40)$$

$$\sum_{j=1}^{\infty} LM_j AM_j = ml_c \qquad (41)$$

$$\sum_{j=1}^{\infty} AM_j^2 = J \qquad (42)$$

NM_{ij} are used for the normalization of mode shape functions. Generally, these coefficients have been chosen equal to 1 or the total moment of inertia of the link.

3.2 Centrifugal and Coriolis force

The velocity coupling matrix which are consist of coefficients of centrifugal and Coriolis force can be derived from the mass matrix using the Christoffel symbol [13,14].

$$C_{jk}(i) = \frac{1}{2}\{\frac{\partial M_{ij}}{\partial q_k} + \frac{\partial M_{ik}}{\partial q_j} - \frac{\partial M_{jk}}{\partial q_i}\} \qquad (43)$$

$C_{jk}(i)$ characterizes the effects on link i which are caused by the coupled velocities of link j and k. The diagonal elements for j = k are the coefficients of the centrifugal force. The off-diagonal elements for j $\neq$ k are the coefficients of the Coriolis force.

In the flexible arm dynamics, the states can be partitioned into the rigid states θ and the flexible states δ.

$$\sum_{i=1}^{2} A_{ij}\ddot{\theta}_j + \sum_{j=3}^{6} B_{ij}\ddot{\delta}_j + \sum_{j=1}^{2}\sum_{k=1}^{2} P_{jk}(i)\dot{\theta}_j\dot{\theta}_k + \sum_{j=1}^{2}\sum_{k=3}^{6} Q_{jk}(i)\dot{\theta}_j\dot{\delta}_k$$

$$+\sum_{j=3}^{6}\sum_{k=3}^{6} R_{jk}(i)\dot{\delta}_j\dot{\delta}_k + G_i = \tau_i \quad (i=1,2) \tag{44}$$

$$\sum_{i=1}^{2} B_{ji}\ddot{\theta}_j + \sum_{j=3}^{6} D_{ij}\ddot{\delta}_j + \sum_{j=1}^{2}\sum_{k=1}^{2} \hat{P}_{jk}(i)\dot{\theta}_j\dot{\theta}_k + \sum_{j=1}^{2}\sum_{k=3}^{6} \hat{Q}_{jk}(i)\dot{\theta}_j\dot{\delta}_k$$

$$+\sum_{j=3}^{6}\sum_{k=3}^{6} \hat{R}_{jk}(i)\dot{\delta}_j\dot{\delta}_k + \sum_{j=1}^{2} K_{ij}\delta_j = 0 \quad (i=3,6) \tag{45}$$

Therefore, each velocity coupling matrix can be written as follows:

$$P_{jk}(i) = \frac{1}{2}\{\frac{\partial A_{ij}}{\partial q_k} + \frac{\partial A_{ik}}{\partial q_j} - \frac{\partial A_{jk}}{\partial q_i}\} \tag{46}$$

$$Q_{jk}(i) = \frac{1}{2}\{\frac{\partial A_{ij}}{\partial q_k} + \frac{\partial B_{ik}}{\partial q_j} - \frac{\partial B_{jk}}{\partial q_i}\} \tag{47}$$

$$R_{jk}(i) = \frac{1}{2}\{\frac{\partial B_{ij}}{\partial q_k} + \frac{\partial B_{ik}}{\partial q_j} - \frac{\partial D_{jk}}{\partial q_i}\} \tag{48}$$

$$\hat{P}_{jk}(i) = \frac{1}{2}\{\frac{\partial B_{ij}}{\partial q_k} + \frac{\partial B_{ik}}{\partial q_j} - \frac{\partial A_{jk}}{\partial q_i}\} \tag{49}$$

$$\hat{Q}_{jk}(i) = \frac{1}{2}\{\frac{\partial B_{ij}}{\partial q_k} + \frac{\partial D_{ik}}{\partial q_j} - \frac{\partial B_{jk}}{\partial q_i}\} \tag{50}$$

$$\hat{R}_{jk}(i) = \frac{1}{2}\{\frac{\partial D_{ij}}{\partial q_k} + \frac{\partial D_{ik}}{\partial q_j} - \frac{\partial D_{jk}}{\partial q_i}\} \tag{51}$$

Because mass submatrix D_{ij} are not the function of elastic state δ_i in equation (29), $\hat{R}_{jk}(i)$ is eliminated. The number of independent centrifugal and Coriolis coefficients also can be reduced using the symmetry and the reflective coupling properties [13,14].

$$C_{jk}(i) = C_{kj}(i) \tag{52}$$

$$C_{jk}(i) = -C_{ji}(k) \quad for \quad j \le i,k \tag{53}$$

The reflective coupling property that Tourassis and Neuman finds for rigid arms is not always valid in the flexible case. Therefore, even though the symbolic manipulation program can be used as the computational tool, the simplication procedure must be completed under the supervision of the analyst.

Using these properties, the following independent terms are drawn from elements of the velocity coupling matrix $C_{jk}(i)$.

$$d_1 = \int_0^{l_2}\{(u_{1e}C_2 - l_1S_2)x_2 - (u_{1e}S_2 + l_1C_2)u_2\rho_2A_2dx_2\}$$

$$d_{21} = \int_0^{l_1} \psi_{11}^2 q_{11}\rho_1A_1dx_1$$

$$+\psi_{11e}[\int_0^{l_2}(S_2x_2 + C_2u_2 + u_{1e})\rho_2A_2dx_2]$$

$$d_{22} = \int_0^{l_1} \psi_{12}^2 q_{12}\rho_1A_1dx_1$$

$$+\psi_{12e}[(\int_0^{l_2}(S_2x_2 + C_2u_2 + u_{1e})\rho_2A_2dx_2]$$

$$d_{31} = \psi_{11e}\int_0^{l_2}(S_2x_2 + C_2u_2)\rho_2A_2dx_2$$

$$d_{32} = \psi_{12e}\int_0^{l_2}(S_2x_2 + C_2u_2)\rho_2A_2dx_2$$

$$d_{41} = \int_0^{l_2}\psi_{21}(\psi_{21}q_{21} + \psi_{22}q_{22})\rho_2A_2dx_2$$

$$d_{42} = \int_0^{l_2}\psi_{22}(\psi_{21}q_{21} + \psi_{22}q_{22})\rho_2A_2dx_2 \tag{54}$$

$$d_{51} = \int_0^{l_2}\psi_{21}\{(\psi_{21}q_{21}+\psi_{22}q_{22})+(u_{1e}C_2-l_1S_2)\}\rho_2A_2dx_2$$

$$d_{52} = \int_0^{l_2}\psi_{22}\{(\psi_{21}q_{21}+\psi_{22}q_{22})+(u_{1e}C_2-l_1S_2)\}\rho_2A_2dx_2$$

$$d_{61} = \psi_{11e}S_2\int_0^{l_2}\psi_{21}\rho_2A_2dx_2$$

$$d_{62} = \psi_{11e}S_2\int_0^{l_2}\psi_{22}\rho_2A_2dx_2$$

$$d_{71} = \psi_{12e}S_2\int_0^{l_2}\psi_{21}\rho_2A_2dx_2$$

$$d_{72} = \psi_{12e}S_2\int_0^{l_2}\psi_{22}\rho_2A_2dx_2$$

Using these coefficients, the velocity coupling matrix for the two link example can be simplified as follows:

$$C(1) = \begin{bmatrix} 0 & d_1 & d_{21} & d_{22} & d_{41} & d_{42} \\ & d_1 & 0 & 0 & d_{41} & d_{42} \\ & & 0 & 0 & 0 & 0 \\ & & & 0 & 0 & 0 \\ & & & & 0 & 0 \\ & & & & & 0 \end{bmatrix} \tag{55}$$

$$C(2) = \begin{bmatrix} -d_1 & 0 & d_{31} & d_{32} & d_{51} & d_{52} \\ & 0 & 0 & 0 & d_{51} & d_{52} \\ & & 0 & 0 & -d_{61}/2 & -d_{62}/2 \\ & & & 0 & -d_{71}/2 & -d_{72}/2 \\ & & & & 0 & 0 \\ & & & & & 0 \end{bmatrix} \tag{56}$$

$$C(3) = \begin{bmatrix} -d_{21} & -d_{31} & 0 & 0 & -d_{61} & -d_{62} \\ & -d_{31} & 0 & 0 & -d_{61}/2 & -d_{62}/2 \\ & & 0 & 0 & 0 & 0 \\ & & & 0 & 0 & 0 \\ & & & & 0 & 0 \\ & & & & & 0 \end{bmatrix} \quad (57)$$

$$C(4) = \begin{bmatrix} -d_{22} & -d_{32} & 0 & 0 & -d_{71} & -d_{72} \\ & -d_{32} & 0 & 0 & -d_{71}/2 & -d_{72}/2 \\ & & 0 & 0 & 0 & 0 \\ & & & 0 & 0 & 0 \\ & & & & 0 & 0 \\ & & & & & 0 \end{bmatrix} \quad (58)$$

$$C(5) = \begin{bmatrix} -d_{41} & -d_{51} & d_{61} & d_{71} & 0 & 0 \\ & -d_{51} & d_{61}/2 & d_{71}/2 & 0 & 0 \\ & & 0 & 0 & 0 & 0 \\ & & & 0 & 0 & 0 \\ & & & & 0 & 0 \\ & & & & & 0 \end{bmatrix} \quad (59)$$

$$C(6) = \begin{bmatrix} -d_{42} & -d_{52} & d_{62} & d_{72} & 0 & 0 \\ & -d_{52} & d_{62}/2 & d_{72}/2 & 0 & 0 \\ & & 0 & 0 & 0 & 0 \\ & & & 0 & 0 & 0 \\ & & & & 0 & 0 \\ & & & & & 0 \end{bmatrix} \quad (60)$$

4 Conclusion

Mass matrices and gravity vectors are directly derived from the Jacobian matrices which are easily calculated from positon vectors by SMP. Because the deriving procedure is simple, it reduces the possibility of producing the incorrect equations. Furthermore, this form can easily expand the model to higher modes expanding elastic deformations as series of mode shape functions. The coefficients of centrifugal and Coriolis force are derived from the mass matrices by Christoffel symbol and are simplified by using several structural properties. The resulting velocity coupling matrices have a structure which is useful to reduce the number of terms calculated, to check correctness, or to extend the model to higher order. Some procedures for deriving the velocity coupling are not computerized. In the future, an even more systematic derivation method may be possible.

References

[1] Asada, H.. and Slotine, J.-J.E., "Robot Analysis and Control," *John Wiley & Sons, Inc*, 1986.

[2] Book, W.J., " Analysis of Massless Elastic Chains With Servo Controlled Joints," *ASME Journal of Dynamic Systems, Measurement, and Control*, 101(3), Sep. 1979, pp 187-192

[3] Book, W.J., "Recursive Lagrangian Dynamics of Flexible Manipulator Arms," *The International Journal of Robotics Research*, 3(3), Fall 1984, pp 87-101.

[4] Burdick, J., "An Algorithm for Generation of Efficient Manipulator Dynamic Equations," *Proc. IEEE International Conf. on Robotics and Automation*, San Francisco, CA, 1986, pp 212-218.

[5] Cetinkunt, S., "Symbolic Modelling and Dynamic Analysis of Flexible Manipulators," *Proc. IEEE International Conf. on Robotics and Automation*, Rayleigh, NC, 1987, pp -

[6] Hollerbach, J.M., "A Recursive Lagrangian Formulation of Manipulator Dynamics and a Comparative Study of Dynamic Formulation Complexity," *IEEE Trans. Systems, Man, and Cybernetics*, 10(11), Nov. 1980, pp 730-736.

[7] Hughes, P.C., "Modal Identities for Elastic Bodies with Application to Vehicle Dynamics and Control," *Journal of Applied Mechanics*, 47(1), Mar. 1980, pp 177-184.

[8] Kane, T.R., and Levinson, D.A., "The Use of Kane's Dynamical Equations in Robotics," *The International Journal of Robotics Research*, 2(3), Fall 1983, pp 3-20.

[9] Low, K.H., "A Systematic Formulation of Dynamic Equations for Robot Manipulators with Elastic link," *Journal of Robotic Systems*, 4(3) 1987, pp 435-456.

[10] Luh, J.Y.S., Walker, M.W., and Paul, R.P.C., " On-Line Computational Scheme for Mechanical Manipulators," *ASME Journal of Dynamic Systems, Measurement, and Control*, 102, Jun. 1980, pp 69- 76.

[11] Maizza - Neto, O., "Modal Analysis and Control of Flexible Manipulator Arms," PhD Thesis, Dept. of Mechanical Engineering, MIT, 1974.

[12] *SMP Reference Manual*, Inference Corporation, 1983

[13] Tourassis, V.D., and Neuman, C.P., "Properties and Structure of Dynamic Robot Models for Control Engineering Applications," *Mechanism and Machine Theory*, 20(1), 1985, pp 27-40.

[14] Tourassis, V.D., and Neuman, C.P., "The Inertial Characteristics of Dynamic Robot Models," *Mechanism and Machine Theory*, 20(1), 1985, pp 41-52.

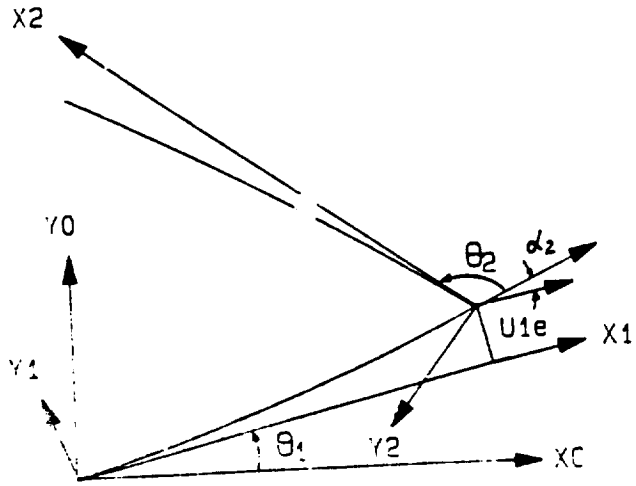

Fig. 1.a Serial Link

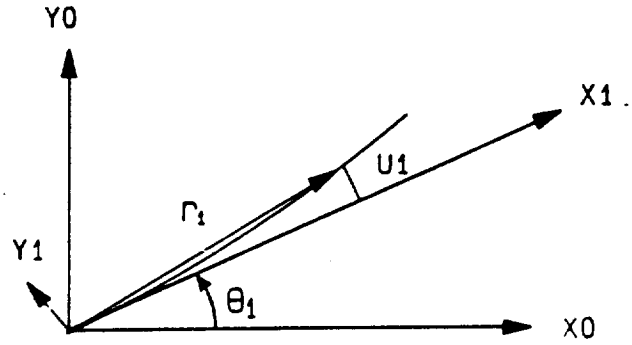

Fig. 2.a Position Vector of Lower Link

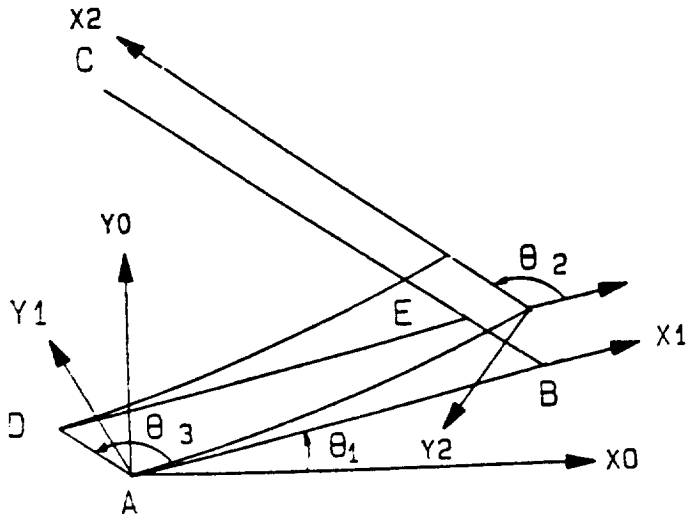

Fig. 1.b Parallel Link

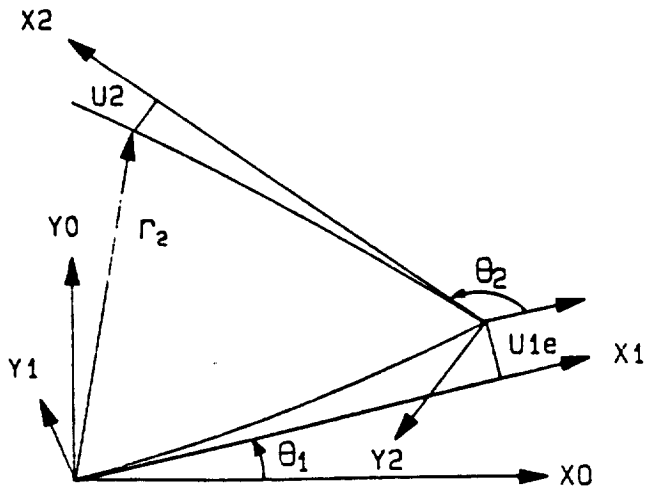

Fig. 2.b Position Vector of Upper Link

ABSTRACT

Submitted to ACC '90

CONTROL OF A SMALL WORKING ROBOT ON A LARGE FLEXIBLE MANIPULATOR FOR SUPPRESSING VIBRATIONS

Soo Han Lee
Wayne J. Book
The George W. Woodruff School of Mechanical Engineering
Georgia Institute of Technology
Atlanta, Georgia 30332

The vibrations of flexible manipulators have been usually damped out by using the joint actuators. The joint actuators must have a larger bandwidth than flexible vibrations. This means that the additional use of joint actuators has larger torque per link weight ratio (or actuator weight per link weight ratio) compared to a rigid link robot. The high weight ratio degrades an advantage of flexible manipulator, light weight, especially when a flexible manipulator is long. A simple solution to decrease the weight ratio is to use joint actuators for only nominal position control. The vibrations are suppressed by a passive damping treatment or momentum exchange devices that increase total weight. A flexible manipulator at Georgia Institute of Technology gives another solution, that is, damping out the vibrations by using inertial forces of a small rigid robot carried by large flexible manipulator.

An approximately human scale three degree of freedom research robot designated SAM (Small Articulated Manipulator) can change the direction of inertial force by changing joint angles and joint torque directions. The direction of the inertial forces affects the vibration suppression effectiveness. The most effective angles and torque directions of the small robot depend on the mode shape of a large flexible manipulator designated RALF (Robotic Arm, Large and Flexible). Also the mode shape of flexible vibrations varies with the angles and joint torque directions of the large manipulator. The issues related with the angles (nominal position) and torque direction (inertial force management scheme) are addressed.

A small robot carried by a large flexible manipulator suffers from relatively large acceleration and nonlinear forces. The controller of a small robot should keep the robot at a nominal position and follow a predetermined inertial force management scheme for damping the vibration of the large manipulator. The control law should be simple and effective in order to overcome the speed limit of computations. Studies on this control issue are also addressed.

Proceedings, 1989 American Control Conference, June 21-23, 1989,
Pittsburgh, PA

SMALL MOTION EXPERIMENTS ON A LARGE FLEXIBLE ARM WITH STRAIN FEEDBACK[1]

B. S. Yuan
American Semiconductor Equipment Technologies
Woodland Hills, California

J. D. Huggins
W. J. Book
Georgia W. Woodruff School of Mechanical Engineering
Georgia Institute of Technology
Atlanta, Georgia

ABSTRACT

Initial experiments on state space feedback control of a large flexible manipulator with a parallel linkage drive are described. A linear controller using joint angle and strain measurements was designed to minimize a quadratic performance index with a prescribed stability margin. It is based on a simplified model that accounts for the constraints of the parallel linkage kinematically rather than through constraint forces. The results show substantial improvement over a simple P.D. joint control.

INTRODUCTION

A large, two link flexible manipulator designated RALF (Robotic Arm, Large and Flexible) is the subject of modeling and control research at Georgia Institute of Technology. It is hydraulically actuated with the second joint powered through a parallelogram linkage. This drive linkage is representative of drives found in many large articulated arms. It allows the substantial weight of the actuators to be located near the base hence reducing the weight that must be supported and the inertia that must be moved. A parallelogram arrangement allows the drive for the second joint to carry some of the bending load on link 1 as well. Most control researchers have avoided this practical configuration, especially when the links are flexible for the more tractable direct drive, serial link problem. The direct drive concept has not been employed for large articulated arms in earth's gravity and may never be practical in that application.

The difficulty of research with the parallelogram mechanism is the conceptual difficulty of modeling a system with nonlinear large motion dynamics, distributed flexibility, and constraints of closed kinematic chains. One valuable contribution of the research described here is the determination of a simple yet adequate model for RALF and other arms of this type. The second contribution is the analytical development and experimental testing of simple linear state space controllers.

DYNAMIC MODELING

Dynamic models for RALF have been developed and compared to experiment as reported in Lee, et.al. [1]. That model included an assumed modes approximation for the link deformation and algebraic constraint equations representing the closed chain topology of the parallel actuating link. A simpler model is used here as the result of two key assumptions. First, the kinematics of the deflection assumed allows no beam extension. Hence the distances between pin joints in the parallelogram remains constant and deflection of the lower or actuating link causes no rotation in the upper link. The thicker cross section of the upper link between the pins (points E and F in the schematic of Fig. 1) makes reasonable the second assumption: rigidity in that segment of the upper link. Consequently, the segment E-F remains parallel to the same line while deflections rotate the lower link. This is in sharp contrast to serial link arms. These facts will now be incorporated into the description of the arm's motion.

As proposed in Book [2], kinematics of serial flexible arms is readily described by 4x4 transformation matrices. In particular, consider the two link arm of Fig. 1. The transformation matrix between link-fixed coordinates and base coordinates is composed of joint transformation matrices A_i and flexible link transformation coordinates E_i. The transformation to a point located a distance l_2 along the beam from the second joint is

$$T_2 = A_1 E_1 A_2 E_2. \tag{1}$$

The point on the second link is located at ${}^2r_2$ in the link-fixed frame or at point r_2 in the base frame, where

[1]This work was partially supported through NASA Grant NAG1-623 and the Computer Integrated Manufacturing Systems Program at the Georgia Institute of Technology.

$$r_2 = T_2\,{}^2r_2. \qquad (2)$$

The constraints of the parallelogram mechanism on link two can be readily incorporated in the rotation matrix of E_1. In general (for small deflections)

$$E_i = \sum_{j=1}^{m_i} \delta_{ij} \begin{bmatrix} 0 & -\theta_{zij} & \theta_{yij} & u_{ij} \\ \theta_{zij} & 0 & -\theta_{xij} & v_{ij} \\ -\theta_{yij} & \theta_{xij} & 0 & w_{ij} \\ 0 & 0 & 0 & 0 \end{bmatrix} + \begin{bmatrix} 1 & 0 & 0 & 0 \\ 0 & 1 & 0 & 0 \\ 0 & 0 & 1 & 1_i \\ 0 & 0 & 0 & 0 \end{bmatrix}$$

where

δ_{ij} is the time varying amplitude of the shape function,

u_{ij}, v_{ij} and w_{ij} are the x, y, and z components, respectively, of the shape functions,

θ_{xij}, θ_{yij}, and θ_{zij} are the small rotations of the body-fixed coordinate system at the point of interest,

m_i is the number of shape functions needed to represent the flexible kinematics to the degree of accuracy needed, and l_i is the distance to the point of interest along the links neutral axis, which is L_i, the length of the link, when the point at r_k is not on link i.

In the special case at hand the rotations θ_{x1j}, θ_{y1j}, and θ_{z1j} are zero as seen by link two. Only translations of the tip of link one are experienced by link two.

It should be made clear that the model still accounts for rotations of the beams in the equations, but that the kinematic constraints prevent those rotations from propagating to link two in the ideal case of the joint rotational axis on the beam neutral axis. Comparing the drawing and the schematic of Fig. 1 will show a substantial offset in the laboratory hardware. This is an additional approximation in the dynamic model.

Given the above description of the arm kinematics, 8.4 the derivation of the dynamic equations of motion can proceed using Lagrange's equations substantially the same as described in Book [2]. The method shown here for two links can be extended to additional parallelogram actuated links.

It is desirable to account for the cumulative compliance of the actuating link, pin joints, and hydraulic fluid in the actuator. Including a simple massless spring effectively accomplishes this. One end of the spring is attached to the second link and the spring compression is prescribed by the actuator displacement. Lagrange's equations can accommodate this model simply with an additional term in the system kinetic energy. The method employed here differs somewhat, however. The actuator force, instead of displacement, is chosen as the input. The force acting through a massless spring is instantaneously felt by the link and the spring is of no direct consequence. The actuator spring is of consequence in the selection of assumed mode shapes for the links, however, as described below.

The transformation matrix E_i contains deflection displacements and rotations as a function of position l_i along the link. The spatial dependence of these deflections, their shape, is theoretically required only to meet modest restrictions at the link boundaries in an infinite order model. A finite element approach was used in this research to determine the shapes from detailed models of the link geometry and material properties. Of crucial importance to the accuracy of a low order model are the boundary conditions applied in deriving the shapes. Equivalent springs were used to represent the actuators for both links. Equivalent masses and inertias were also placed at the end of each link, yielding boundary conditions at 3 points on each link: at each end and where pinned in the middle. At these points on

Link 1: pinned, spring, inertia
Link 2: pinned, spring, mass

The final nonlinear equations derived by Lagrangian or other equivalent method is of the form

$$M(x)\,\ddot{x} + H(x,\dot{x})\,\dot{x} + K\,x = Q \qquad (4)$$

where

x is a vector containing the joint angles θ_i and the deflection amplitudes δ_{ij}

M is the inertia matrix

$H(x,\dot{x})$ contains the nonlinear velocity dependent functions

K is a spring constant matrix

Q is a vector of actuator torques.

CONTROL

Using the model developed in above, an LQR (Linear Quadratic Regulator) controller was developed for RALF. The points about which the model was linearized are $\theta_1 = 0°$ and $\theta_2 = 90°$. The LQR controller utilizes strain feedback from strain gages mounted near the base of the links to control vibrations of the links.

The linearized form of the equations of motion is:

$$[M]\,\ddot{(\bar{x})} + [K](\bar{x}) = (Q)$$

where $\bar{x}$, M, K, and Q are given by:

$$(\bar{x}) = \begin{Bmatrix} \bar{\theta}_1 \\ \delta_1 \\ \bar{\theta}_2 \\ \delta_2 \end{Bmatrix}; \quad [M] = \begin{bmatrix} 1949.92 & 12.47 & 317.74 & 2.365 \\ 12.47 & .0998 & 0 & 0 \\ 317.74 & 0 & 317.74 & 2.365 \\ 2.365 & 0 & 2.365 & 1.786\ E\text{-}2 \end{bmatrix}$$

$$(Q) = \begin{Bmatrix} \tau_1 \\ 0 \\ \tau_2 \\ 0 \end{Bmatrix}; \quad [K] = \begin{bmatrix} 6124860 & 0 & 0 & 0 \\ 0 & 157.02 & 0 & 0 \\ 0 & 0 & 1814400 & 0 \\ 0 & 0 & 0 & 60.94 \end{bmatrix}$$

Note that: $\theta_1 = \theta_{10} + \bar{\theta}_1$
$\theta_2 = \theta_{20} + \bar{\theta}_2$

where $\theta_{10} = 0°$ and $\theta_{20} = 90°$. See Figure 24.

writing this in state space form yields:

$$\frac{d}{dt}[X] = \frac{d}{dt}\begin{bmatrix} \bar{x} \\ \dot{x} \end{bmatrix} = \begin{bmatrix} 0 & I \\ -M^{-1}K & 0 \end{bmatrix}\begin{Bmatrix} \bar{x} \\ \dot{x} \end{Bmatrix} + \begin{bmatrix} 0 \\ M^{-1} Q \end{bmatrix} u$$

For this LQR controller the following quadratic cost criteria was used to obtain a prescribed degree of stability:

$$PI = \frac{1}{2}\int_0^t e^{2\alpha t}\,[X^T PX + u^T Ru]\,dt$$

with α, P, and R given by:

$\alpha = 2$

$$R = 1.E\text{-}5\begin{bmatrix} 1 & 0 \\ 0 & 1 \end{bmatrix}$$

$$P = \begin{bmatrix} 1E11 & 0 & 0 & \cdots & 0 \\ 0 & 1 & & & \\ & & 1E11 & & \\ & & & 1 & \\ & & & & 1 \\ 0 & & & & 1 \end{bmatrix}$$

and $u = -F(x - x_r)$ where x_r is the reference state variable. Notice the large values in the [Q] matrix corresponding to the joint position variables. Two factors influenced these numbers. First, the system model was derived using inches as the unit of length. This resulted in very small numbers when $[M]^{-1}$ is formed. Secondly, the hydraulics actuators are very stiff and inherently have a high gain. The large numbers in the [P] matrix compensate for these factors. The small numbers in the [R] matrix also resulted because of the system of units used in deriving the model.

Using a controller design software, CTRL-C, the LQR feedback gains were found as follows:

$$F = \begin{bmatrix} 2.8161E7 & 1.3518E4 & 3.1388E4 & 8.3383E3 & 2.8013E5 \\ 1.5035E5 & -4.4833E3 & 3.0015E7 & 1.0065E4 & 4.6735E4 \\ 1138.4 & 4.483E4 & 248.226 & & \\ -12.9825 & 7.7616E4 & 268.2405 & & \end{bmatrix}$$

This yields a state space system of the form:

$$\dot{X} = (A - BF)X + BX_R$$

It should be mentioned here that the feedback gains found by solving the LQR equations do not result in absolute values. What is important is the relative magnitude of the gains. When the controller was implemented, the gains were scaled to match the physical capabilities of the system.

The controller for RALF was then implemented on a Microvax II computer with a sampling rate of 8 milliseconds. The language used is FORTRAN. All path planning is calculated before movement starts. The following graphs show the results of the LQR controller compared to a controller that does not utilize strain feedback, ie., a controller using joint position feedback only. The LQR regulator uses differentiation and filtering to estimate all rates.

Figure 3 is a plot of the strain in the lower link when the manipulator is subjected to a step input. Figure 3-a. shows the strain in the lower link when the controller uses joint position feedback only. Figure 3-b. is a graph of the strain in the lower link when subjected to the same input but using the LQR controller with strain feedback instead. As can be seen in Fig. 3-b., the vibration amplitude in the lower link is reduced much more rapidly when the LQR controller is used.

Figure 4-a. shows the strain in the lower link when the controller uses joint position feedback only. Figure 4-b. is a graph of the strain in the lower link when subjected to the same input but using the LQR controller with strain feedback instead. Again the vibration amplitude is reduced much more quickly when the LQR controller incorporating strain feedback is used.

Figure 5-a. shows the strain in the lower link in response to a disturbance to the manipulator's structure. In this case, the manipulator's position is being maintained by the controller that uses joint position feedback only. Figure 5-b. shows a graph of the strain in the lower link when subjected to the same disturbance when using the LQR controller to maintain the manipulator's position. Much better disturbance rejection is seen in Fig. 5-b. than in Fig. 5-a.

SUMMARY AND FUTURE WORK

It is seen from these experiments that a suitable controller utilizing strain information from the links can

successfully damp out the vibration in the manipulator. The LQR controller is a good example of these. Since the structure's dynamics are non-linear, a better controller might be one that incorporates some nonlinearities and adapts to changes in configuration. Work on this aspect is underway.

REFERENCES

1. Lee, J. W., Huggins, J. D., and Book, W. J., "Experimental Verification of a Large Flexible Manipulator," Proceedings of the 1988 American Control Conference, June 15-17, 1988, Atlanta, Georgia 1021-1028.

2. Book, W. J., "Recursive Lagrangian Dynamics of Flexible Manipulators Arm," The Int. J. of Robotics Research, Vol. 3, No. 3, 1984, pp. 87-101.

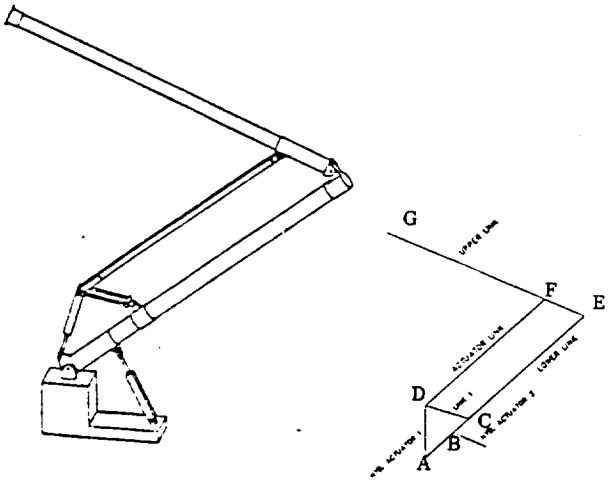

Figure 1. Robotic Arm Large and Flexible (RALF); Actual and Idealized.

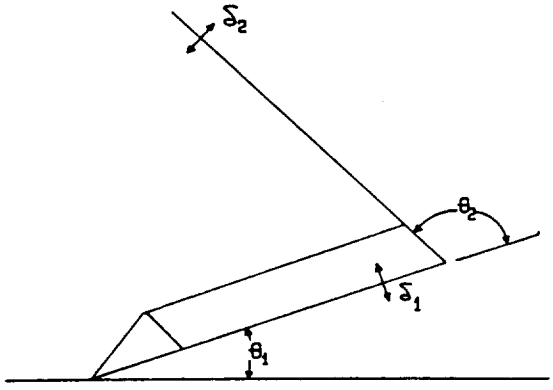

Figure 2. Variables in RALF Model

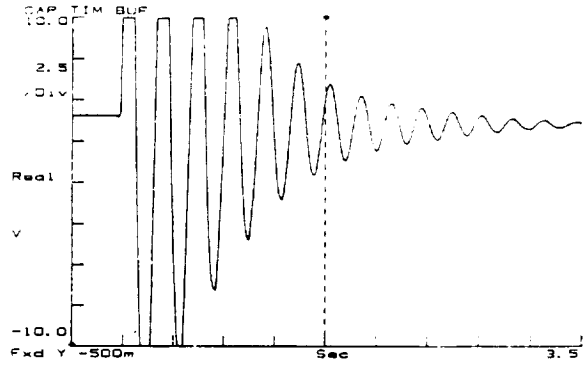

Figure 3a. Lower Link Strain for Joint P.D. Control, Step Input.

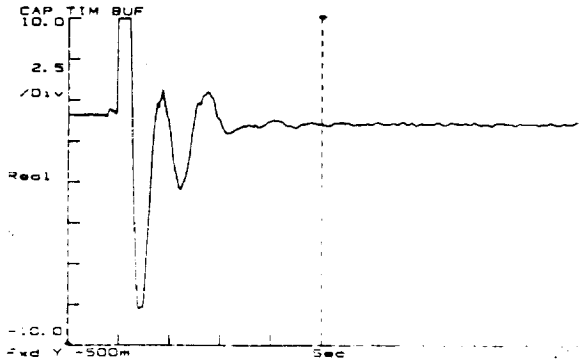

Figure 3b. Lower Link Strain for Strain Feedback LQR, Step Input.

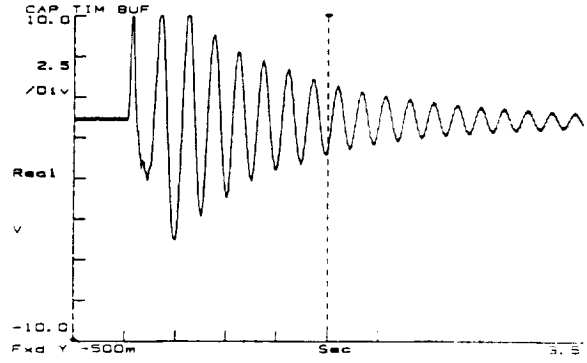

Figure 4a. Lower Link Strain for Joint P.D. Control, Step Input.

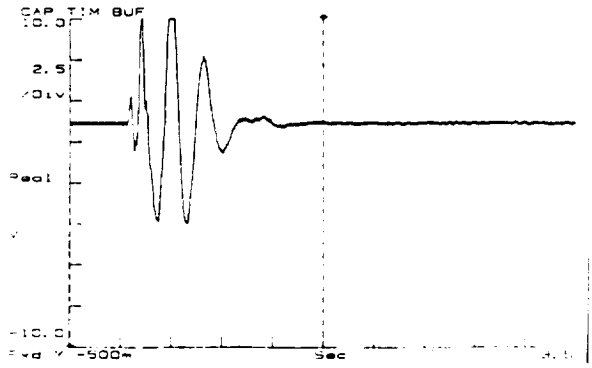

Figure 4b. Lower Link Strain for Strain Feedback LQR, Step Input.

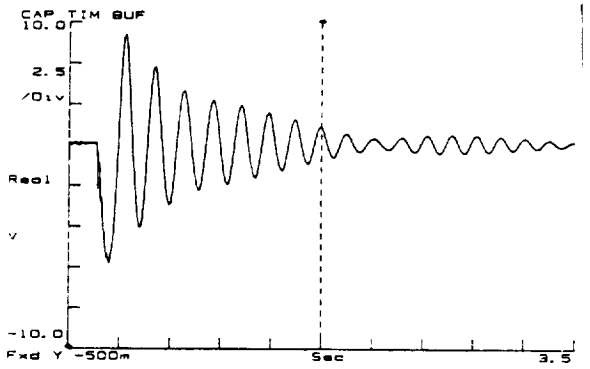

Figure 5a. Lower Link Strain for Joint P.D. Control, Impulse Disturbance.

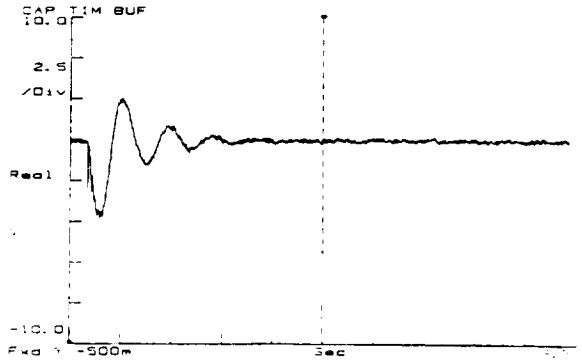

Figure 5b. Lower Link Strain for Strain Feedback LQR, Impulse Disturbance.

To be presented at the 1989 ASME Winter Annual Meeting and to appear in its Proceedings.

DECENTRALIZED ADAPTIVE CONTROL OF A TWO DEGREE OF FREEDOM FLEXIBLE ARM

B.S. Yuan W.J. Book J.D. Huggins

School of Mechanical Engineering
Georgia Institute of Technology
Atlanta, GA 30332-0405

ABSTRACT

A robust adaptive control is derived by signal-synthesis methods for a light, flexible two degree-of-freedom manipulator. The controller for each joint is decentralized, using measurements of one joint's position as well as one link's strain. The coupling to other dynamics is treated as a bounded uncertainty in the model. A stability proof has been developed and is outlined. Performance of the advanced controller is compared to a Linear Quadratic Regulator (LQR) and to an independent joint control. Both simulations and experiments are presented. The cases of payload variations are considered at this point.

I. INTRODUCTION

The industrial robotic arm has been designed for rigidity by implementing short link lengths and heavy steel construction in order to achieve positional accuracy and stability of the robot's movement. The resulting disadvantages include slow motion speed, low payload to weight ratio and high power consumption. To overcome these issues, a robotic arm with a light-weight structure poses an important solution for the designer of the next generation of robots. The main problem with light-weight structures is in the resulting flexible vibrations which are naturally excited as the arm is commanded to move or is disturbed. An effective control is one key to moving the flexible arm with high-speed motion and fast vibration settling time [1,2].

In order to demonstrate the control system of a flexible arm, a large flexible manipulator arm, designated RALF (Robotic Arm, Large and Flexible), is used in the experiment. The robotic system with the independent joint PD (Proportional-Derivative) controller, which is proven to be stable via the Lyapunov criterion, leads to the development of an advanced control algorithm using a decentralized scheme. In other words, each flexible link can be considered as a subsystem of the overall system. Under consideration of the uncertainty for interconnected terms of each subsystem, the dynamic system of the manipulator motion is illustrated to be bounded by the reference model, which is chosen to be stable. The possible magnitude of the uncertainty is presumed known, making the statistical information for a stochastic approach unnecessary [3]. Thus, the feedback systems are also insensitive to other uncertainties such as friction, measurement error, backlash and etc.

Certain matching conditions are assumed to guarantee that the uncertainty vector does not influence the dynamics more than the control input does [4]. The signal-synthesis adaptation approach used here results in a robust design that reduces the burden of on-line computation, while an auxiliary input with the update action should have faster convergence rate and smaller steady-state error.

Simulations and experiments are carried out to compare this controller to the independent joint PD controller and an LQR controller. The sensitivity of the control performance to variations in payload ranging from 0% to 40% of the arm structure is considered.

II. DYNAMIC MODELING AND INDEPENDENT JOINT CONTROLLER

To specify the robot controller, the dynamical equations of motion need to be developed for the system design [5]. A rigid arm will have one generalized coordinate per joint, but a flexible arm may have many. Transformations representing the joint coordinates and link deflection can be used to represent the position r_i of a point. The velocity can be related to the coordinate derivatives as [7]

$$\dot{r}_i = J_i \dot{X}_i \ , \qquad (2.1)$$

where

- r is the velocity vector in the Cartesian coordinates,
- J_i is the 3xL matrix of Jacobian,
- X_i represents the time derivative vector including i joints, say, $q_1, q_2, \ldots q_i$, and L_i-i time dependent flexible coordinates.

The kinetic energy of the n-link flexible arm is then:

$$KE = \frac{1}{2} \sum_{i=1}^{n} \int_{link_i} \dot{r}_i^T \dot{r}_i \, dm \qquad (2.2a)$$

$$= \frac{1}{2} \sum_{i=1}^{n} \dot{X}_i^T \left(\int_{link_i} J_i^T J_i \, dm \right) \dot{X}_i$$

$$= \frac{1}{2} \dot{X}_n^T \, M \, \dot{X}_n ,$$

where

$$M = \sum_{i=1}^{n} \int_{link_i} \left(J_i^T J_i \right) dm \ . \qquad (2.2b)$$

It is mentioned that the inertia matrix M, a function of position, is symmetric and positive definite. The kinetic energy of rigid robotic arms have the same structure as (2.2a)

Without the effect of gravity, the potential energy of the flexible arm which includes the elastic joint and strain energy is expressed as

$$PE = \frac{1}{2} \bar{X} K \bar{X}, \qquad (2.3)$$

where

$\bar{X} = X - Xo$, Xo is the unstretched coordinate at the "home" position.

K is the stiffness matrix, which has the corresponding value as described in Ref. [7].

By applying the Lagrangian formula, the equation of motion in the Matrix-Vector form is:

$$M\ddot{X} + H\dot{X} + K\bar{X} = Q, \qquad (2.4)$$

where

Q is the generalized force, which acts on the joint q only.

H represents nonlinear terms and (M - 2H) is skew symmetric.

The similar form has also been found in the rigid arms without the stiffness term K.

Hence, a multi-link flexible arm with independent joint controllers will be stable. The case of a rigid-link manipulator has been illustrated by Asada and Slotine [5]. The frequency domain approach has been taken by Book [1] for flexible arms, and physically, the feedback system effectively equips each joint with an equivalent rotary spring and damper. The input torque then has the following form:

$$T_i = K_{pi}\bar{q}_i + K_{di}\dot{\bar{q}}_i, \qquad (2.5)$$

where

K_{pi} and K_{di} are positive constants,

$\bar{q}_i = q_i - q_{io}$, q_{io} is the reference path and assumed to be constant. $\dot{q}_i = \dot{q}_i$.

Because the torque acts only on each joint, the following equality exists

$$Q^T\dot{X} = \tau^T q, \qquad (2.6)$$

where

$$\tau^T = [\tau_1, \tau_2, \ldots\ldots \tau_n], \quad q^T = [q_1, q_2, \ldots\ldots q_n],$$

Choose a Lyapunov candidate V associated with the total energy of the feedback system:

$$V(\dot{X},\bar{X},q) = \frac{1}{2}[\dot{X}^T M\dot{X} + \bar{X}^T K\bar{X} + \bar{q}^T K_p \bar{q}], \qquad (2.7)$$

where

$$K_p = diag\,[K_{pi}]$$

Differentiating V with respect to time gives

$$\dot{V} = \dot{q}^T K_p \bar{q} + \dot{X}^T M\ddot{X} + \frac{1}{2}\dot{X}^T\dot{M}\dot{X} + \dot{X}^T K\bar{X} \qquad (2.8a)$$

$$= \dot{q}^T K_p \bar{q} + \dot{X}^T(M\ddot{X} + K\bar{X}) + \frac{1}{2}\dot{X}^T\dot{M}\dot{X}$$

By substituting (2.5), (2.6), (2.4) and the skew-symmetry of (M-2H) into above,

$$\dot{V} = \dot{q}^T K_p \bar{q} + \dot{X}(Q - H\dot{X}) + \frac{1}{2}\dot{X}^T\dot{M}\dot{X}$$

$$= \dot{q}^T K_p \bar{q} + \dot{X}^T Q + \frac{1}{2}\dot{X}^T(\dot{M} - 2H)\dot{X}$$

$$= \dot{q}^T K_p \bar{q} + \dot{q}^T\tau$$

$$= -\dot{q} K_D \dot{q} \le 0$$

where

$k_D = diag[k_{di}]$ is a positive matrix.

Therefore, the system with a local joint PD controller leads to the development of an advanced control algorithm using a decentralized scheme which is restrictive on information transfer from one group of sensors and actuators to others.

III. DECENTRALIZED ADAPTIVE CONTROL

Without loss of generality, the system of a two-degree-of-freedom flexible manipulator with the effect of gravity is considered from the control viewpoint; i.e, n=2. To combine with friction and other disturbances that are treated as uncertainties R(X,$\dot{X}$), the equations of motion are, then, rewritten as follows:

$$M(X)\ddot{X} + H(X,\dot{X})\dot{X} + K\bar{X} + G(X) + R(X,\dot{X}) = Q \qquad (3.1)$$

The actuator dynamics is ignored.

Since the inertia matrix, M(X), is square, symmetric and positive definite, one can always find a constant matrix β such that the elements of β corresponding to the coupling subsystem are zero and

$$|\beta| \ge |M^{-1}(X) - \beta| \qquad (3.2)$$

where $|\cdot|$ is an induced norm.

Equation (3.1) can be rearranged as

$$\ddot{X} = -M^{-1}[H\dot{X} + K\bar{X} + G + R] + \beta Q + (M^{-1} - \beta)Q \qquad (3.3)$$

With i = 1,2 , let $z_i = [x_i, \dot{x}_i]^T$ and equation (3.3) is divided into two equations for two subsystems,

$$\dot{Z}_i = A_i Z_i + b_i u_i + F_i(Z) + f_i(Z)u_i \qquad (3.4)$$

where $u_i = \tau_i$ in (2.6); $f_i(Z)u_i$ = the coupling terms of $(M^{-1} - \beta)Q$ for subsystem i. A_i is a constant matrix which represents the linear time invariant part of $-M^{-1}K$,

$$A_i = \begin{bmatrix} 0 & I \\ a_{i1} & a_{i2} \end{bmatrix} \qquad (3.5)$$

while $F_i(Z)$ represents the rest of $-M^{-1}K$ and the nonlinear terms of $-M^{-1}[H+R+G]$. b_i, then , becomes a vector form with zero elements on the upper half.

It is assumed that F_i and f_i are bounded and have the following properties:

$$F_i(Z) = b_i D_i(Z) \qquad (3.6)$$

$$f_i(Z) = b_i E_i(Z)$$

where D_i and E_i have the corresponding dimensions; $|E_i| < 1$ from (3.2).

These conditions, called the matching conditions [8], guarantee that the uncertainty does not influence the dynamics more than the control input does [4]. The one degree-of-freedom system, has been illustrated by the previous works [9] , and for the two degree-of-freedom flexible arm, each link is considered as a subsystem.

The objective of model reference adaptive control is to eliminate the state error between the plant and the reference model so that the behavior of the plant follows the model. Consider the reference model first,

$$\dot{Z}_{mi} = A_{mi} Z_{mi} + b_{mi} r_i \qquad (3.7a)$$

where

$$Z_{mi} = [X_{mi} , \dot{X}_{mi}]^T$$

r_i is the reference input,

and let

$$A_{mi} = A_i + b_i K_{zi} \qquad (3.7b)$$

$$b_{mi} = b_i K_{bi}$$

where K_{zi} and K_{bi} are constant matrices with the corresponding dimensions.

Also, A_{mi}, which is a stable matrix, satisfies the Lyapunov equation,

$$A_{mi}^T P_i + P_i A_{mi} = - L_i \qquad (3.7c)$$

where P_i and L_i are positive definite and symmetric matrices.

The signal-synthesis method [10] implemented here seeks to control the system by adjusting the input u_i which is as described in the following equation

$$u_i = K_{zi} Z_i + K_{bi} r_i + \psi_i(e_i) \qquad (3.8)$$

where $e_i = z_{mi} - z_i$ is referred to as the state error and the function ψ_i is the control input to compensate the system uncertainty. Thus, let ψ_i be

$$\psi_i = \begin{cases} \dfrac{b_i^T P_i e_i}{|b_i^T P_i e_i|} \rho_i(Z, e_i, r_i), & \text{when } |b_i^T P_i e_i| > \delta_i \\ \dfrac{b_i^T P_i e_i}{\delta_i} \rho_i(Z, e_i, r_i), & \text{when } |b_i^T P_i e_i| \le \delta_i \end{cases} \qquad (3.9)$$

where δ_i is a prescribed positive constant and ρ_i is a positive constant to be specified subsequently.

As a result, the error dynamics of the subsystem is derived from the difference between equation (3.4) and (3.7) along with (3.8) and (3.9):

$$\dot{e}_i = \dot{Z}_{mi} - \dot{Z}_i = A_{mi} e_i - b_i(\psi_i + \nu_i), \qquad (3.10a)$$

where

$$\nu_i = D_i + E_i(K_{zi} + K_{bi} r_i + \psi_i) \qquad (3.10b)$$

Given the boundedness of the state variable z_i and the reference input r_i, equation (3.10b) with (3.9) has the following inequality:

$$|\nu_i| \le \rho_i (Z, \rho_i, r_i) , \qquad (3.11a)$$

where

$$\rho_i \triangleq |D_i| + |E_i|(|K_{zi} Z_i| + |K_{bi} r_i| + |\psi_i|) \qquad (3.11b)$$

This definition involving ρ_i on both sides of the equation is valid; i.e., (3.11) can be solved, since (3.2) is satisfied. Therefore, we have

$$\rho_i = (1 - |E_i|)^{-1} [|D_i| + |E_i|(|K_{zi} Z_i| + |K_{bi} r_i|)] \qquad (3.12)$$

To specify that the error dynamics (3.10) is uniformly bounded, the approach is also based on the Lyapunov criterion and similar to ref. [8]. Given a candidate

$$V_i = e_i^T P_i e_i , \qquad (3.13a)$$

and there exists

$$\dot{V}_i = \dot{e}_i^T L_i e_i - 2 e_i^T P_i b_i (\psi_i + \nu_i)$$

$$\le e_i^T L_i e_i - 2[b_i^T P_i e_i][\psi_i - \frac{b_i P_i e_i}{|b_i^T P_i e_i|} \rho_i] \qquad (3.13)$$

Consequently, $\dot{V}_i \le 0$

Furthermore, to improve the convergence rate of equation (3.10), an auxiliary input $w_i(t)$ is introduced and applied to the input u_i in (3.8) [7]. This input is apparently an integral action and

$$\dot{W}_i(t) = - \alpha_i W_i(t) + S_i^{-1} b_i^T P_i e_i , \qquad (3.14)$$

where

$$\alpha_i \ge \frac{4 \delta_i \rho_i - \lambda_{min}(L_i) |\rho_i|^2}{2 \lambda_{min}(S_i) |W_i|^2}$$

$$S_i > 0$$

Note that λ_{min} represents the minimum eigenvalue.

The error dynamics of the total system can be proven stable by summing the individual Lyapunov function (3.13) [7]. The block diagram of the decentralized adaptive control is shown in Figure 1.

IV. SIMULATIONS AND EXPERIMENTS

The following section will demonstrate the results obtained from the analytical works using RALF, which is in the Flexible Automation Laboratory at Georgia Tech. The arm is constructed of two ten foot links and two rotary joints. The second joint is actuated through a parallelogram mechanism by a hydraulic cylinder at the base [11]. A simple yet adequate dynamical model for RALF has been established, wherein the parallel link is described simply as a spring [7].

A MicroVax II running the VMS operating system is used to provide high speed calculation for real-time control and data-acquisition. The resolution of D/A and A/D is 12 bits/10 Volts, and the sampling time is 8 ms. For the initial measurement, the bandwidth of both hydraulic motors is above 45 Hz and the lowest frequencies of the RALF are 5.69 Hz and 9.12 Hz. The parallel link's lowest frequency is about 30 Hz, which cannot be controlled. A linear variable differential transformer (LVDT) is the position transducer mounted on the hydraulic piston rod, so that the noncollocation problem existing in the feedback control of flexible structures may be avoided. The link deflection is obtained by utilizing a strain gage mounted near the joint. One flexible mode is adopted for each link in this work.

The first joint position of 35° and the second joint position of 109° are set to be the "home" position for RALF. A linearized dynamical equation is used to derive the constant gains Kz_i and Kb_i in (3.7) and (3.8), while the payload is not considered at this moment [11]. Kz_i (i=1,2) are:

$$K_{zi} = [-2.8E7 \ -1.35E4 \ -2.8E5 \ -1.14E3] \ , \quad (4.1)$$

$$K_{z2} = [-3.0E7 \ -1.01E4 \ -7.76E4 \ -2.68E2] \ ,$$

and $Kb_i = 1$.

The gains associated with the joint positions and velocities turn out to be the independent joint controller in (2.5) as follows:

$$K_p = \begin{bmatrix} 2.8E7 & 0 \\ 0 & 3.0E7 \end{bmatrix} \quad (4.2)$$

$$K_D = \begin{bmatrix} 2.8E5 & 0 \\ 0 & 7.76E4 \end{bmatrix}$$

To get b_i, equation (3.2) needs to be satisfied and β has the interconnecting elements of zero. Thus, b_1 and b_2 are:

$$b_1 = \begin{bmatrix} 0 \\ 0 \\ 0.002 \\ -0.259 \end{bmatrix} \quad (4.3)$$

$$b_2 = \begin{bmatrix} 0 \\ 0 \\ 0.0373 \\ -5.267 \end{bmatrix}$$

The values of ρ_i and δ_i are chosen as 3.0E5 and 2.0 respectively. For the decentralized adaptive control, S_i^1 is 3.0E2 and α_i is simply set to zero.

The distal ends of both the lower and the upper links are moved 24.3 inches in 1 second for joint point-to-point control. Figures 2a-d show the time responses of the feedback system without payload, and Figures 3a-d show results with a 30 lb payload. Note that the best tracking and fast oscillation-setting time of each link occurs with adaptation but that the link oscillations damped out more slowly for the joint PD control and LQR, when the system has the payload on the tip. However, all of the three controllers demonstrate the robustness with the variation of payload. When the controller is implemented in the experiment, the gains are scaled to match the physical capability of the system. Figures 4a,b show the time responses of the joints with the PD controller and with the decentralized adaptive controller without payload. The strain responses are demonstrated in Figures 4c-f. With payload, the response is as shown in Figures 5. It should be mentioned that the gravitational effect provides the partial reason for the steady-state error in the joint PD control.

The results from simulations are compared with the experiments to illustrate certain agreement. The fact that the simplified model, (the actuator dynamics ignored and one flexible mode used), implemented in the simulation may cause small deviation from the measured experimental data is, however, expected and acceptable from the engineering point of view.

V. CONCLUSION

A flexible arm with positive gains and negative feedback independently controlling each joint is shown theoretically and experimentally to be stable. The decentralized algorithm results have shown much improvement of the system responses. To achieve insensitivity to variations of the payload, the adaptive scheme of control is superior. The assumption of banded and small interconnecting action between subsystems is consequently appropriate.

ACKNOWLEDGEMENTS

This work was partially supported through NASA Grant NAG1-623 and the Computer Integrated Manufacturing Systems Program at the Georgia Institute of Technology.

REFERENCES

[1] Book, W. J.,"Model, design and control flexible manipulator arms," Ph.D. Thesis, Dept. of Mech. Engr. MIT, April 1974.

[2] Cannon, R. M., Schmitz, E.,"Initial experiments on the end-point control of a flexible one-link robot," Int. J. of Robotics Research, Fall 1984, pp. 62-75.

[3] Chen, Y. H. ,"On the deterministic performance of uncertain dynamical systems," Int. J. Control, Vol.43, 1986, pp.521-525.

[4] Gutman, S.,"Uncertain dynamical systems - a Lyapunov Min-Max approach," IEEE Trans. on Auto. Control, June 1979.

[5] Asada, H., Slotine, J. J., Robot analysis and control, John Wiley and Sons, 1986.

[6] Book, W. J.,"Recursive Lagrangian dynamics of flexible manipulator arms," Int. J. of Robotics Research, Vol.3, No.3, 1984, pp.87-101.

[7] Yuan, B.,"Adaptive strategies for controls of flexible arms," Ph.D. Thesis, Dept. of Mech. Engr., Ga. Tech., April 1989.

[8] Leitmann, G.,"On the efficacy of nonlinear control in uncertain linear systems," ASME J. of Dynamic Systems, Measurement and Control, 1981, PP.95.

[9] Yuan, B., Book, W. J., Siciliano, B.,"Direct adaptive control of a one-link flexible arm with tracking," Accepted to be published in J. of Robotic Systems.

[10] Landau, Y. D., Adaptive Control - the Model Reference Approach, Marcel Dekker Inc., 1979.

[11] Yuan, B. S., Book, W. J., Huggins, J. D.,"Small motion experiments on large flexible arm with strain feedback," 1989 American Control Conference, June 1989.

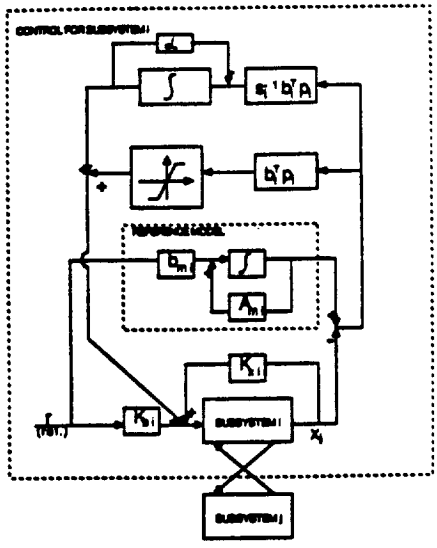

Figure 1. Block Diagram of the Decentralized Adaptive Control.

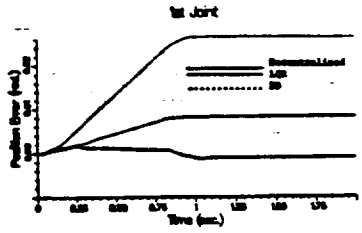

Figure 2a. Error Response of 1st Joint (Without Payload).

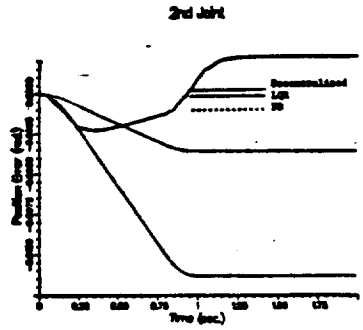

Figure 2b. Error Responses of 2nd Joint (Without Payload).

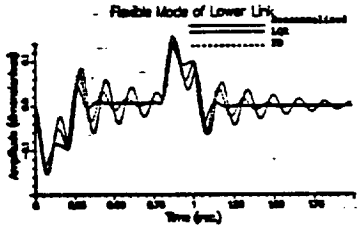

Figure 2c. Strain Responses of Lower Link (Without Payload).

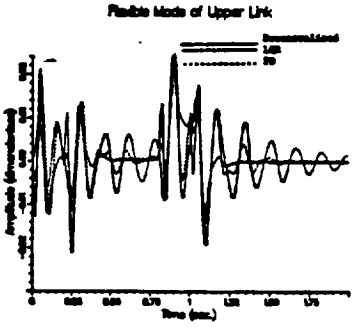

Figure 2d. Strain Responses of Upper Link (Without Payload).

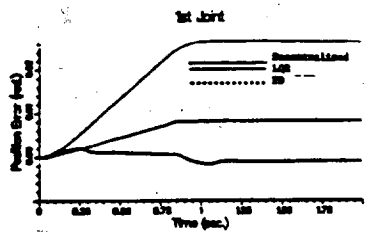

Figure 3a. Error Responses of 2st Joint (With Payload).

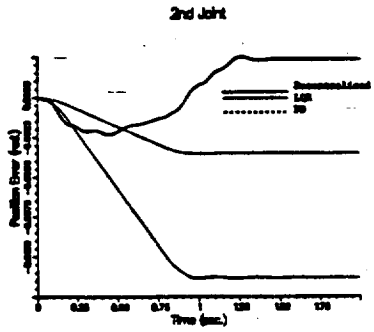

Figure 3b. Error Responses of 2nd Joint (With Payload).

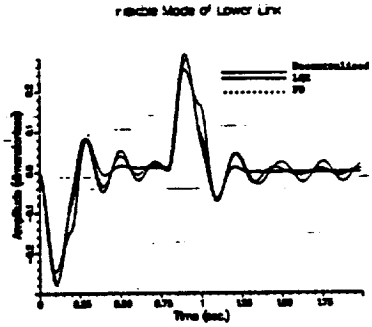

Figure 3c. Strain Responses of Lower Link (With Payload).

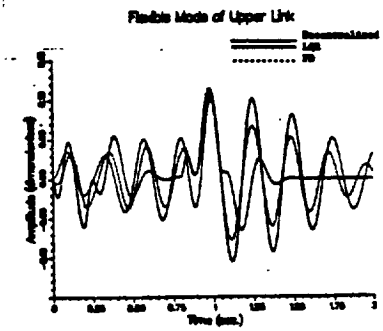

Figure 3d. Strain Responses of Upper Link (With Payload).

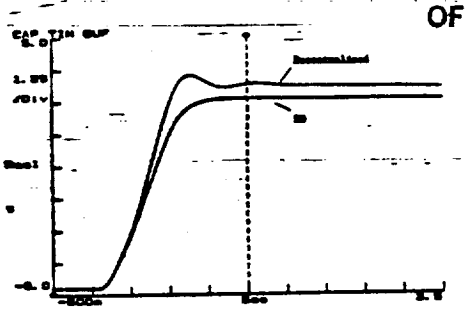

Figure 4a. Time Responses of 1st LVDT (Without Payload).

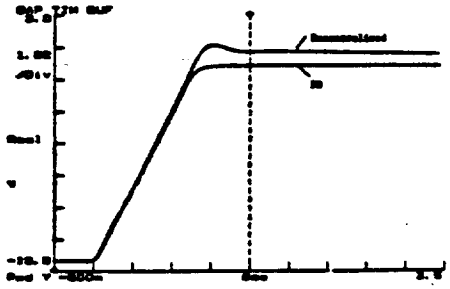

Figure 4b. Time Responses of 2nd LVDT (Without Payload).

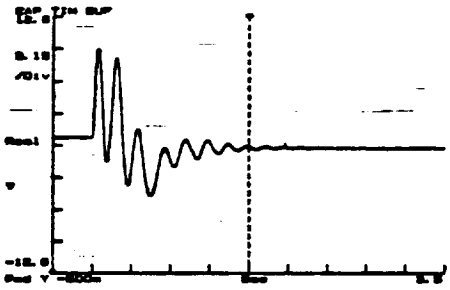

Figure 4c. Strain Responses of Lower Link (PD, Without Payload).

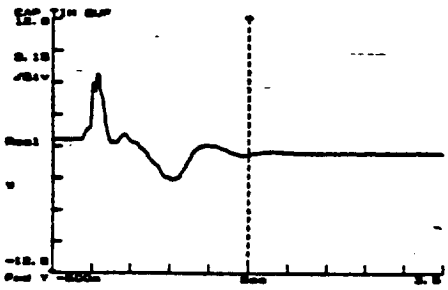

Figure 4d. Strain Response of Lower Link (Decentralized, Without Payload).

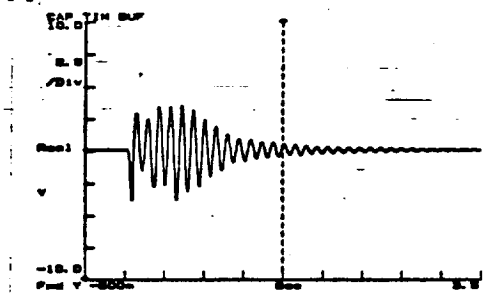

Figure 4e. Strain Response of Upper Link (PD, Without Payload).

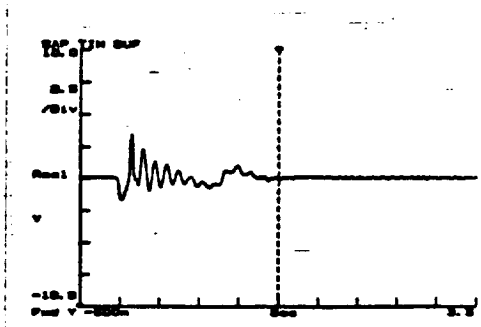

Figure 4f. Strain Response of Upper Link (Decentralized, Without Payload).

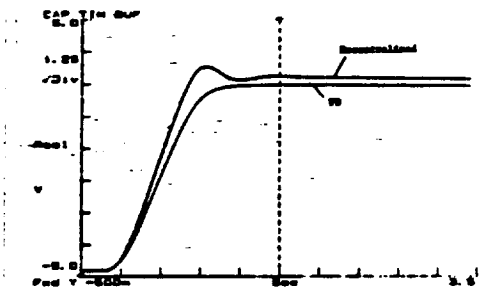

Figure 5a. Time Responses of 1st LVDT (With Payload).

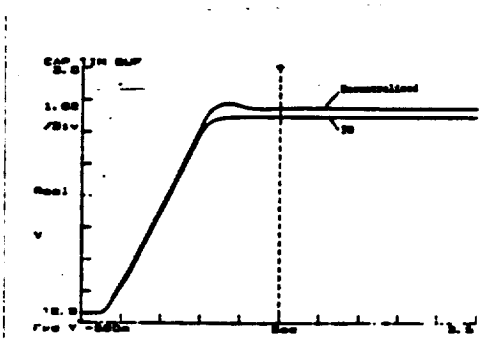

Figure 5b. Time Response of 2nd LVDT (With Payload).

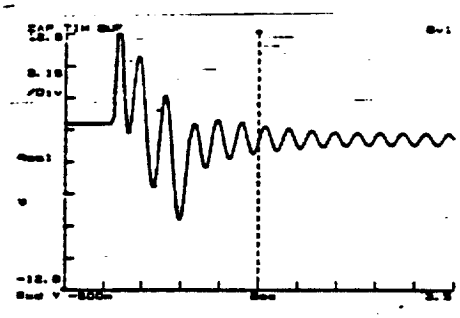

Figure 5c. Strain Response of Lower Link (PD, With Payload).

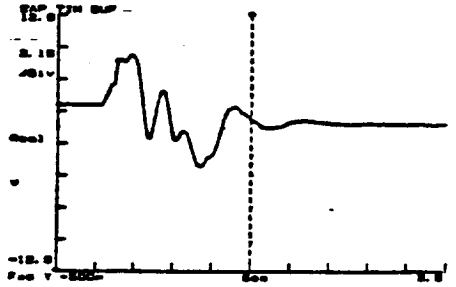

Figure 5d. Strain Response of Lower Link (Decentralized, With Payload).

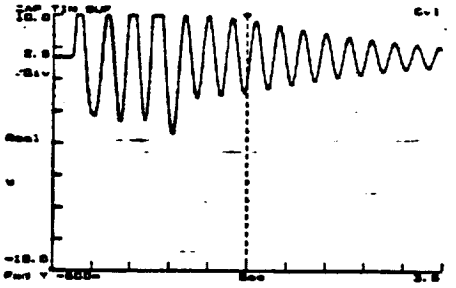

Figure 5e. Strain Response of Upper Link (PD, With Payload).

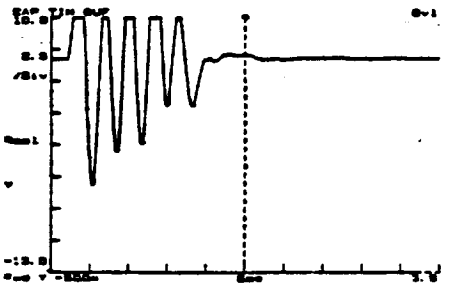

Figure 5f. Strain Response of Upper Link (Decentralized, With Payload).

To appear, J. of Robotic Systems.

Direct Adaptive Control of a One-Link Flexible Arm with Tracking

Bau-San Yuan* Wayne J. Book* and Bruno Siciliano•

*George W. Woodruff School of Mechanical Engineering
Georgia Institute of Technology
Atlanta, GA 30332, U.S.A.

•Dipartimento di Informatica e Sistemistica
Universita' di Napoli
Via Claudio 21; 80125 Napoli, Italy

Abstract

A robust tracking controller for a one link flexible arm based on a model reference adaptive control approach is proposed. In order to satisfy the model matching conditions, the reference model is chosen to be the optimally controlled linearized model of the system. The resulting controller overcomes the fundamental limitation in previously published research on direct adaptive control of flexible robots which required additional actuators solely to control the flexible degrees of freedom. The nominal trajectory is commanded by means of a tracking control. Simulation results for the prototype in the laboratory show improvements obtained with the outer adaptive feedback loop compared to a pure optimal regulator control. Robustness is tested by varying the payload mass.

Introduction

Lightweight arms are a challenging research topic with potential to improve over today's robot performance. Control is one key to effective use of lighter arms,[1,2] but it is limited by uncertainties in the arm's behavior and in the environment. The main problem with light-weight structures is the flexible vibrations which are naturally excited as the arm is commanded to move.[3]

The first step in designing a control system consists of developing a dynamic model for the flexible arm. A general dynamic modeling technique was established by Book,[4] based on a recursive Lagrangian-assumed modes method. If one is interested in the regulator control problem requiring that the arm reach a pre-specified nominal state with satisfactory response, the approach of linearizing the dynamic equations by assuming small motions around the nominal state and neglecting terms of higher order, proves effective. An optimal control for a one-link flexible arm was experimentally tested by Hastings and Book.[5] Also, experimental results with linear models were reported by Cannon and Schmitz[6], by Fukuda[7], by Sakawa et al.[8], and by Chalhoub and Ulsoy.[9] Frequency domain techniques, instead, were adopted by Book and Majette[10] and recently revisited by Ower and Van de Vegte.[11]

On the other hand, if one is concerned with controlling the arm while it is moving along a pre-defined path with given velocity and acceleration of the joint variables, the technique of linearizing the system is likely to fail. Furthermore, linearization around a sequence of nominal states, as done by Sunada and Dubowski[12] for instance, seems expensive

computationally and not necessarily very robust when applied to the overall nonlinear dynamics.

This paper describes research on control for a one link flexible arm moving along a pre-defined trajectories. The resulting controller overcomes the fundamental limitation in previously published research on direct adaptive control of flexible robots which required additional actuators solely to control the flexible degrees of freedom. Previous efforts aimed at designing tracking controllers for flexible arms have been produced by Singh and Schy[13] with a nonlinear inversion control, and by Davis and Hirschorn[14] with a linear control. They have both taken advantage, however, of additional active tip actuators. A nonlinear joint tracking controller has been devised by DeLuca and Siciliano[15]. A singular perturbation approach has been pursued, instead, by Siciliano and Book.[16]

The approach adopted here is based on Model Reference Adaptive Control (MRAC),[17] as recently proposed by Siciliano et al.[18] In order to assure the satisfaction of the so-called model matching conditions, the reference model is chosen as the linearized system (2nd order terms neglected) as optimally controlled. Integral type adaptive actions guarantee the stability of the overall system, as is proved via the Lyapunov direct method. However, since the reference model turns out not to be decoupled, the reference trajectory is forced on the system by means of a tracking controller.[19] A direct adaptive controller for a linear model of a flexible arm was also designed by Meldrum and Balas[20], but stability was guaranteed only for a special class of trajectories. An indirect adaptive control conversely, with dynamic parameter identification was proposed by Canudas, De Wit and Van den Bossche.[21]

A case study based on a laboratory prototype, whose dynamic model is described in Hastings and Book[22] shows that the control performs well when tracking a fast trajectory. The whole nonlinear system is considered for simulation purposes. Moreover, the control proves robust to parameter variations such as payload changes.

It must be mentioned that full state availability is assumed for control synthesis. While the state variables representing deflection can be obtained from strain gage measurements,[5] their derivatives need to be reconstructed by means of an observer.[23]

Problem Formulation

Nonlinear equations of motion for a flexible arm can be derived using the Lagrangian approach.[4] The deflection of the elastic members is represented as a linear combination of admissible functions multiplied by time dependent generalized coordinates.[24] The flexible motion of a link is then described by

$$u(\eta,t) = \sum_{i=1}^{n} \phi_i(\eta)\ \delta_i(t) \tag{1}$$

where the $\phi_i(\eta)$ are assumed in this paper to be eigenfunctions of a clamped-free beam, $\delta_i(t)$ are the generalized coordinates, and η is any point along the undeformed link (see Fig. 1). Furthermore, assuming that the amplitudes of the higher modes of the flexible link are very small compared to the lower modes, $n = 2$ will be accurate enough to describe the flexible motion.[22,25]

The derivation of the dynamic equations for the one link arm follows then as in Book[4] and Siciliano and Book[16] i.e. (dropping the explicit reference to time dependence)

$$M(\theta,\delta)\begin{bmatrix}\ddot{\theta}\\ \ddot{\delta}\end{bmatrix}+\begin{bmatrix}f_1\\ f_2\end{bmatrix}+\begin{bmatrix}0\\ K\delta\end{bmatrix}=\begin{bmatrix}u\\ 0\end{bmatrix} \tag{2}$$

where θ is the joint angle.

M is the inertia matrix.

f_1 and f_2 are vectors containing nonlinear dynamic terms

(interactions of angular rates and deflections).

K is the effective spring matrix.

u is the net input torque.

Notice that in the model no actuator dynamics is considered, and no friction at the joints nor in the structural vibrations is explicitly included. Define the full state vector

$$X^T = [x^{pT}, x^{vT}] \quad \text{and} \quad x^{vT} = [\dot{\theta}, \dot{\delta}^T] = \dot{x}^{pT} \tag{3}$$

The dynamic model of the flexible arm of Fig. 1 can be expressed in state variable form as

$$\frac{d}{dt}\begin{bmatrix}x^p\\ x^v\end{bmatrix}=\begin{bmatrix}0 & I\\ A_1(x^p) & A_2(x^p,x^v)\end{bmatrix}\begin{bmatrix}x^p\\ x^v\end{bmatrix}+\begin{bmatrix}0\\ B_2(x^p)\end{bmatrix}u \tag{4}$$

C - 2

$$\dot{X} = A(X)X + b(X)u \tag{5}$$

where

$$A_1(x^p)x^p = M^{-1}\begin{bmatrix} 0 \\ K\delta \end{bmatrix}$$

$$A_2(x^p, x^v)x^v = M^{-1}\begin{bmatrix} f_1 \\ f_2 \end{bmatrix}$$

$$B_2(x^p) = M^{-1}\begin{bmatrix} 1 \\ 0 \end{bmatrix}$$

At this point it becomes clear why the tracking control problem is difficult. If the goal is just to require that the arm reaches a pre-specified nominal state, linearizing (5) around the nominal state leads naturally to an optimal regulator in which one can eventually specify the closed loop poles of the linearized system with an arbitrary degree of stability. However, if one desires to control the arm while it moves along a pre-defined trajectory, in terms of joint angle rates and accelerations, a different approach must be sought, rather than trying to linearize (5) around a sequence of nominal states.

In order to obtain good trajectory tracking and steady-state accuracy, a direct MRAC approach[17] is pursued in the following. The basic idea of this approach is to define a linear time-invariant reference model and directly synthesize a controller that assures that the error between the states of the system and those of the model tends to zero. To this purpose let

$$\dot{X}_m = A_m X_m + b_m u_m \tag{6a}$$

$$A_m = \begin{bmatrix} 0 & I \\ A_{10} & A_{20} \end{bmatrix} \qquad b_m = \begin{bmatrix} 0 \\ b_0 \end{bmatrix} \tag{6b}$$

be a linear time-invariant reference model of the same dimension as the system described by eqs. (5).

As in the work on MRAC for rigid manipulators,[26,27] it would seem appropriate to select a decoupled model for (6), i.e. $A_{10} = \text{diag}(a_{11}\ a_{12}\ a_{13})$, $a_{1i} < 0$, $A_{20} = \text{diag}(a_{21}\ a_{22}\ a_{23})$, $a_{2i} < 0$. However the model matching conditions which are the basis of an MRAC approach[28] cannot be satisfied independent from the particular values of A, A_m, b, b_m. This can be confirmed by observing that the system described in (5) does not have as many control inputs as nontrivial state variables (θ, δ_1, δ_2), i.e. the lower block of vector b_0 in (6b) is not a square block (a row vector in this case).

In the particular case of the system in (5), however, the nonlinear terms do not play a dominant role, thus it appears adequate to choose a reference model on the basis of the linearized model of the system (2nd order terms neglected) as optimally controlled; this approach will be outlined in the next section.

Control Law Development

Following the basic MRAC scheme in Landau[17] a control for the overall system (5) - (6) is proposed in the form

$$u = u_1 + u_2 \tag{7a}$$

$$u_1 = -K_x^T X + K_u u_m \qquad u_2 = -\Delta K_x^T X + \Delta K_u u_m \tag{7b}$$

where u_1 is a linear model following control and u_2 represents the adaptive control which is devoted to assuring the stability of the whole system. Under the action of control (7), the system (5) becomes

$$\dot{X} = A_s(X)X + b_s(X)u_m \tag{8a}$$

$$A_s = A - b(K_x^T + \Delta K_x^T), \qquad b_s = b(K_u + \Delta K_u)\,. \tag{8b}$$

Let then

$$e = X_m - X \tag{9}$$

be the error between the model and system states. On reduction of (6) and (8), the error dynamics are found to be

$$\dot{e} = A_m e + (A_m - A_s)X + (b_m - b_s)u_m \tag{10}$$

In order to satisfy the model matching conditions, the following should hold:[28]

$$A_m = \tilde{A} - \tilde{b}K_x^T \qquad b_m = \tilde{b}K_u \tag{11}$$

where $\tilde{A}$ and $\tilde{b}$ are the linearized forms of A and b, respectively. Assuming that the pair $(\tilde{A},\tilde{b})$ is stabilizable, K_x^T can be designed by means of optimal control techniques for the linearized system in (A,b). K_u is chosen equal to 1 for simplicity. Substituting (8b) and (11) into (10) gives

$$\dot{e} = A_m e + [\Delta A - \Delta b K_u^T + b\Delta K_x^T]x + [\Delta b K_u - b\Delta K_u]u_m \tag{12}$$

where $\tilde{A} - A = \Delta A$ (13a)

and $\tilde{b} - b = \Delta b$ (13b)

express the difference between the actual system and its linearized parts. In order to guarantee the stability of the overall system, a candidate Lyapunov function is

$$V = e^T P e + tr[(A_m - A_s)^T F_a^{-1}(A_m - A_s)] + tr[(b_m - b_s)^T F_b^{-1}(b_m - b_s)] \tag{14}$$

where P, F_a, F_b are positive definite matrices. The derivative of V including (12) yields :

$$\dot{V} = e^T(A_m^T P + P A_m)e + 2tr[(\Delta A - \Delta b K_u^T + b\Delta K_x^T)^T(PeX^T - F_a^{-1}\dot{A}_s)] + 2tr[(\Delta b K_u - b\Delta K_u)T(Pe u_m - F_b^{-1}\dot{b}_s)] \tag{15}$$

Setting, as is usual,

$$A_m^T P + P A_m = -H \tag{16}$$

where H is a positive definite matrix, and assuming that the rate of the adjustable gains is larger than that of the system, $\Delta\dot{K}_x$, $\Delta\dot{K}_u >> \dot{A}, \dot{b}$, leads to

$$\dot{V} = -e^T He + 2tr[(\Delta A - \Delta b K_u^T + b\Delta K_x^T)^T(PeX^T + F_a^{-1}b\Delta\dot{K}_x^T)]$$
$$+ 2tr[(\Delta b K_u - b\Delta K_u)^T(Peu_m - F_b^{-1}b\Delta\dot{K}_u)] \tag{17}$$

At this point the choice of

$$\Delta\dot{K}_x^T = -(b^T F_a^{-1} b)^{-1} b^T PeX^T,$$
$$\Delta K_x^T\big|_{t=o} = \Delta K_{xo}^T \tag{18a}$$

$$\Delta\dot{K}_u = (b^T F_b^{-1} b)^{-1} b^T Peu_m,$$
$$\Delta K_u\big|_{t=o} = \Delta K_{uo} \tag{18b}$$

results in cancellation of the last two terms in (17), and assures that $\dot{V}$ is negative definite, thus guaranteeing that $e \to 0$ ($X \to X_m$).

The only problem now remaining is to force the system to track a desired trajectory. This point has been addressed by Meldrum and Balas[20] but, even with an equal number of controls

and output variables, only a sinusoidal reference trajectory could be commanded of the rigid body motion. An inverse model technique of the type proposed in Balestrino et al.[26] cannot be adopted since the model (6), satisfying (11), turns out not to be decoupled. However, the state-space design existing in the reference model (6) appears to provide a possible way out of this dilemma by specifying the development of systematic design procedures for both the optimal regulator and the tracking problems.[19]

Tracking Controller

The tracking problem was initially conceived in order to extend state-space regulator methods to problems having external command inputs. Therefore, consider an output form

$$Y = C X_m \tag{19}$$

where Y is the output to be tracked.

C is a constant matrix.

Meanwhile, a control system for the reference model (6) and (19) must be synthesized such that in the steady-state condition, the output Y becomes equal to some arbitrary desired constant reference output $Y_r(t) = Y_r$. In order to pursue this goal, the integral error W between the reference and the actual outputs is defined as follows :

$$\dot{W} = Y_r - Y \quad \text{or} \quad W = \int^t (Y_r - Y)dt \tag{20}$$

and the tracking control law can thus be written as

$$u_m = -K_m X_m - K_I W \tag{21}$$

where K_m, K_I are the proportional and the integral gains respectively. Adjoining (20) and (21) to (6), gives

$$\dot{Z} = A_o Z + B_o Y_r \tag{22}$$

where $Z^T = [X_m^T, W]$

$$A_O = \begin{bmatrix} A_m - b_m K_m & -b_m K_I \\ -C & 0 \end{bmatrix}$$

$$B_O = \begin{bmatrix} 0 \\ I \end{bmatrix}$$

It is claimed that the dynamic system (22) is asymptotically stable, if K_I is chosen appropriately. Then, in the steady state,

$$\lim_{t\to\infty} Z = Z_\infty = \begin{bmatrix} X_\infty \\ W_\infty \end{bmatrix} = -\begin{bmatrix} A_m + b_m K_m & -b_m K_I \\ -C & 0 \end{bmatrix}^{-1} \begin{bmatrix} 0 \\ I \end{bmatrix} Y_r \tag{23}$$

where the inverse matrix exists due to the asymptotical stability. Clearly, the desired zero error between Y and Y_r is also obtained in the steady state. i.e. $\lim_{t\to\infty} Y(t) = Y_r$ or $\lim_{t\to\infty} W(t) = 0$.

Now, the objective is to find the gains K_m and K_I. Define

$$\Delta X_m = X_m - X_\infty \quad \Delta W = W - W_\infty \quad \Delta u_m = u_m - u_\infty \tag{24}$$

where $u_\infty = -K_m X_\infty - K_I W_\infty$

The transient response is then governed by the set of differential equations

$$\frac{d}{dt}\begin{bmatrix} \Delta X_m \\ \Delta W \end{bmatrix} = \begin{bmatrix} A_m & 0 \\ -C & 0 \end{bmatrix}\begin{bmatrix} \Delta X_m \\ \Delta W \end{bmatrix} + \begin{bmatrix} b_m \\ 0 \end{bmatrix}\Delta u_m \tag{25}$$

An LQR design is utilized to minimize the performance functional for (25)

$$J = \int_0^\infty ([\Delta X_m{}^T \; \Delta W]\; Q \begin{bmatrix} \Delta X_m \\ \Delta W \end{bmatrix} + R\Delta u_m{}^2)\; dt \tag{26}$$

This results in

$$K_m = R^{-1} b_m S_{11} \tag{27a}$$

$$K_I = R^{-1} b_m S_{12} \tag{27b}$$

where $S = \begin{bmatrix} S_{11} & S_{12} \\ S_{12} & S_{22} \end{bmatrix} > 0$ is the solution of the Riccati equation.

In summary, since the constant matrix C is determined by the output Y, one needs at least as many inputs as the number of outputs to be tracked and needs the dynamical system (25) to be controllable.[19] Therefore, K_m and K_I are simultaneously derived as in (27). With

only one input, for example, the dynamical system (25) in the case of a one-link flexible arm may be uncontrollable when the joint velocity is to tracked as is shown in the following example. This may result in a singular solution for the Riccati equation (27). Finally, the total control problem becomes one of choosing the feedback constant gains K_x, K_u, along with the adaptive gains ΔK_x, ΔK_u for system stability, and K_m as well as the integral gain K_I for the desired reference tracking. In other words, u is composed of (7) and (21). The block diagram of the total system is shown in Fig. 2.

The Case Study

In the following a case study is developed for the one link flexible arm existing in the Flexible Automation Laboratory at Georgia Tech, whose specification is fully described in Appendix A.

As far as the joint angle trajectory is concerned, the arm is required to move from $\theta_i = 0$ deg. to $\theta_f = 90$ deg. in 2 seconds, following a standard trapezoidal velocity profile with maximum velocity $\dot{\theta} = 60$ deg./sec. The constant feedback gain resulting is K_x^T = [65.27 -176.13 -2937.23 27.27 -7.50 -67.27] and $K_u = 1$. ΔK_x^T and ΔK_u (18) have been chosen with $F_a = 2I$, $F_b = 0.005$, and $H = I$ in (16) such that the system under adaptive control is guaranteed to be stable. ΔK_{xo}^T and ΔK_{uo} are null here. An LQR design with $Q = 2I$ and $R = 1$, which is used to derive the tracking controller, results in K_m^T = [0.0 -0.635 -8.591 0.06 -0.056 0.046], $K_I = 0.031$ for the joint angular velocity to be tracked (Fig. 4 - 7) (i.e. C^T = [0 0 0 1 0 0]). For the joint angular position to be tracked (Fig. 8 - 11) (i.e. C^T = [1 0 0 0 0 0]), the tracking

controller is K_m^T = [0.616 -0.793 -10.004 0.1335 -0.034 0.05], K_I = 1.414. For the end point position to be tracked (Fig. 12 - 15) (i.e. C^T = [4. 2.02 -1.365 0 0 0]), K_m^T and K_I become [2.41 -1.27 -14.32 0.396 0.05 0.0058] and 1.4142. Also notice that the dynamic system which is linearized around zero states from (4) is used to derive the optimal (constant) gains K_x. This results in unstable responses for the constant (nonadaptive) feedback control system, when the arm travels at high velocity.

Different sets of simulations have been carried out, one with the above design parameters, and another one just with the constant feedback gains K_x^T and K_u, without any outer adaptive control. In order to analyze the control performance the whole nonlinear model has been simulated for the system (5) in both cases. A sampling rate of .1 ms has been adopted. Furthermore, the robustness of the system control to parameter variations has been tested by doubling the payload mass, without changing the constant control gains. Figs. 4 through 15 illustrate the results obtained. It can be recognized that the adaptive control performs better than the simple optimal control, as it results in better tracking accuracy.

First consider the case (Fig. 4 - 7) of joint velocity tracking. Fig. 4 shows the joint position response with and without adaptive control and corresponding reference input. Fig. 5 shows the joint velocity. Note better tracking occurs with adaptation but at the expense of some oscillations as gains adapt. Fig. 6 shows differences in the end point position error with

respect to the reference signal. Fig. 7 shows the joint torque. It should be pointed out that the dynamical system (25) does not satisfy the criteria of controllability. Therefore, the solution of the Riccati equation is singular, which causes undesirable response with inaccurate tracking and oscillations. However, such problems do not arise for joint position and end point tracking.

When the system is used to track a joint position command (Fig. 8 - 11), the nonadaptive control is unstable due to uncompensated nonlinearities and thus not plotted. The joint position response of the adaptive control is shown in Fig. 8 with the reference joint position command and responses for a nominal payload as well as twice the payload used in the design. The low steady-state error and the low effect of payload change illustrate the robust properties of the controller. Joint velocity, end point position error and control torques are illustrated in Fig. 9 - 11.

Another quantity tracked in this analysis is the end point position. Figs. 12 - 15 show the time responses for this simulation. The results are almost identical to the above joint position case, except that the end point position error is comparatively small during this control process. Note that this requires that the reference model predict the end point position.

Conclusions

A model reference adaptive control has been presented for a one link flexible arm which is based on the preliminary results obtained in Siciliano et al.[18] In order to comply with the

model matching conditions, the reference model has been set up to be the linearized arm model of the system as optimally controlled. Since the resulting reference model is not decoupled, the desired joint angle trajectory is commanded through a tracking controller proceeding the overall system. Full state availability has been supposed for control synthesis. The extension of this work to the use of an observer has been initiated and described in Yuan and Book.[23]

A case study has been developed for a prototype in the laboratory. Simulation results have shown the advantage of using an outer adaptive feedback control with respect to the pure optimal control and the robustness of the system control to payload variations. Furthermore, for the tracking controller, only the joint velocity command is not recommended based on the results of this work.

It must be emphasized, however, that for multiple link flexible manipulators the results obtained in this paper appear only partially satisfactory. In the case of more degrees of freedom, the nonlinear coupling terms in the joint variables (which are not present in the one link case) may become dominant, particularly at high speed, and control performance is likely to be derated.

This point, along with the problem of state reconstruction, or eventually considering output feedback, constitute two challenging research issues needing additional investigation.

Acknowledgements

The authors would like to acknowledge that this material is based in part on work supported by the Computer Integrated Manufacturing Systems Program at Georgia Tech, and by the NATO Science Programme (Special Panel on Sensory Systems for Robotic Control) under grant no. 687/86.

References

1. W. J. Book, O. Maizza-Neto and D. E. Whitney, "Feedback control of two beam, two joint systems with distributed flexibility," ASME J. Dyn. Syst., Measur. Contr., 97 (4), 424-431 (1975).

2. M. J. Balas, "Feedback control of flexible systems," IEEE Trans. Automat. Contr., AC-23, (4), 673-679, (1978).

3. A. Truckenbrodt, "Modelling and control of flexible manipulator structures," Proceedings of the 4th CISM-IFToMM Symposium on Theory and Practice of Robots and Manipulators, A. Morecki, G. Bianchi and K. Kedzior (Eds.), Zaborow, Poland, Sept. 8-12, 1981, pp. 90-101.

4. W. J. Book, "Recursive Lagrangian dynamics of flexible manipulator arms," Int. J. of Robotics Research, 3 (3), 87-101 (1984).

5. G. G. Hastings and W. J. Book, "Experiments in optimal control of a flexible arm," Proceedings of the American Control Conference, Boston, MA. June 10-12, 1985, pp. 728-729.

6. R. H. Cannon, Jr. and E. Schmitz, "Initial experiments on the end-point control of a flexible one-link robot," Int. J. Robotics Research, 3(3), 62-75 (1984).

7. T. Fukuda, "Flexibility control of elastic robotic arms," J. Robotic Systems, 2(1), 73-88 (1985).

8. Y. Sakawa, R. Matsumo and S. Fukushima, "Modeling and feedback control of a flexible arm," J. Robotic Systems, 2(4), 453-472 (1985).

9. N. G. Chalhoub and A. G. Ulsoy, "Control of a flexible robot arm: experimental and theoretical results," ASME J. Dyn. Syst. Meas. Contr., 109 (4), 299-309 (1987).

10. W. J. Book and M. Majette, "Controller design for flexible, distributed parameter mechanical arms via combined state space and frequency domain techniques," ASME J. Dyn. Syst. Meas. Contr., 105(4), 245-254 (1983).

11. J. C. Ower and J. Van de Vegte, "Classical control design for a flexible manipulator: modeling and control system design," IEEE J. Robotics, Automation, RA-3 (5), 485-489, (1987).

12. W. H. Sunada and S. Dubowski, "On the dynamics analysis and behavior of industrial robotic manipulators with elastic members," ASME J. Dyn. Syst., Meas., Contr., 105(1), 42-51 (1983).

13. S. N. Singh and A. A. Schy, "Control of elastic robotic systems by nonlinear inversion and modal damping," ASME J. Dyn. Syst., Meas., Contr., 108 (3), 180-189, (1985).

14. J. H. Davis and R. M. Hirschorn, "Tracking Control of a Flexible Robot Link," IEEE Trans. Automat. Contr. AC-33 (3), 2 38-248 (1988).

15. A. De Luca and B. Siciliano, "Joint-based control of a nonlinear model of a flexible arm," Proceedings of the American Control Conference, Atlanta, GA, June 15-17, 1988, pp. 935-940.

16. B. Siciliano and W. J. Book, "A singular perturbation approach to control of light-weight flexible manipulators," Int. J. Robotics Research, 7(4), 79-90, (1988).

17. Y. D. Landau, Adaptive Control: The Model Reference Approach, Marcel Dekker, Inc., NY, 1979.

18. B. Siciliano, B. S. Yuan and W. J. Book, "Model reference adaptive control of a one link flexible arm," Proceedings of the 25th IEEE Conf. on Decision and Control, Athens, Greece, Dec. 10-12, 1986, pp. 91-95.

19. P.C. Young and J. C. Willems, "An approach to the linear multivariable servomechanism problem," Int. J. Control, 15 (5), 961-979 (1972).

20. D. R. Meldrum and M. J. Balas, "Direct adaptive control of a remote manipulator arm," Robotics and Manufacturing Automation (Proceedings of the ASME Winter Annual Meeting), H. Donath and M. Leu (Eds), Miami, FL, Nov. 17-22, 1985, pp. 115-120.

21. C. Canudas De Wit and Van den Bossche, "Adaptive control of a flexible arm with explicit estimation of the payload mass and friction," Preprints of the IFAC/IFIP/IMACS Int. Symposium on Theory of Robots, P. Kopacek, I. Troch and K. Desoyer (Eds)., Vienna, Austria, Dec. 3-5, 1985, pp. 315-320.

22. G. G. Hastings and W. J. Book, "A linear dynamic model for flexible robotic manipulators," IEEE Control Systems Magazine, 7, (1), 61-64 (1987).

23. B. S. Yuan and W. J. Book, "A robust scheme for direct adaptive control of flexible arms," in Modeling and Control of Robotic Manipulators and Manufacturing Processes, R. Shoureshi, K. Youcef-Toumi and H. Kazerooni (Eds.), ASME DSC-Vol. 6, 261-269 (1987).

24. L. Meirovitch, Analytical Methods in Vibrations, Macmillian, NY, 1967.

25. P. C. Hughes, "Space structure vibration modes: How many exists? Which ones are important? " IEEE Control System Magazine, 7 (1), 22-28 (1987).

26. A. Balestrino, G. De Maria and L. Sciavicco, "An adaptive model following control for robotic manipulators," ASME J. Dyn. Syst., Meas., Contr., 105 (3), 143-151 (1983).

27. K. L. Lim and M. Eslami, "Adaptive controller designs for robot manipulator systems using Lyapunov direct method," IEEE Trans. Automat. Contr., AC-30 (12), 1229-1233, (1985).

28. H. Erzberger, "Analysis and design of model following control systems by state space techniques," Proceedings of the Joint American Control Conference, Ann Arbor, MI, June 26-28, 1968, pp. 572-581.

Appendix A : Specification of Experimental Properties

Beam
Length : 48 in
Section : 3/16 * 3/4 in^2
EI : 4120
Material : Aluminum
Alloy : 6065-T6

Payload
Weight : 0.1 lb
Material : Aluminum
Alloy : 6065-T6

Torque Motor
Manufacturer : INLAND MOTOR
Type : T-5730 (Permanet Magnet DC)
Rotor Inertia : 0.06 in-lb-sec^2

Figure Captions

Fig. 1. The one link flexible arm
Fig. 2. Block diagram of the total control scheme
Fig. 3. 1st and 2nd mode shapes
Fig. 4. Joint position profiles (joint velocity to be tracked)
Fig. 5. Joint velocity profiles (joint velocity to be tracked)
Fig. 6. End point position errors (joint velocity to be tracked)
Fig. 7. Control torques (joint velocity to be tracked)
Fig. 8. Joint position profiles (joint position to be tracked)
Fig. 9. Joint velocity profiles (joint position to be tracked)
Fig. 10. End point position errors (joint position to be tracked)
Fig. 11. Control torques (joint position to be tracked)
Fig. 12. Joint position profiles (end point position to be tracked)
Fig. 13. Joint velocity profiles (end point position to be tracked)
Fig. 14. End point position errors (end point position to be tracked)
Fig. 15. Control torques (end point position to be tracked)

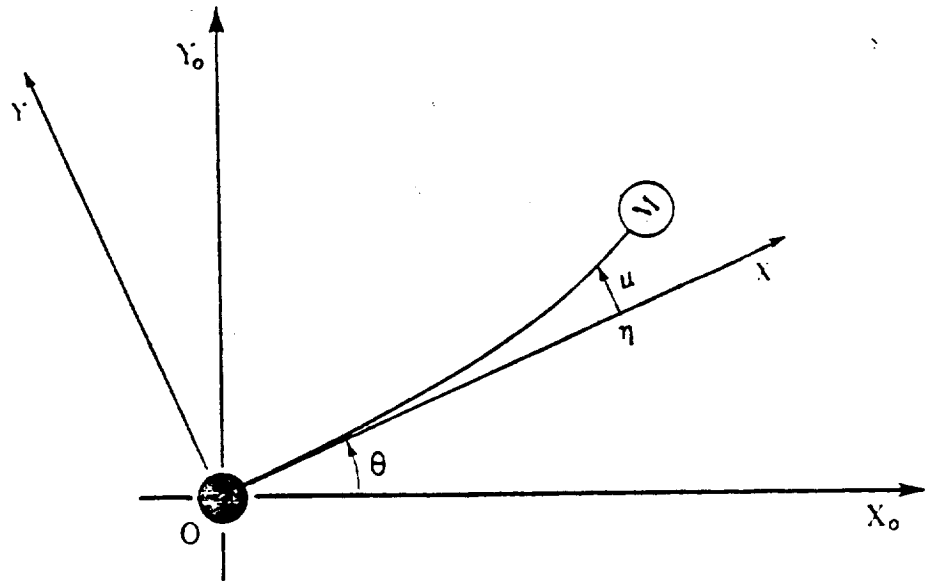

Fig. 1

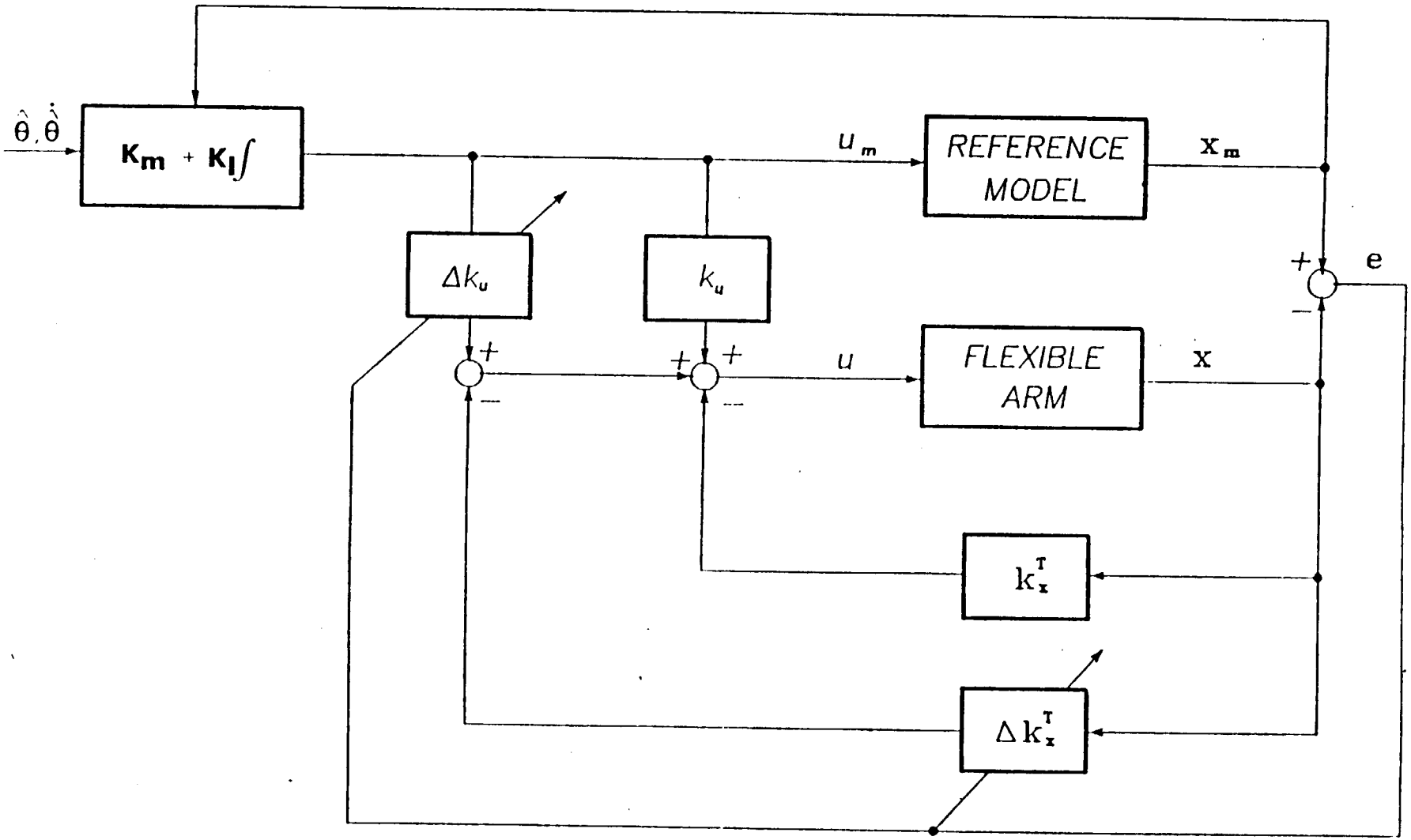
$\hat{\theta}, \dot{\hat{\theta}}$
$K_m + K_I \int$
u_m
REFERENCE MODEL
x_m
Δk_u
k_u
e
+
−
+
+
+
−
−
u
FLEXIBLE ARM
x
k_x^T
Δk_x^T

Fig. 2

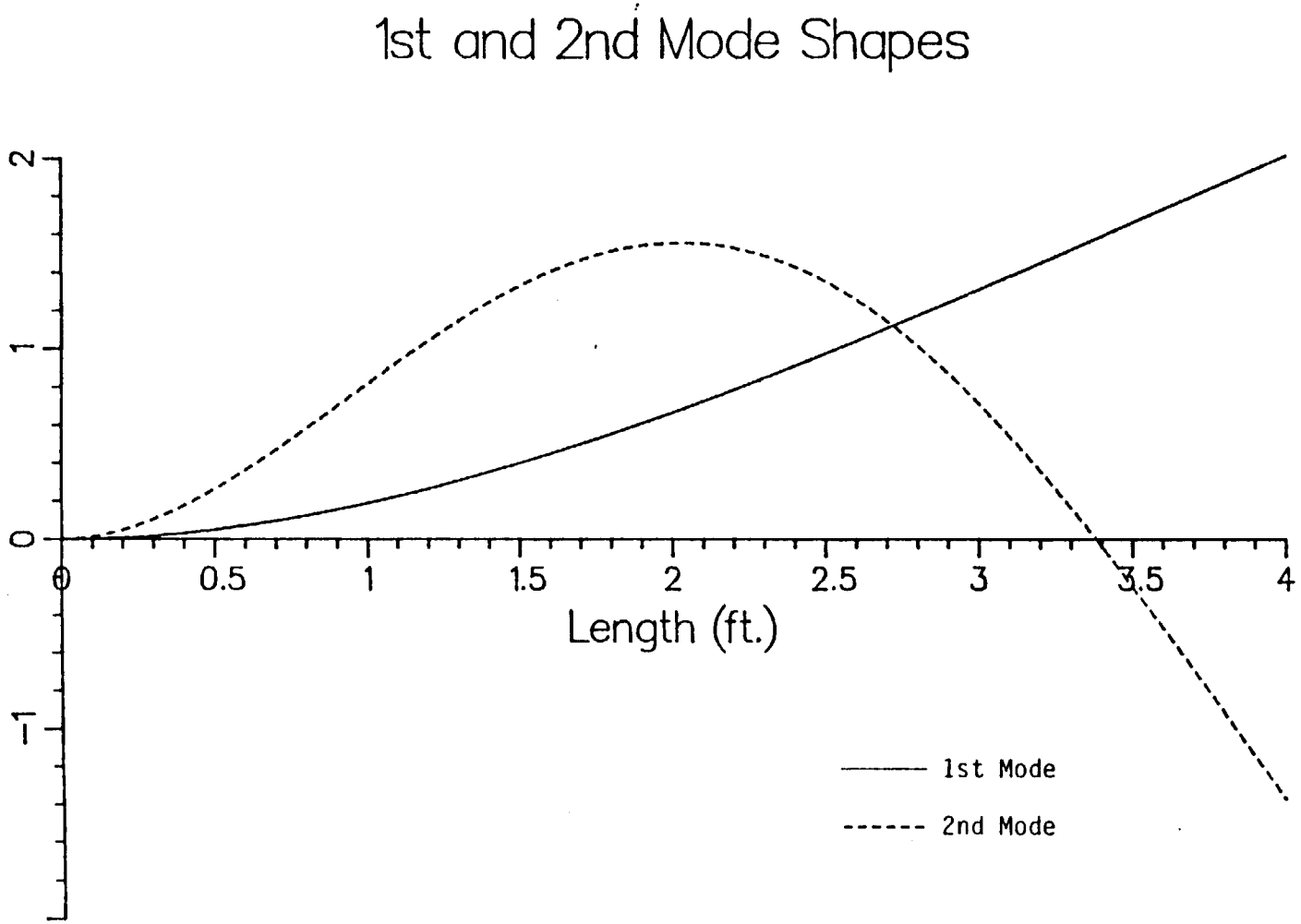
1st and 2nd Mode Shapes
2
1
0
-1
0
0.5
1
1.5
2
2.5
3
3.5
4
Length (ft.)
1st Mode
2nd Mode

Fig. 3

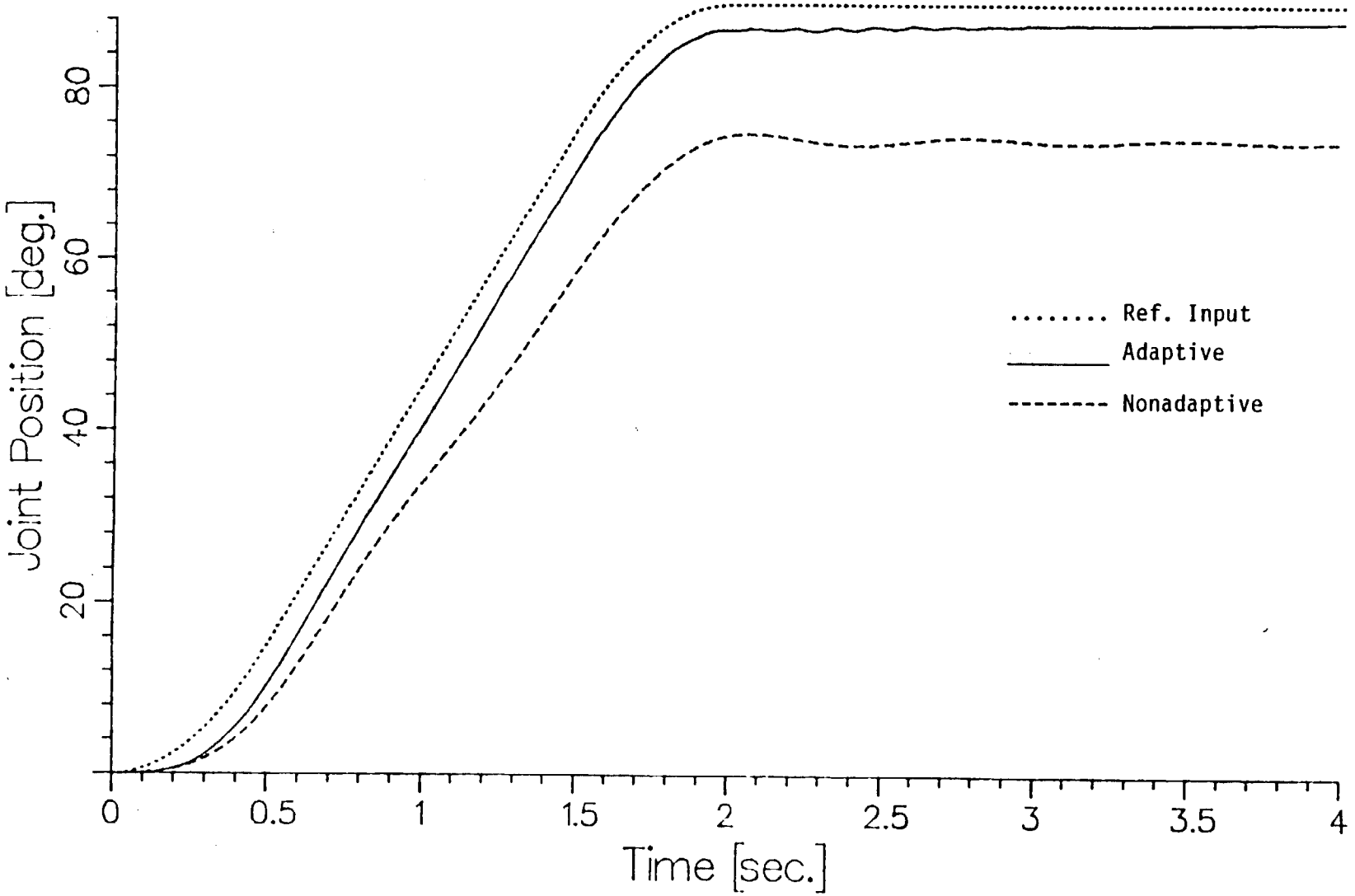
Joint Position [deg.]
20
40
60
80
0
0.5
1
1.5
2
2.5
3
3.5
4
Time [sec.]
..... Ref. Input
_____ Adaptive
------- Nonadaptive

Fig. 4

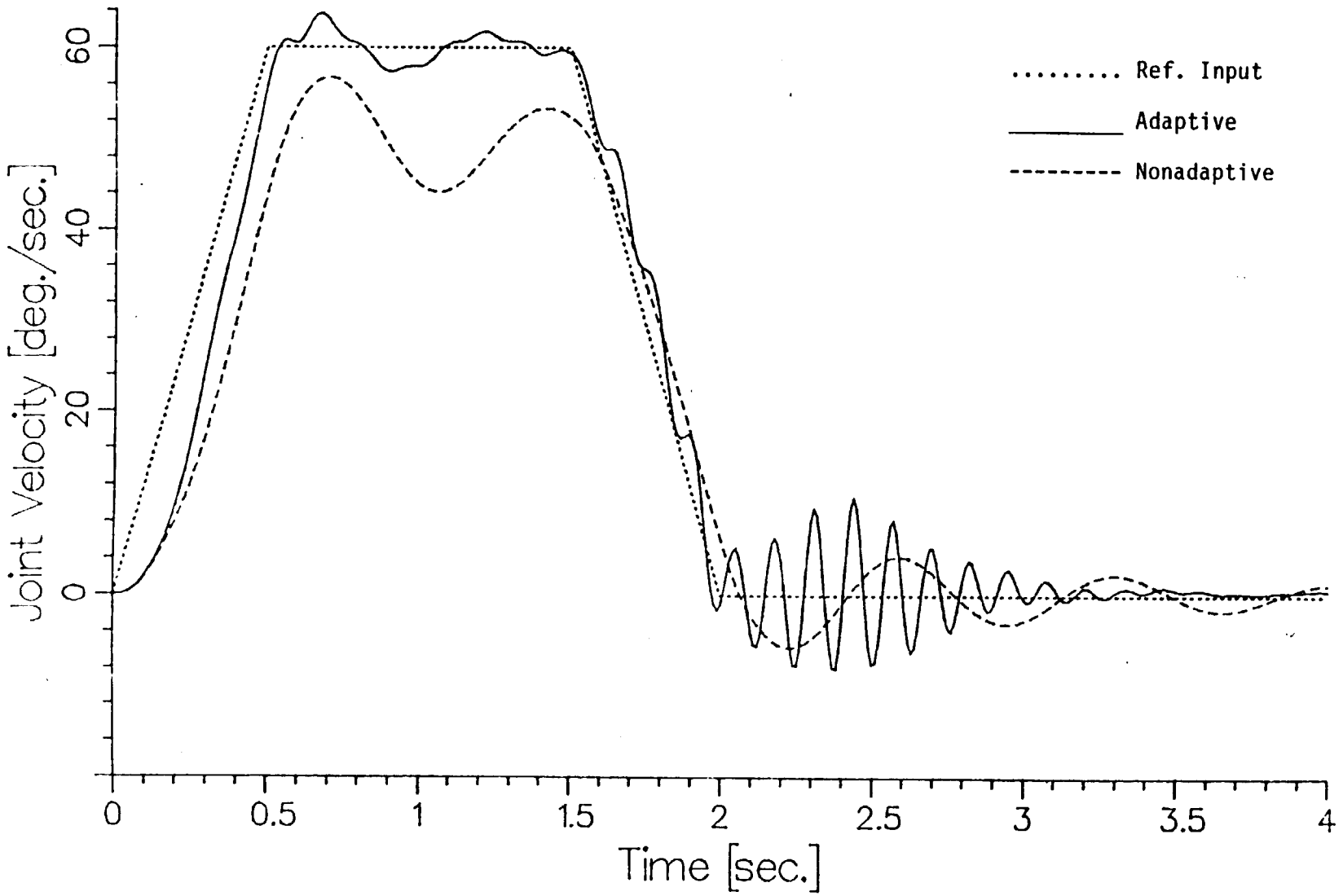
Joint Velocity [deg./sec.]
60
40
20
0
0
0.5
1
1.5
2
2.5
3
3.5
4
Time [sec.]
..... Ref. Input
_____ Adaptive
-------- Nonadaptive

Fig. 5

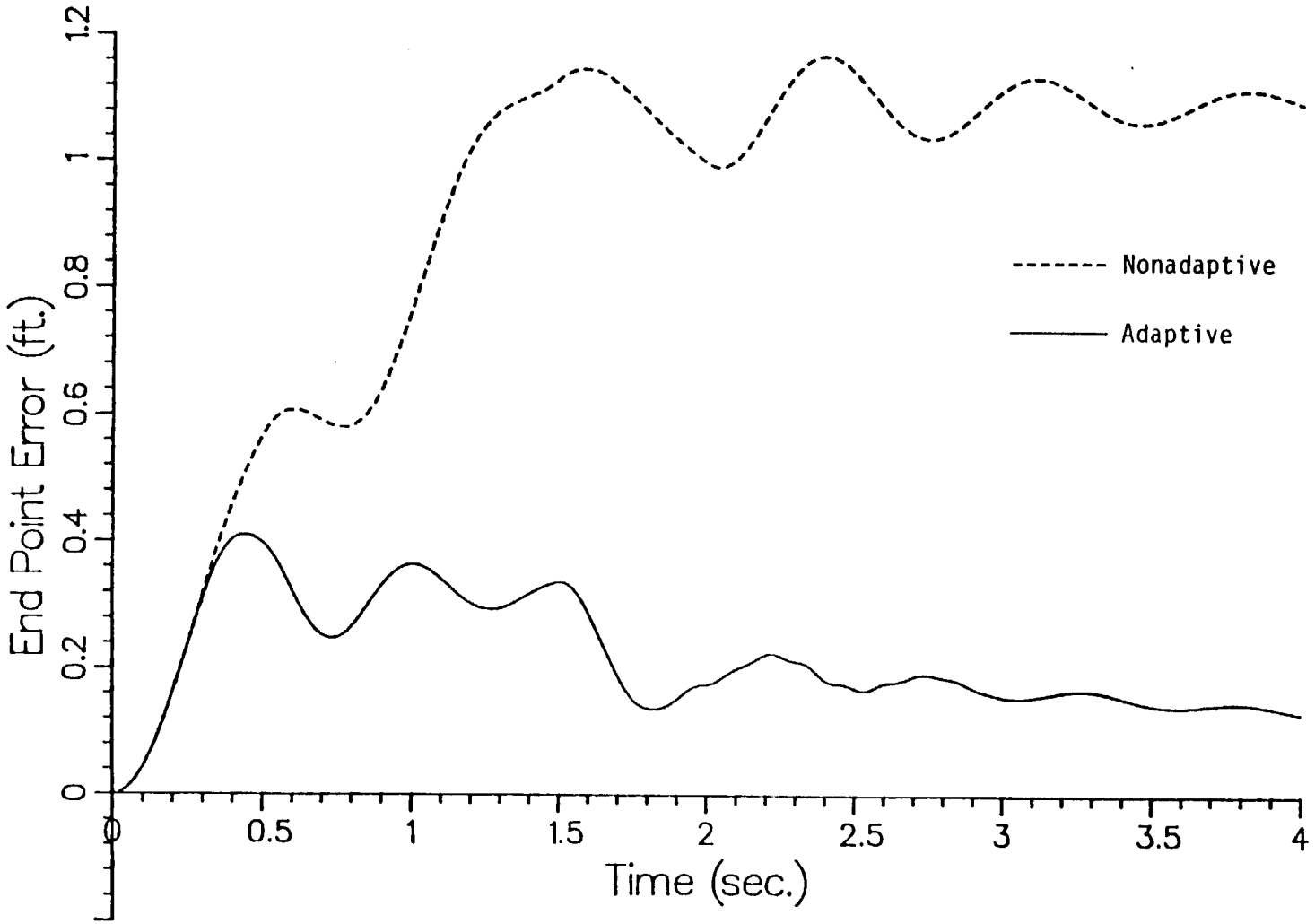
End Point Error (ft.)
0
0.2
0.4
0.6
0.8
1
1.2
0
0.5
1
1.5
2
2.5
3
3.5
4
Time (sec.)
Nonadaptive
Adaptive

Fig. 6

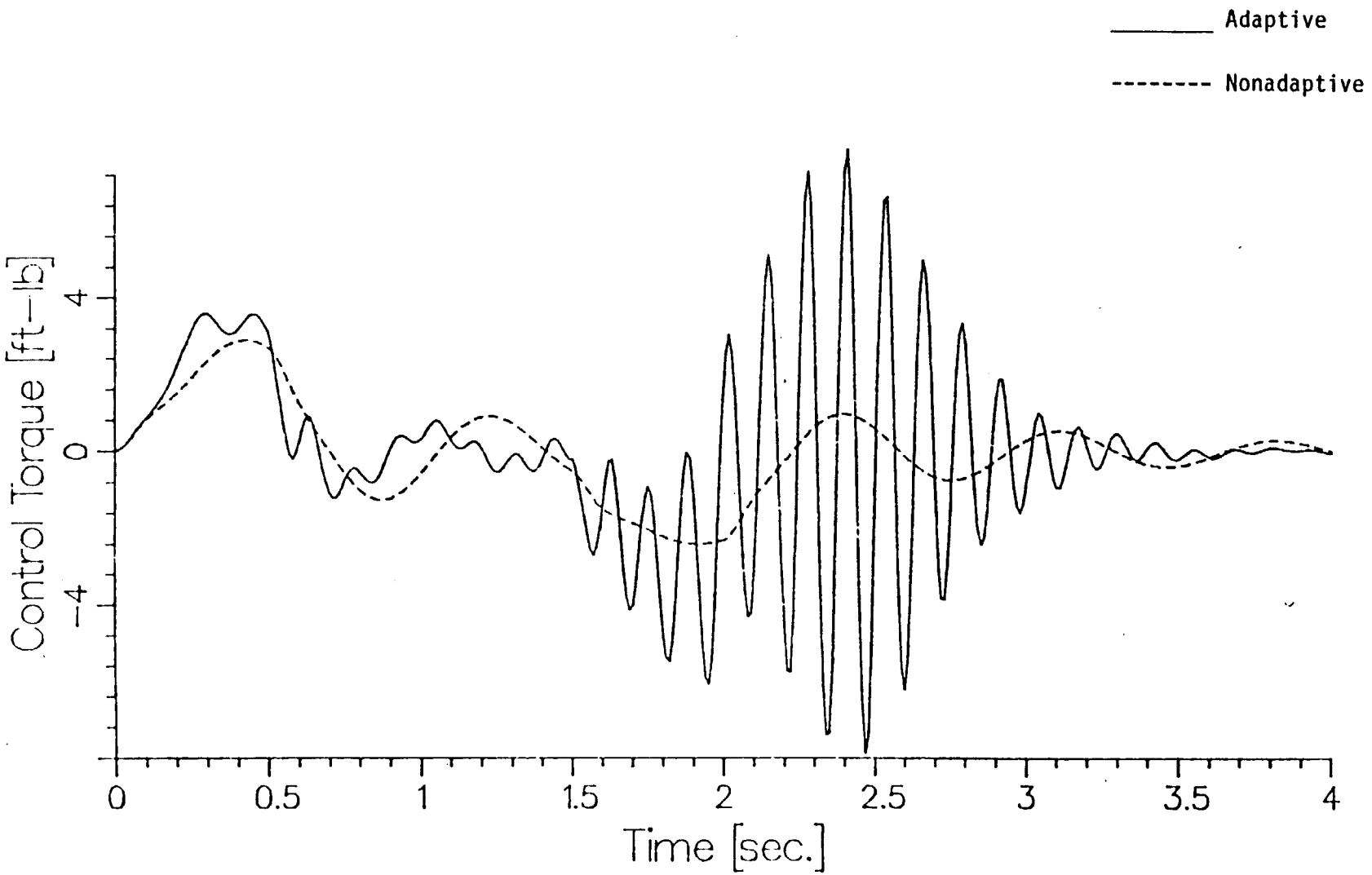
Adaptive
Nonadaptive
Control Torque [ft-lb]
4
0
-4
0
0.5
1
1.5
2
2.5
3
3.5
4
Time [sec.]

Fig. 7

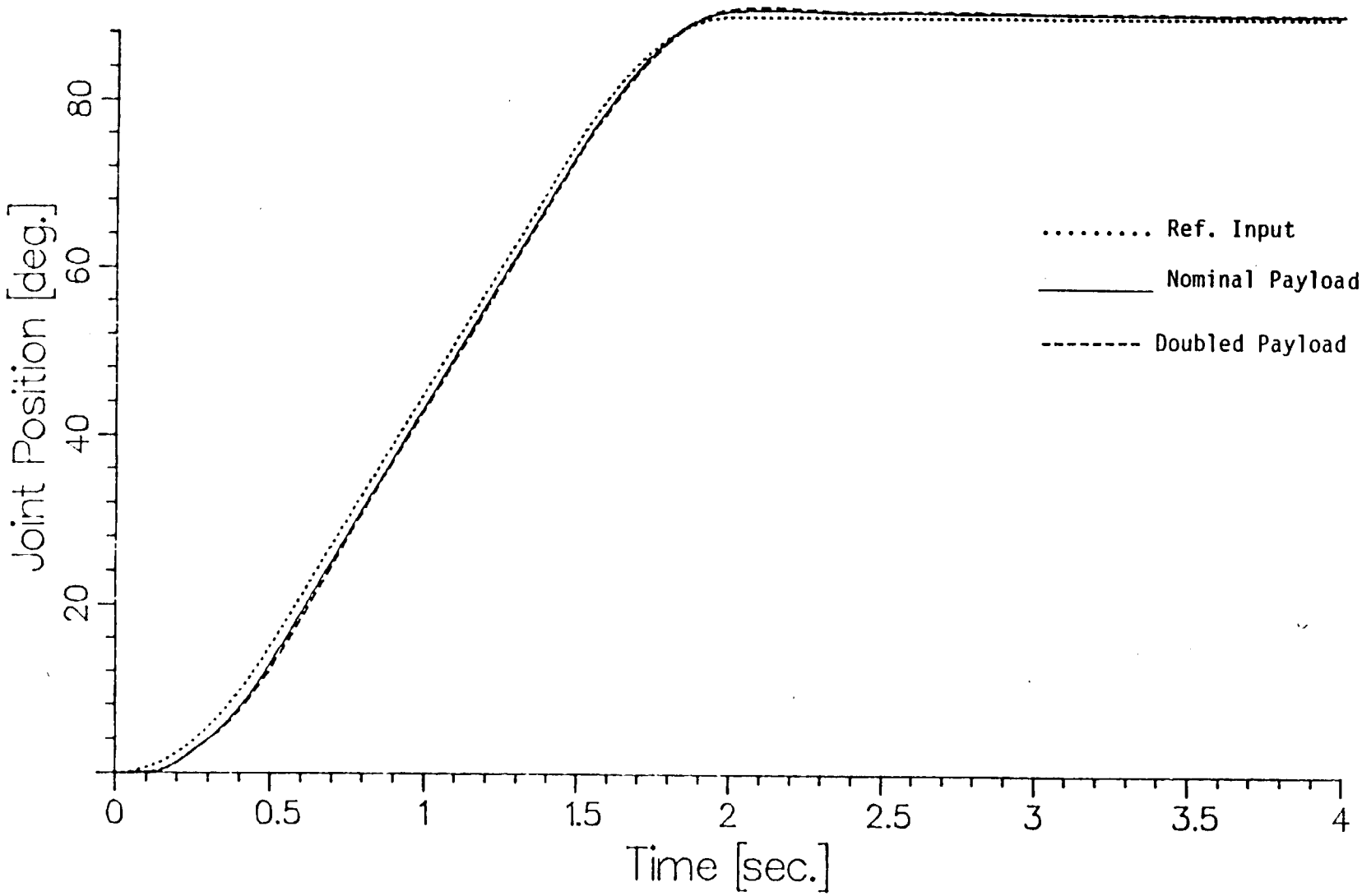
Joint Position [deg.]
20
40
60
80
0
0.5
1
1.5
2
2.5
3
3.5
4
Time [sec.]
..... Ref. Input
_____ Nominal Payload
-------- Doubled Payload

Fig. 8

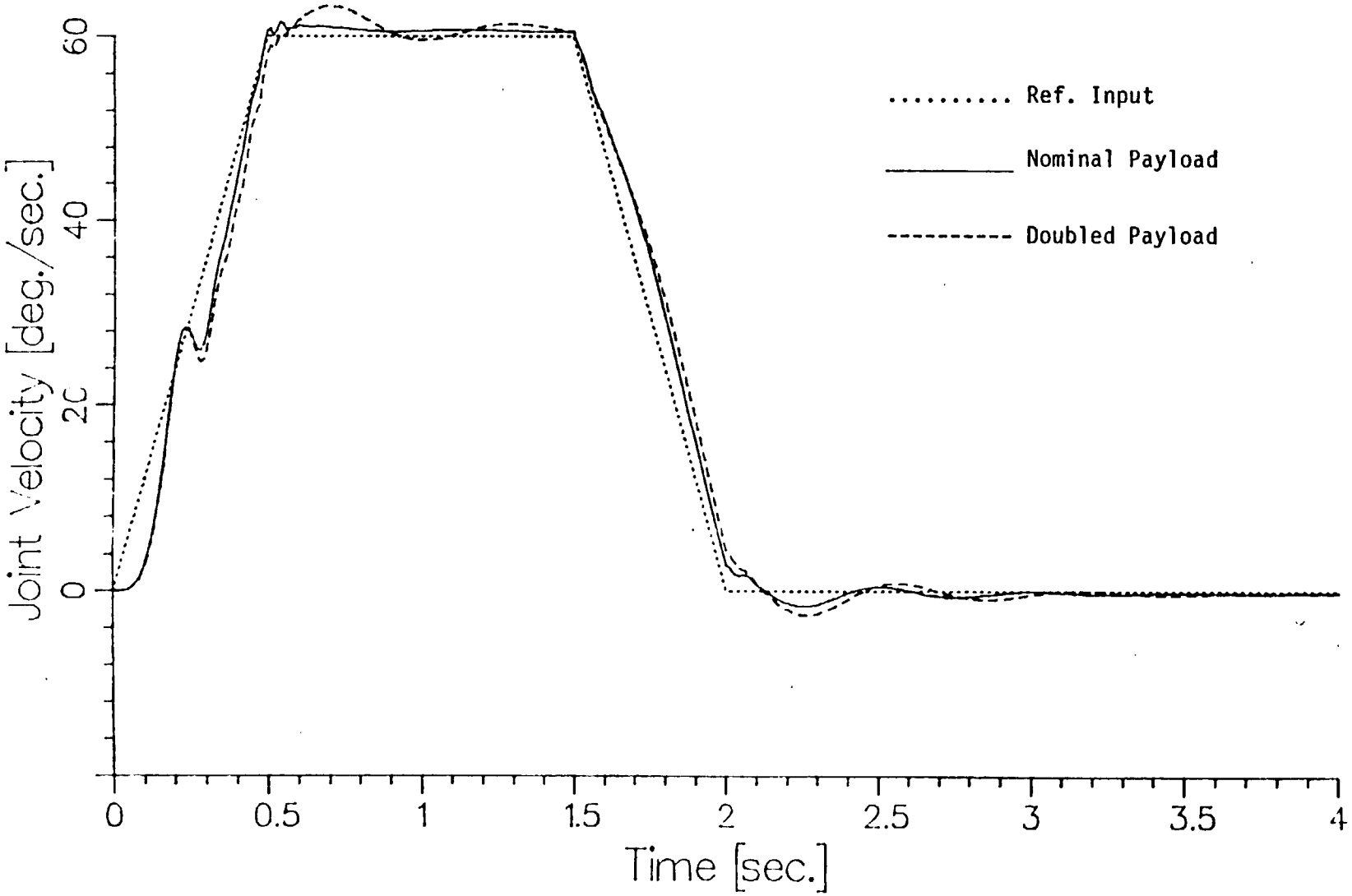
Joint Velocity [deg./sec.]
60
40
20
0
0
0.5
1
1.5
2
2.5
3
3.5
4
Time [sec.]
..... Ref. Input
_____ Nominal Payload
--------- Doubled Payload

Fig. 9

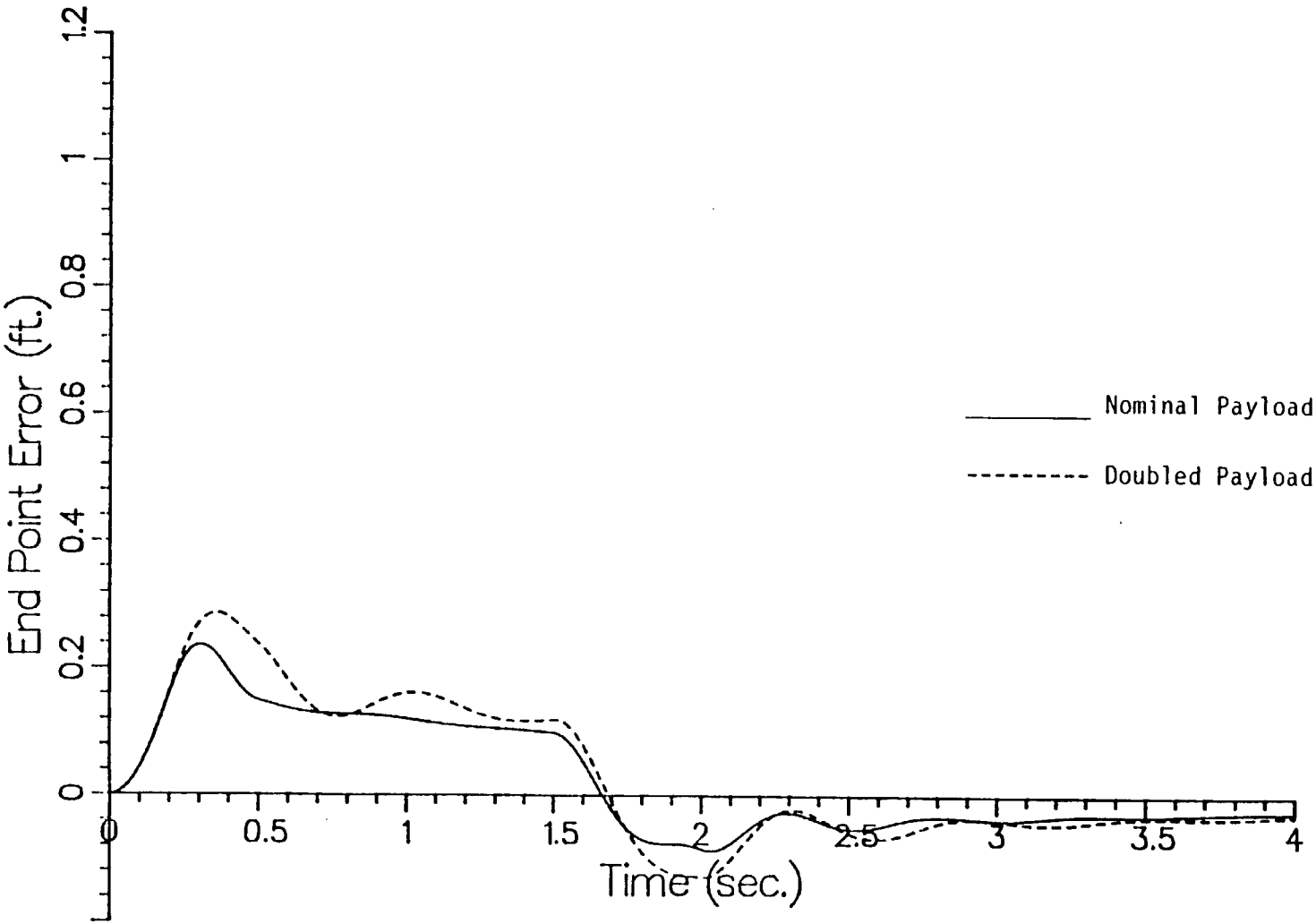
End Point Error (ft.)
0
0.2
0.4
0.6
0.8
1
1.2
0
0.5
1
1.5
2
2.5
3
3.5
4
Time (sec.)
Nominal Payload
Doubled Payload

Fig. 10

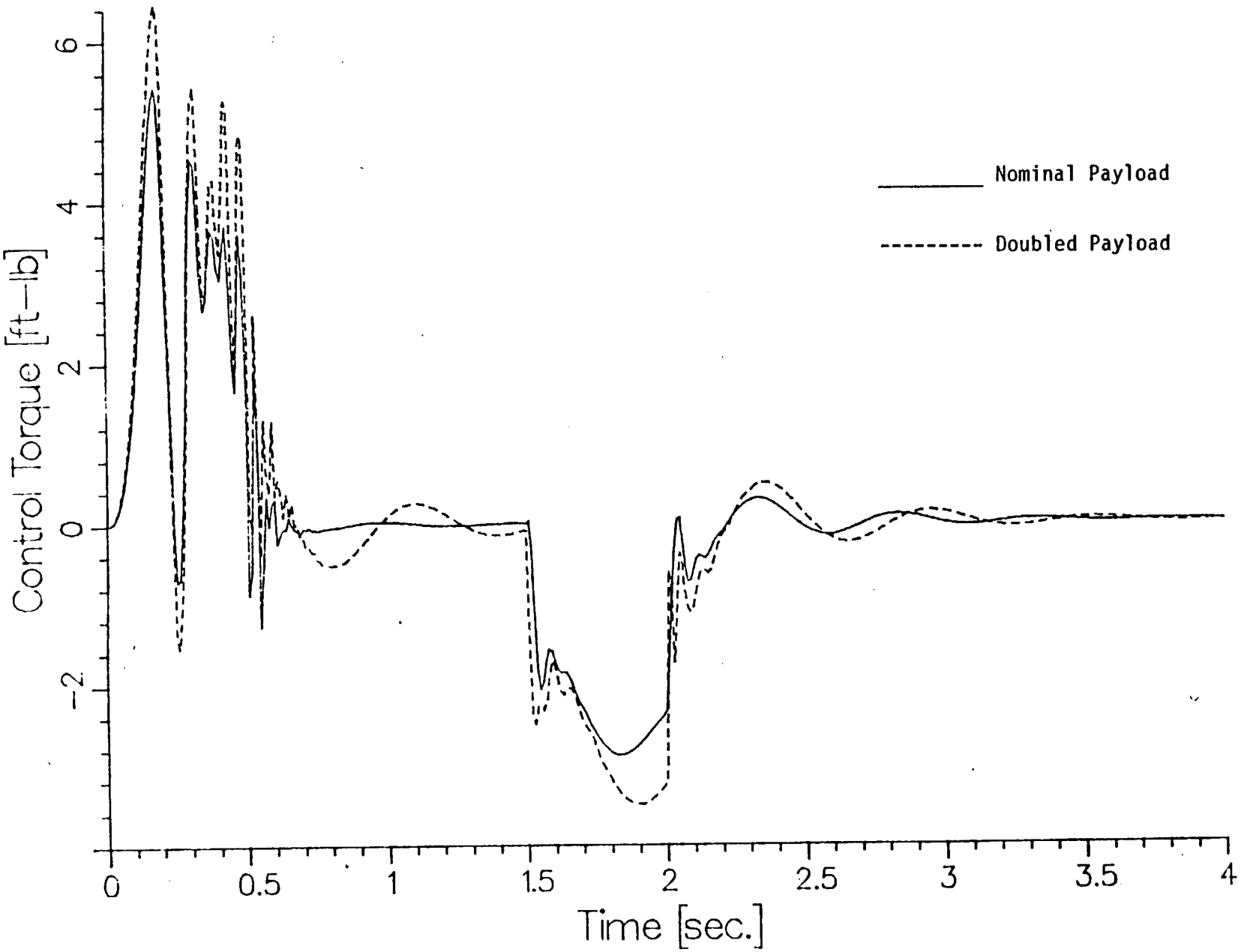
Control Torque [ft-lb]
6
4
2
0
-2
0
0.5
1
1.5
2
2.5
3
3.5
4
Time [sec.]
Nominal Payload
Doubled Payload

Fig. 11

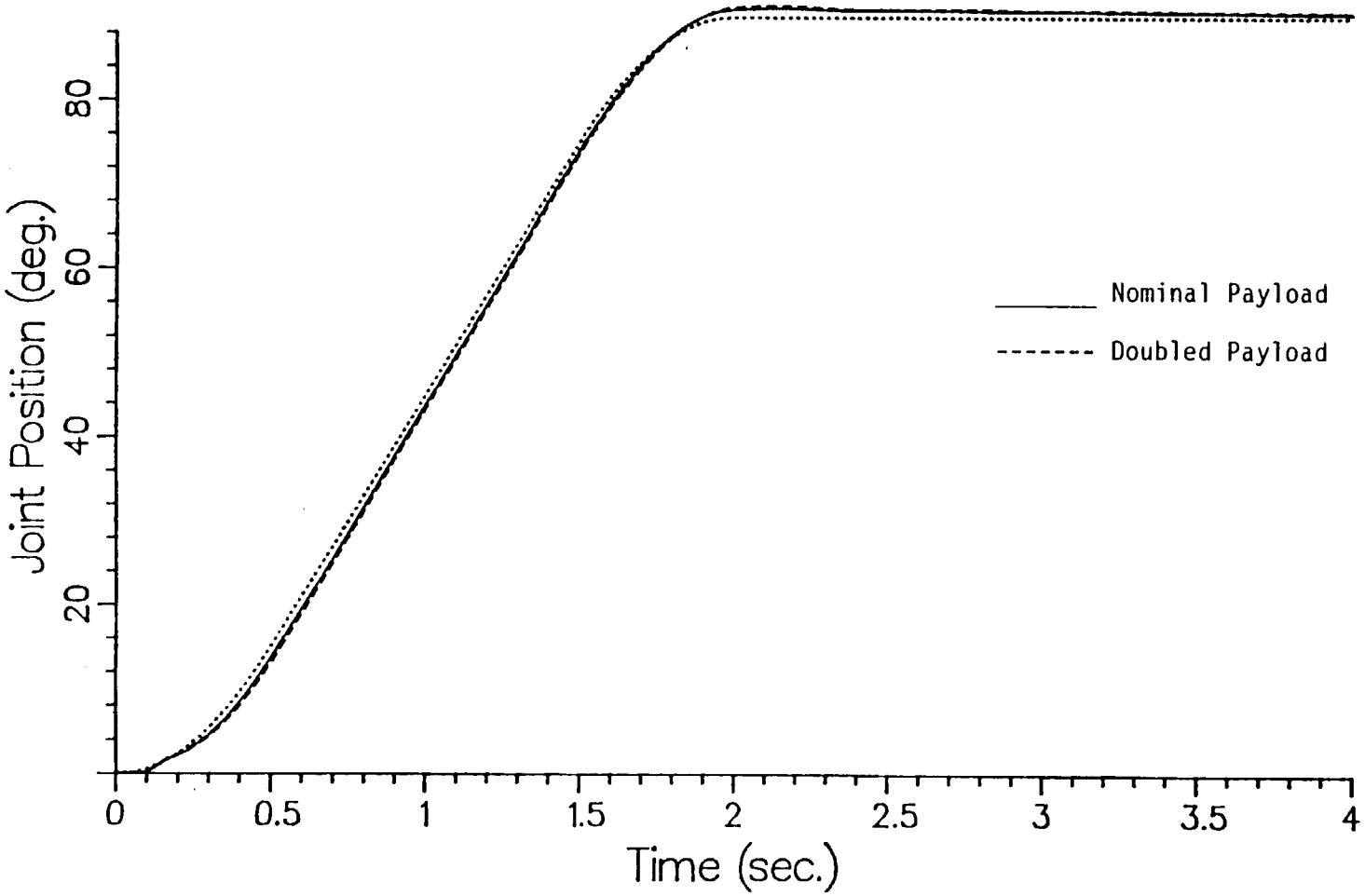
Joint Position (deg.)
20
40
60
80
0
0.5
1
1.5
2
2.5
3
3.5
4
Time (sec.)
Nominal Payload
Doubled Payload

Fig. 12

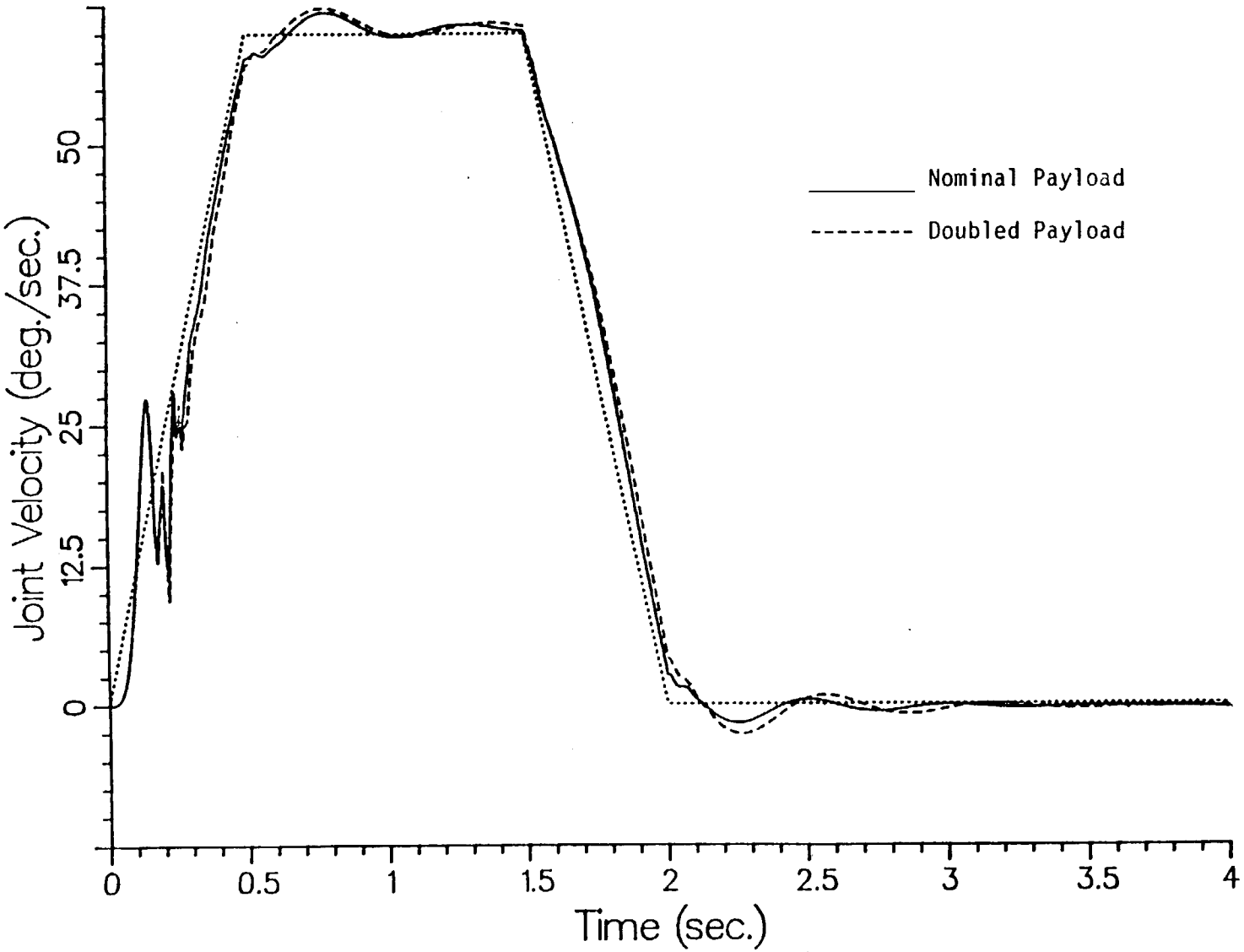
Joint Velocity (deg./sec.)
0
12.5
25
37.5
50
0
0.5
1
1.5
2
2.5
3
3.5
4
Time (sec.)
Nominal Payload
Doubled Payload

Fig. 13

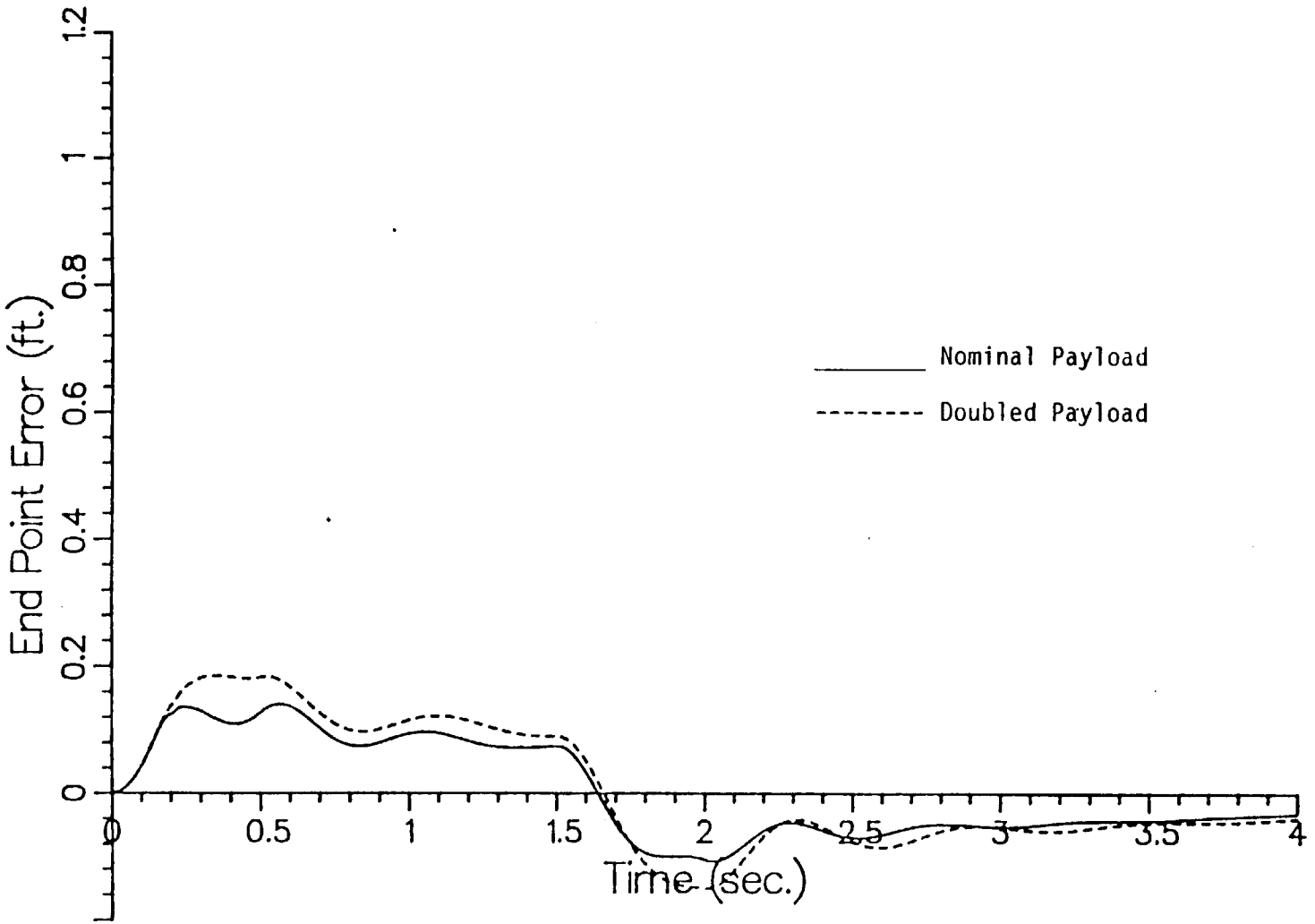
End Point Error (ft.)
0
0.2
0.4
0.6
0.8
1
1.2
0
0.5
1
1.5
2
2.5
3
3.5
4
Time (sec.)
Nominal Payload
Doubled Payload

Fig. 14

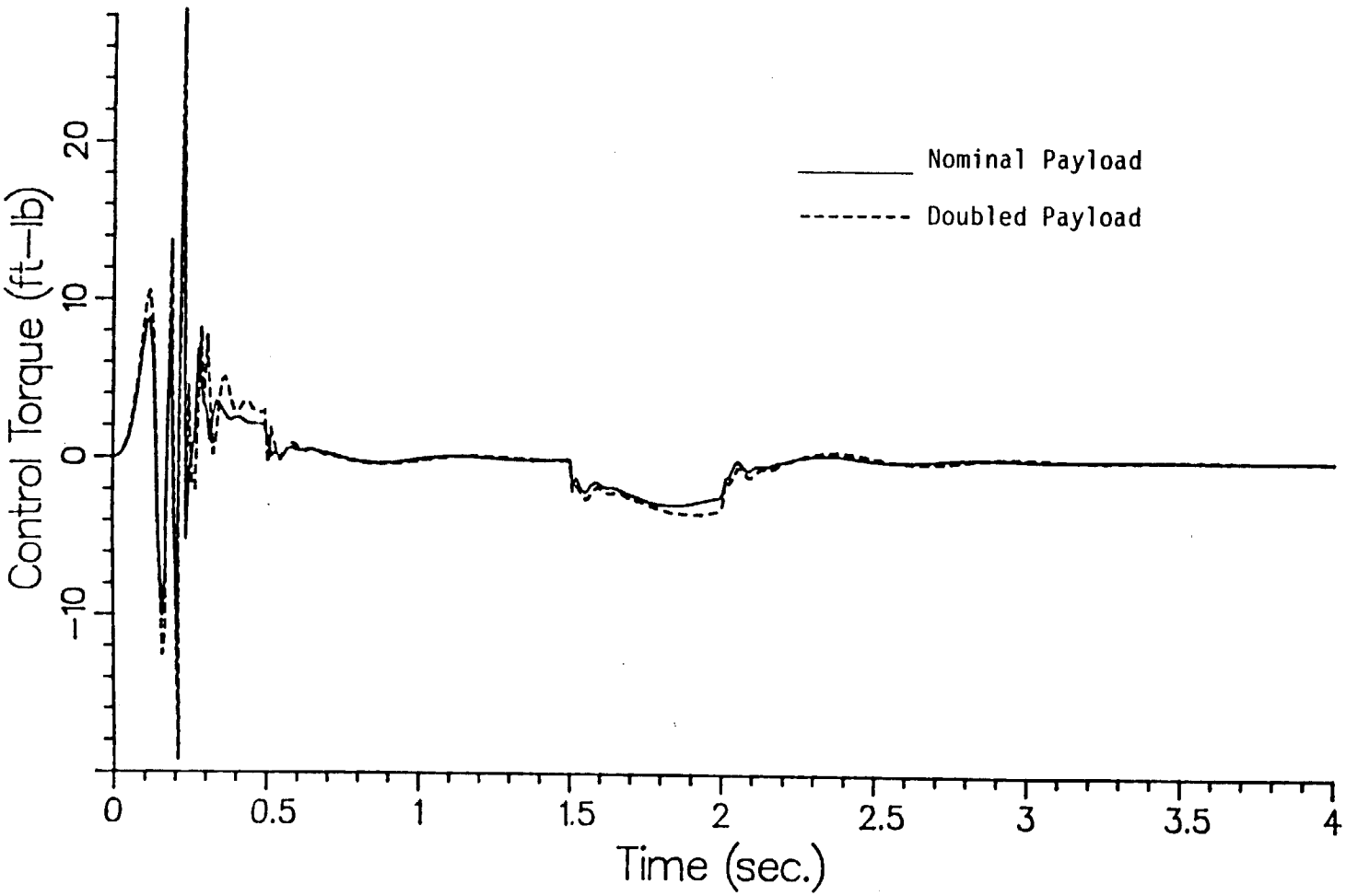
Nominal Payload
Doubled Payload
Control Torque (ft–lb)
20
10
0
–10
0
0.5
1
1.5
2
2.5
3
3.5
4
Time (sec.)

Fig. 15

Submitted to 1990 IFAC World Congress

CONTROL OF A MULTI-LINK FLEXIBLE MANIPULATOR WITH A DECENTRALIZED APPROACH

B. S. Yuan, W. J. Book, J. D. Huggins

School of Mechanical Engineering, Georgia Institute of Technology, Atlanta, GA 30332-0405 U.S.A.

Abstract. This work seeks to provide an effective way for the development of the dynamics of a multi-link flexible manipulator. Due to the presence of nonlinearities, uncertainty, and link flexibility, a decentralized control is implemented here to provide robust stability without increasing the burden of on-line computation. Simulations and experiments show agreement with the analytic work.

INTRODUCTION

The light weight manipulator arm is a challenging research topic with potential to improve the performance of robots and other high performance motion systems [Book, 1974; Cannon, 1984]. The main problem with light-weight structures is in the resulting flexible vibrations naturally excited as the manipulator is commanded to move or is disturbed [Balas, 1978]. Control is one key to effective use of lighter manipulators, but its capability is limited by uncertainties in the manipulator plant and in the environment.

The first step in studying a design is establishing a suitable dynamic model. An assumed mode representation of the structural deflection is combined with a Lagrangian approach to derive the equations. An efficient derivation is possible by recognizing that the inertia matrix is positive and symmetric, and that nonlinear terms exhibit a skew symmetry. The general form of the equations allows the complete nonlinear model to be derived from the Jacobian matrix and the mass properties via symbolic manipulation techniques [Yuan, 1989].

A centralized control is possible and a linear quadratic regulator using link strain and joint angle measurements is considered for comparison to advanced controllers [Yuan, 1989]. A decentralized control, however, will have advantages in terms of implementation in complex cases. The independent control of the joints of a flexible arm is shown to be stable [Yuan, 1989]. Then, an advanced control algorithm using a decentralized scheme with bounded plant uncertainty is proposed. If the rigid dynamics is dominant, the flexible dynamics will contribute most to model uncertainty. Alternatively, the flexibility of each link can be included in the decentralized models. Link interactions then form the major source of uncertainty.

The decentralized control scheme assumes the satisfaction of certain matching conditions [Leitmann, 1981]. These conditions guarantee that the uncertainty vector does not influence the dynamics more than the control input does [Gutman, 1979]. The signal-synthesis adaptation approach used here results in a robust stability design which reduces the burden of on-line computation and satisfies the needs of flexible arms. The design is based on the Lyapunov criterion [Vidyasagar, 1978], with the output error between the system and the reference model used as the signal of interest.

Simulations and experiments are carried out on a two link test case called RALF (Robotic Arm, Large and Flexible), at the Flexible Automation Laboratory at Georgia Tech (Fig. 1). The results compare independent joint control and a decentralized adaptive controller, when a predefined trajectory is followed.

DYNAMIC MODELING OF A MULTI-LINK FLEXIBLE MANIPULATOR

To establish a successful feedback control for a mechanical system, dynamic modeling is an important prerequisite. In contrast to the rigid manipulator, whose equations of motion have been well-developed [Asada, 1986; Paul 1981], the distributed-mass character of the flexible manipulator needs further explanation. The kinetic and potential energies, that are derived using Cartesian coordinates, result in a Lagrangian formulation that simply and systematically produces the dynamics of a multi-link flexible arm.

Kinematics of flexible arms has been described by 4x4 transformation matrices as proposed in Book [Book, 1984]. A point along the link is described in a fixed reference coordinate system by two transformations, A_i and E_i, between the coordinate systems. The transformation, A_i, relates system i', the point before deflection, to system $i-1$. The transformation E_i relates the deflection of system i to system i'. Note that the transformation which is described as the position of an arbitrary point attached to the rigid arm has the form of

$$A = \begin{bmatrix} R & P \\ 0 & 1 \end{bmatrix} , \qquad (2.1)$$

where

R = 3x3 matrix of direction cosines,

P = position vector.

Therefore, the combined relation is

$$h_{i-1} = A_i E_i h_i , \qquad (2.2)$$

where

$h_i = [P_i^T , 1]^T$ = the position of the point in system i.

Considering the ith consecutive coordinate transformation along a serial linkage, we can derive the location (r_i) of a point along the ith coordinate viewed from the base frame,

$$r_i = T_i {}^i r_i \qquad (2.3a)$$

where

$$T_i = A_1 E_1 A_2 E_2 - A_{i-1} E_{i-1} A_i , \qquad (2.3b)$$

and r_i is the position vector related to the ith coordinate without the transformation E_i due to link deflection.

The flexible deflection is assumed to be a finite series of separate modes which are the product of admissible shape functions and time-dependent generalized coordinates. Higher modes are comparatively small in amplitude. With small deflections, the matrix E can then be expressed as

$$E_i = \sum_{j=1}^{m_i} \delta_{ij} \begin{bmatrix} 0 & -\theta_{zij} & \theta_{yij} & U_{ij} \\ \theta_{zij} & 0 & -\theta_{xij} & V_{ij} \\ -\theta_{yij} & \theta_{xij} & 0 & W_{ij} \\ 0 & 0 & 0 & 0 \end{bmatrix} +$$

$$\begin{bmatrix} 1 & 0 & 0 & 0 \\ 0 & 1 & 0 & 0 \\ 0 & 0 & 1 & \ell_i \\ 0 & 0 & 0 & 1 \end{bmatrix} \qquad (2.4)$$

where for link i δ_{ij} is the time varying amplitude of the shape function, u_{ij}, v_{ij}, and w_{ij} are the x, y and z components, respectively, of the shape function, θ_{zij}, θ_{yij} and θ_{zij} are the small rotations of the body-fixed coordinate system at the point of interest, m_i is the number of shape functions needed to represent the flexible kinematics to the degree of accuracy needed, and ℓ_i is the distance to the point of interest along the link's neutral axis, which is L_i, the length of the link, when the point at r_i is not on link i.

Clearly, A_i is a function of the joint displacement (q_i) and E_i is a function of link deflections (δ_{ij}). Transformation equation (2.3) illustrates the functional relationship between the position of a point along the ith link and the displacements of all joints and link deflection involved in the kinematic chain. Then, consider the kinetic energy of a point on the ith link,

$$KE_i = \int_{\text{link } i} dKE_i =$$

$$\frac{1}{2} \int_{\text{link } i} \text{Trace} \left[\frac{dr_i}{dt}^T \frac{dr_i}{dt} \right] dm \ , \qquad (2.5)$$

where $\frac{dr}{dt}$ is called the velocity vector.

Taking the derivative of the transformation (2.3a) with respect to time

$$\dot{r}_i = \dot{T}_i \, {}^i r_i + T_i \, {}^i \dot{r}_i \qquad (2.6)$$

Summing over all n links, one finds the system kinetic energy to be

$$KE = \sum_{i=1}^{n} \int_{\text{link } i} dKE_i \qquad (2.7)$$

Equation (2.6) can also be written as

$$\dot{r}_i = J_i \dot{X} \ , \qquad (2.8)$$

where

J_i is the $4x[nx(m_i+1)]$ matrix,
X includes all q_i's and δ_{ij}'s.

Then,

$$KE = \sum_{i=1}^{n} \frac{1}{2} \int_{\text{link } i} \text{Trace} \, (\dot{X}^T J_i^T J_i \dot{X}) \, dm, \qquad (2.9a)$$

$$= \dot{X}^T \left[\sum_{i=1}^{n} \frac{1}{2} \int_{\text{link } i} \text{Trace} \, (J_i^T J_i) \, dm \right] \dot{X}, \qquad (2.9b)$$

where $J_i^T J_i$ is symmetric and positive.

To assign indexes i and j to X,

$$x_{ij} = \begin{cases} q_i & j = 0 \\ d_{ij} & j = 1, 2, \ldots, m_i \end{cases} \qquad (2.10)$$

equation (2.9), then, becomes

$$KE = \frac{1}{2} \sum_{i=1}^{n} \sum_{j=0}^{m_i} \sum_{\alpha=1}^{n} \sum_{\beta=0}^{m_\alpha} M_{ij\alpha\beta} \dot{x}_{ij} \dot{x}_{\alpha\beta} \qquad (2.11)$$

In addition to the computation of the kinetic energy, we need to find the potential energy, which arises from three sources as considered here: joint elasticity, gravity and link deformation.

We consider an n-link manipulator with revolute joints, and model the elasticity of the ith joint as an equivalent torsional spring with spring constant K_{ei}. The formula for this potential energy is

$$PE_e = \sum_{i=1}^{n} PE_{ei} = \frac{1}{2} \sum_{i=1}^{n} K_{ei} \bar{q}_i^2 \ , \qquad (2.12)$$

where $\bar{q}_i$ is the joint coordinate measured from the unstretched position $\bar{q}_{oi}$ to q_i.

The gravity potential energy for a differential element on the ith link is

$$dPE_{gi} = - g^T T_i \, {}^i r_i \, dm, \qquad (2.13a)$$

where the gravity vector g has the form

$$g^T = [g_x, g_y, g_z, 0]. \qquad (2.13b)$$

Integrating over the link and summing over all links, the total potential energy is

$$PE_g = -g^T \sum_{i=1}^{n} T_i h_i \ , \qquad (2.14a)$$

where $h_i = M_i h_{mi} + \sum_{k=1}^{m_i} \delta_{ik} E_{ik}$, (2.14b)

and M_i = the total mass of link i, $h_{mi} = [0,0,h_{zi},1]^T$ = a vector to the center of gravity from joint i (undeformed),

$$E_{ik} = \int_{\text{link } i} [\, U_{ik}, V_{ik}, W_{ik}, 0 \,]^T \, dm$$

The strain energy of link i is related to the link deformation integrated along the z-axis coincident with the link is described as

$$PE_{di} = \frac{1}{2} \int_{\text{link}i} \left[EI_x \left(\frac{\partial^2 U_{xi}}{\partial Z_i^2} \right)^2 + EI_y \left(\frac{\partial^2 V_{yi}}{\partial Z_i^2} \right)^2 + \right.$$

$$\left. + E_g J_z \left(\frac{\partial \theta_{zi}}{\partial Z_i} \right)^2 \right] dz_i \qquad (2.15)$$

where E and E_g are Young's modulus and shear modulus of elasticity, I_x and I_y are the area moments of inertia of the link, while J_z is the polar area moment,

and

$$U_{xi} = \sum_{k=1}^{m_i} \delta_{ik} U_{ik}$$

$$V_{yi} = \sum_{k=1}^{m_i} \delta_{ik} V_{ik}$$

$$\theta_{iz} = \sum_{k=1}^{m_i} \delta_{ik} \theta_{zik}$$

Note that compression is not initially included as it is generally much smaller.

Then, the total strain energy PE_d can be written as

$$PE_d = \frac{1}{2} \sum_{i=1}^{n} \sum_{j=1}^{m_i} \sum_{k=1}^{m_i} K_{dijk}\, \delta_{ij} \delta_{ik} \qquad (2.16)$$

where

$$K_{dijk} = K_{xijk} + K_{yijk} + K_{zijk}$$

and

$$K_{xijk} = \int_{link\ i} EI_x \frac{d^2 U_{ij}}{d Z_i^2} \frac{d^2 U_{ik}}{d Z_i^2} \, dZ_i$$

$$K_{yijk}\ ,\ K_{zijk} = \text{etc.}$$

Now, we are going to derive the Lagrangian equation of motion. First, the following expressions need to be obtained for any coordinate state x_{pq}.

$$\frac{d}{dt}\left(\frac{\partial KE}{\partial \dot{x}_{pq}}\right) = \frac{d}{dt}\left(\sum_{i=1}^{n} \sum_{j=0}^{m_i} M_{ijpq}\, \dot{x}_{ij}\right) \qquad (2.17)$$

$$= \sum_{i=1}^{n} \sum_{j=0}^{m_i} M_{ijpq}\, \ddot{x}_{ij} + \sum_{i=1}^{n} \sum_{j=0}^{m_i} \sum_{\alpha=1}^{n} \sum_{\beta=0}^{m_\alpha} \frac{\partial M_{ijpq}}{\partial x_{\alpha\beta}}\, \dot{x}_{ij}\, \dot{x}_{\alpha\beta}$$

and

$$\frac{\partial KE}{\partial x_{pq}} = \frac{1}{2} \sum_{i=1}^{n} \sum_{j=0}^{m_i} \sum_{\alpha=1}^{n} \sum_{\beta=0}^{m_\alpha} \frac{\partial M_{ij\alpha\beta}}{\partial x_{pq}}\, \dot{x}_{ij}\, \dot{x}_{\alpha\beta} \qquad (2.18)$$

Taking the partial derivative of the potential energies of the elastic joint and the link deflection leads to

$$\frac{\partial (PE_e + PE_d)}{\partial x_{pq}} = \sum_{\ell=0}^{m_\ell} K_{p\ell q}\, x_{p\ell}, \qquad (2.19)$$

where

$$K_{p\ell q}\, x_{p\ell} = \begin{cases} K_e \bar{q} & \text{in (2.12)}, \text{ when } \ell = 0 \\ K_d \delta & \text{in (2.16)}, \text{ when } \ell \neq 0 \end{cases}$$

and the gravity term is

$$\frac{\partial PE_g}{\partial x_{pq}} = \begin{cases} -g^T \sum_{i=p}^{n} \frac{\partial T_i}{\partial x_{pq}} h_i - g^T T_p E_{pq}, & \text{when } q \neq 0 \\ -g^T \sum_{i=p}^{n} \frac{\partial T_i}{\partial x_{pq}} h_i, & \text{when } q = 0 \end{cases} \qquad (2.20)$$

Note that $\sum_{i=p}^{n} \frac{\partial T_i}{\partial x_{pq}} = \frac{\partial A_n}{\partial q_n} = 0$, when $p=n$ and $q \neq 0$

Finally, combining (2.17), (2.18), (2.19) and (2.20) gives the equation of motion for x_{pq}:

$$\sum_{i=1}^{n} \sum_{j=0}^{m_i} m_{ijpq}\, \ddot{x}_{ij} + \sum_{i=1}^{n} \sum_{j=0}^{m_i} \sum_{\alpha=1}^{n} \sum_{\beta=0}^{m_\alpha} H_{ij\alpha\beta pq}\, \dot{x}_{ij}\, \dot{x}_{\alpha\beta} + \sum_{\ell=0}^{m_\ell} K_{p\ell q}\, x_{p\ell} + G_{pq} = Q_{pq}, \qquad (2.21a)$$

where

$$H_{ij\alpha\beta pq} = \frac{\partial m_{ijpq}}{\partial x_{\alpha\beta}} = \frac{1}{2} \frac{\partial m_{ij\alpha\beta}}{\partial x_{pq}} \ ,$$

G_{pq} is the gravity term in (2.20),

Q_{pq} is the generalized force.

In matrix-vector form,

$$M(X)\ddot{X} + H(X,\dot{X})\dot{X} + K\bar{X} + G(X) = Q\ . \qquad (2.22)$$

where $\bar{X}$ is the state variable measured from the reference (unstretched) position.

The structures of the equations of motion for rigid and flexible robotic arms are very similar as given above, while the generalized coordinate variables are different. Additional variables, namely the deflection coordinate δ_{ij}, are used to describe the link deformation so that the stiffness coefficient K in (2.22) originates from the strain energy. Therefore, the condition of a skew symmetry (M - 2H) can be obtained in (2.22) [Yuan, 1989] as it has been found in the case of rigid manipulators [Asada, 1986].

III. CONTROL ALGORITHM

Independent linear controllers at each joint, commonly called joint proportional-derivative (PD) controllers, have provided adequate position control for rigid robotic arms [Asada, 1986], similarly for flexible arms [Book, 1974]. The system with flexibility is shown to have the passive nature from both the frequency-dominant [Book, 1974] and time-dominant [Yuan, 1989] approaches. This decentralized approach is carried forward with the development of an advanced control algorithm using the decentralized scheme that treats the overall system as several subsystems (local systems). The designer for such systems determines a control structure which assigns inputs to a set of local controllers, and observes only local system output. The interconnecting terms between subsystems are considered as uncertainties in the system and are bounded [Yuan, 1989].

In a multi-link flexible manipulator, M(X), the inertia matrix, is symmetric and positive definite. Therefore, one can define a positive matrix β such that

$$|\beta| \geq |M^{-1}(X) - \beta| \qquad (3.1)$$

where $|\ |$ is an induced norm.

Equation (2.22) can then be rewritten as

$$\ddot{X} = -M^{-1}(X)[H(X,\dot{X})\dot{X} + K\bar{X} + G(X)] + \beta Q + [M^{-1}(X) - \beta]Q \qquad (3.2)$$

Take each link i as a subsystem and define state variables $Z_i^T = [\bar{X}_i^T, \dot{X}_i^T]$, where the vector X_i is includes one joint coordinate and generalized deflection coordinates for link i (2.21). Equation (3.2) is divided into n equations for the n interconnected subsystems. Therefore, each subsystem is described by a first-order differential equation of the form

$$\dot{z}_i = A_i z_i + b_i u_i + F_i(Z) + f_i(Z) u_i, \qquad (3.3)$$

where

$i = 1,2,\ldots,n$; $Z = [z_1, z_2, \ldots, z_n]^T$

and

$u_i = Q_{zo}$ in (2.21), $f_i(Z)u_i$ = the coupling terms of $[M^{-1}(X)-\beta]Q$ for subsystem i. A_i is a constant matrix which represents the linear time-invariant part of $-M^{-1}(X)K$

$$A_i = \begin{bmatrix} 0 & I \\ a_{i1} & a_{i2} \end{bmatrix}, \tag{3.4}$$

while $F_i(Z)$ represents the rest of $-M^{-1}K$ and the nonlinear terms of $-M^{-1}[H+G]$. b_i becomes a vector form with zero elements on the upper half.

(i) $F_i(Z)$ and $f_i(Z)$ are assumed to be bounded and are modeled as system uncertainties assumed to have the properties [Leitmann, 1981]

$$F_i(Z) \triangleq F_i(Z,\sigma) \tag{3.5a}$$

$$f_i(Z) \triangleq f_i(Z,\sigma) \tag{3.5b}$$

where $\sigma \in R^p$ represent the system uncertainty and is continuous on R^p as well as the uncertainty bounding set.
(ii) (A_i,b_i) is controllable.
(iii) There exist matrix functions $D_i(\cdot)$ and $E_i(\cdot)$ such that

$$F_i(Z,\sigma) = b_iD_i(Z,\sigma) \tag{3.6a}$$

$$f_i(Z,\sigma) = b_iE_i(Z,\sigma) \tag{3.6b}$$

where $|E| < 1$ from (3.1)

A model reference control with signal-synthesis adaptation is implemented here and the satisfaction of the matching conditions (3.6) is assumed. These conditions guarantee that the uncertainty vector does not influence the dynamics more than the control input does [Gutman, 1979]. The objective of model reference adaptive control is eliminate the state error between the plant and the reference model so that the behavior of the plant follows the model. Consider the reference model first,

$$\dot{z}_{mi} = A_{mi}z_{mi} + b_{mi}\gamma_i \ , \tag{3.7}$$

where

$z_{mi}=[x_{mi},\dot{x}_{mi}]^T$ and γ_i is the reference input.

And let

$$A_{mi} = A_i + b_iK_{zi} \tag{3.8a}$$

$$b_{mi} = b_iK_{bi} \tag{3.8b}$$

where K_{zi} and K_{bi} are constant matrices of compatible dimension. Also, Am_i a stable matrix satisfies the Lyapunov equation,

$$A_{mi}^T P_i + P_iA_{mi} = L_i \tag{3.9}$$

where P_i and L_i are positive definite and symmetric matrices.

The signal-synthesis method [Landau, 1979] implemented here seeks to control the system by adjusting the input u which is as described in the following equation

$$u_i = K_{zi}\ z_i + K_{bi}\ \gamma_i + \psi_i(e_i) \tag{3.10}$$

where $e_i = z_{mi} - z_i$ is referred to as state error and the function ψ_i is the control input to compensate the system uncertainty. Thus, let ψ_i be

$$\psi_i(e_i) = \begin{cases} \dfrac{b_i^T P_i e_i}{|b_i^T P_i e_i|}\ \rho_i(Z,\rho_i,\gamma_i), & \text{when } |b_i^T P_i e_i| > \delta_i \\ \dfrac{b_i^T P_i e_i}{A_i}\ \rho_i(Z,\rho_i,\gamma_i), & \text{when } |b_i^T P_i e_i| \le \delta_i \end{cases} \tag{3.11}$$

where A_i is a prescribed positive constant and ρ_i is a positive constant which will be specified subsequently.

As a result, the error dynamics of the subsystem is derived from the difference between equations (3.3) and (3.7) along with (3.11) and (3.6):

$$\dot{e}_i = A_{mi}e_i - b_i(\psi_i + \nu_i) \ , \tag{3.12a}$$

where

$$\nu_i = D_i+E_i(kz_i\ z_i + k_{bi}\gamma_i + \psi_i). \tag{3.12b}$$

Given the boundedness of the state variable z_i and the reference input γ_i, equations (3.11) and (3.12b) give the following inequality:

$$|\nu_i| \le \rho_i(Z,\ e_i,\ \gamma_i) \tag{3.13a}$$

where

$$\rho_i(Z,e_i\gamma_i) \triangleq |D_i(Z)| + |E_i(Z)|(|K_{zi}z_i| + |K_{bi}z_i| + |\psi_i(e_i)|) \tag{3.13b}$$

The definition of ρ_i in (3.13b) is valid; i.e. (3.13) can be solved since (3.1) is satisfied. Therefore, we have

$$\rho_i=(1-|E_i|)^{-1}[|D_i|+|E_i|(|K_{zi}||z_i| + |K_{bi}||\gamma_i|)] \tag{3.14}$$

To insure that the error dynamics (3.12) is uniformly bounded, the approach relies on the Lyapunov criterion [Vidyasagar, 1978]. Given a Lyapunov function candidate

$$V(e_i) = e_i^TP_ie_i \tag{3.15}$$

and there exists

$$\dot{V} = \dot{e}_i^TP_ie_i + e_i^T\ P_i\dot{e}_i \tag{3.16}$$

$$= -e_i^TL_ie_i - 2e_i^TP_ib_i(\psi_i+\nu_i)$$

$$\le e_i^TL_ie_i - 2[b_i^T\ P_ie_i]^T\ [\psi_i - \frac{b_i^TP_ie_i}{|b_i^TP_ie_i|}\ \rho_i] \ .$$

Consequently, $\dot{V} < 0$.

Furthermore, the error dynamics of the total system can be proven to be stable by summing the individual Lyapunov function [Yuan, 1989]. To improve the convergence rate of equation (3.12), an auxiliary input w (t) is introduced and applied to the input u_i in (3.102) [4,13]. This input is effectively an integral action. Thus,

$$u_i = K_{zi} Z_i + K_{bi} \gamma_i + \psi_i + \omega_i \qquad (3.17)$$

where

$$\omega_i = -\alpha_i \omega_i + S_i^{-1} b_i^T P_i e_i \qquad (3.18a)$$

and

$$\alpha_i \geq \frac{(4A_i \rho_i - \lambda_{min}(L_i)\|e_i\|^2)}{2\lambda_{min}(S_i)\|\omega_i\|^2} \qquad (3.18b)$$

$$S_i > 0$$

Note that λ_{min} represents the minimum eigenvalue.

IV. SIMULATIONS AND EXPERIMENTS

In the previous section, the dynamic model of motion for a multi-link flexible manipulator has been derived and the control algorithm implemented here has been proven to be theoretically feasible. Computer simulations and physical experiments should be carried out to test the work. A computer-controlled prototype two link manipulator, RALF with a parallel actuation mechanism, driven by hydraulic rams is used to perform this verification. Each link is a cylindrical hollow beam, ten feet long. The parallel mechanism's function is force transmission to the upper link. The weight of the robotic structure is about seventy pounds. More details are given [Yuan, 1989].

The transformation matrix E_i contains deflection displacements and rotations as a function of position l along the link. The spatial dependence of these deflections, their shape, is theoretically required only to meet modest restrictions at the link boundaries in an infinite order model. A finite element approach was used to in this research to determine the shapes from detailed models of the link geometry and material properties. Of crucial importance to the accuracy of a low order model are the boundary conditions applied in deriving the shapes. Equivalent springs were used to represent the actuators for both links. Equivalent masses and inertias were also placed at the end of each link, yielding boundary conditions on each link [Yuan, 1989]. The parallel mechanism is simplied as a corresponding spring so that equations of motion as given in (2.22) are obtained.

A Micro-Vax II running under the VMS operating system is used to provide high-speed calculation during real-time control and data acquisition. The control program is written in Fortran and the resolution of D/A and A/D is 12 bits/10 volt. It results in sampling and calculation time of 7 ms. When the advanced control is applied, computation time is increased by approximately 1 ms to a total of 8 ms. However, this sampling rate is feasible to control the RALF since the bandwidth of both hydraulic actuators is above 45 Hz and the lowest two frequencies of the RALF are 5.69 Hz and 9.12 Hz, while the higher mode frequencies are hardly measurable. The third mode primarily consisting of vibration of the actuating link is about 30Hz, and can not be controlled.

The measurement of the piston position is used for feedback instead of the joint angle. A linear variable differential transformer (LVDT) is the transducer. Because the LVDT is located at the same position as the actuator, the non-collocation problem existing in the feedback control of flexible structures can be avoided [Balas, 1978]. Strain gages mounted near the base and midpoint of each link provide measurements of the link deflections. The servo valve of the hydraulic actuator is driven by a power amplifier based on the voltage signal.

The controller design is carried out assuming no payload on the end and the configuration of the RALF at "home" position; i.e., the first joint of 35° and the second joint of 109°. Therefore, the constant gains (K_{zi}) are obtained as [Yuan, 1989].

$$K_{z1} = [-2.82E7 \ -1.35E4 \ -2.80E5 \ -1.14E3] \qquad (4.1a)$$

$$K_{z2} = [-3.00E7 \ -1.01E4 \ -7.76E4 \ -2.68E2] \qquad (4.1b)$$

while the gains associated with joint positions and velocities are needed to specify a joint PD controller as follows:

$$u = -K_p q - K_D \dot{q}$$

$$K_p = \begin{bmatrix} 2.82E7 & 0 \\ 0 & 3.0E7 \end{bmatrix}, \qquad (4.2)$$

$$K_D = \begin{bmatrix} 2.8E5 & 0 \\ 0 & 7.76E4 \end{bmatrix}.$$

Equation (3.1) needs to be satisfied in deriving b_i such that β^{-1} is here chosen as the inertia matrix with the interconnecting terms of zero. b_1 and b_2 are, thus ,

$$b_1 = \begin{bmatrix} 0 \\ 0 \\ 0.002 \\ -0.259 \end{bmatrix}, \qquad (4.3)$$

$$b_2 = \begin{bmatrix} 0 \\ 0 \\ 0.0373 \\ -5.267 \end{bmatrix}. \qquad (4.3)$$

The value of ρ_i in (3.11), is related to assumed uncertainties by (3.14). ρ_i is set to be 3.05E5 from the engineering viewpoint; and the value of is then 2.0. For the decentralized adaptive controller, S_i is chosen to be 3.33E-3 , while α_i is simply set to zero.

The end point of each link is moved about 8.5 inches in 0.4 seconds for point-to-point control. Figures 2a,b show the joint (error) responses and Figures 2c,d represent the strain responses in simulations. Obviously, the decentralized adaptive control results in the best performance in the joint position tracking as well as flexible link damping, while the joint PD control displays the low relative stability of that feedback system. When the controller is implemented in the experiments, the gains are scaled to match the physical characteristics of the system. The Figures 3a,b show time responses of the joints with a PD controller and with an adaptive decentralized controller. Figures 4a,b and 5a,b illustrate the strain responses occurred in the lower and the upper links with different controllers. The decentralized controller settles in less than 1/3 the time needed by the PD controller.

The results from simulations can be compared with experiments to illustrate qualitative agreement. In light of model simplifications the deviation between the experiment and the simulation should, however, be tolerable.

V. CONCLUSIONS

An effective approach based on Lagrange's formula and the assumed mode method has been developed to derive the dynamical equations of a multi-link flexible manipulator. By applying positive control gains K_p and K_D on individual joint position and velocity feedbacks, the system is known to be stable. This simple independent joint control leads to an adaptive decentralized scheme to improve the convergence rate. In the experiments, time responses show compatibility with the theoretical analysis and simulation. The vibration is damped out in under 2 cycles.

Long distance motion and variations of payload must be performed in the experiments in order to test control robustness.

REFERENCES

Asada, H., Slotine, J-J.E., "Robot Analysis and Control," John Wiley and Sons, 1986.

Balas, M. J., "Feedback Control of Flexible System," IEEE Trans. on Auto. Contro., April, 1978, pp. 673-679.

Book, W. J., "Modeling, Design and Control Flexible Manipulator Arms," Ph.D. Thesis, Dept. of Mech. Engr. MIT, April, 1974.

Book, W. J., "Recusive Lagrangian Dynamics of Flexible Manipulator Arms," Int. J. of Robotcs Research, Vol. 3, No. 3, 1984, pp. 87-101.

Cannon, R. M., Schmitz, E., "Intial Experiments on the End-Point Control of a Flexible One-Link Robot," Int. J. of Robotics Research, Fall, 1984, pp. 62-75.

Gutman, S., "Uncertain Dynamical Systems - A Lyapunov Min-Max Approach," IEEE Trans. on Auto. Contr. June, 1979.

Landau, Y. D., "Adaptive Control. - The Model Reference Approach," Marcel Dekker Inc., 1979.

Leitmann, G., "On the Efficacy of Nonlinear Control in Uncertain Linear Systems," ASME J. of Dynamic Systems, Measurement and Control, 1981, p. 95.

Lim, K. Y., Eslami, M., "Adaptive Controller Design for Robot Manipulator System Using Lyapunov Direct Method," IEEE Trans. on Auto. Control, Dec., 1985.

Paul, R., "Robot Manipulators," MIT press, 1981.

Vidyasagar, M., "Nonlinear System Analysis," Prentice Hall, 1978.

Yuan, B. S., "Adaptive Strategies for Controls of Flexible Arms," Ph.D. Thesis, Dept. of Mech. Engr., Ga. Tech, April 1989.

Yuan, B. S., Book, W. J., Huggins, J. D., "Small Motion Experiments on Large Flexible Arm with Strain Feedback," JACC, June, 1989.

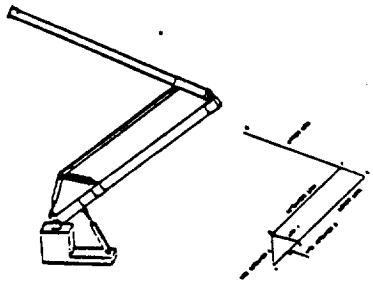

Flexible Manipulator at Georgia Tech

Figure 1. RALF (Robotic Arm, Large and Flexible).

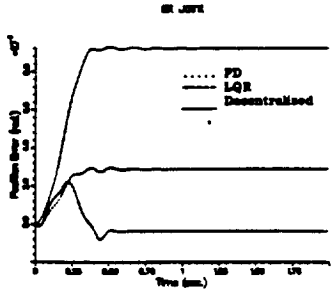

Figure 2a. Joint Error Responses of 1st Joint. (Simulation)

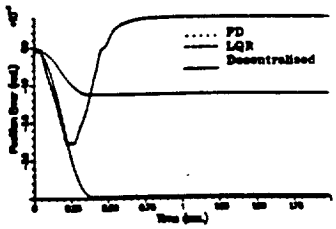

Figure 2b. Joint Error Responses of 2nd Joint. (Simulation)

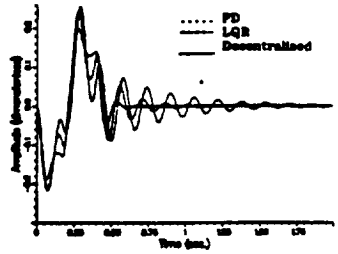

Figure 2c. Strain Responses of Lower Link. (Simulation)

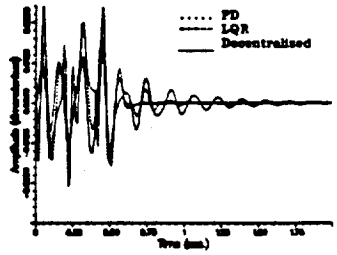

Figure 2d. Strain Responses of Upper Link. (Simulation)

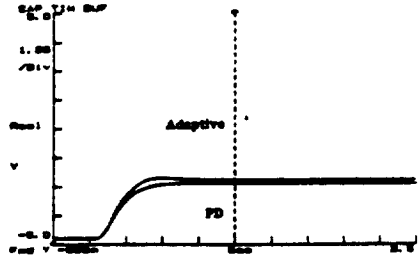

Figure 3a. LVDT Responses for First Actuator. (Experiment)

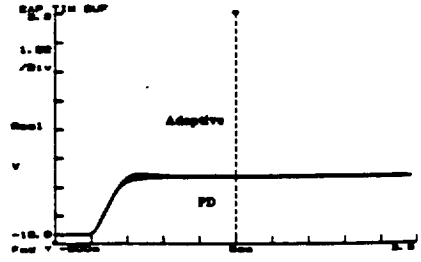

Figure 3b. LVDT Responses of Second Actuator. (Experiment)

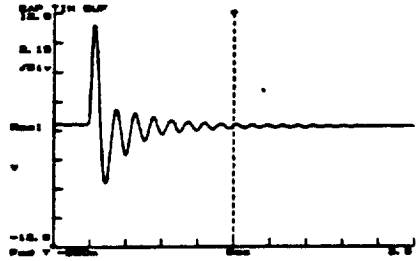

Figure 4a. Strain Response of Lower Link (PD). (Experiment)

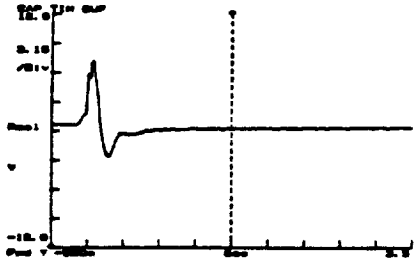

Figure 4b. Strain Response of Lower Link (Decentralised). (Experiment)

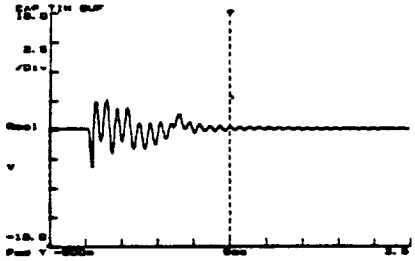

Figure 5a. Strain Response of Upper Link (PD). (Experiment)

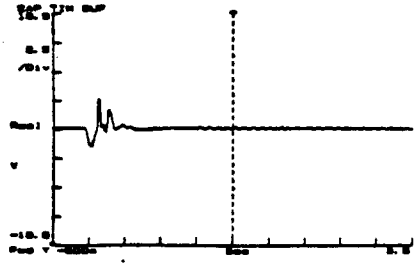

Figure 5b. Strain Response of Upper Link (Decentralised). (Experiment)